RICE UNIVERSITY

The Role of Alpha-Hemoglobin Stabilizing Protein in Human Hemoglobin Assembly

By

Todd Mollan

A THESIS SUBMITTED
IN PARTIAL FULFILLMENT OF THE
REQUIREMENTS FOR THE DEGREE

Doctor of Philosophy

APPROVED, THESIS COMMITTEE:

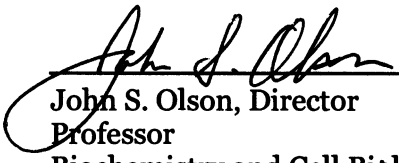

John S. Olson, Director
Professor
Biochemistry and Cell Biology

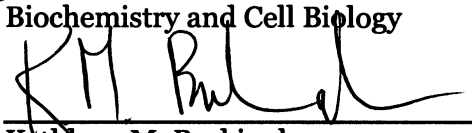

Kathleen M. Beckingham
Professor
Biochemistry and Cell Biology

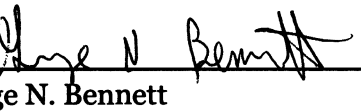

George N. Bennett
Professor
Biochemistry and Cell Biology

Yousif Shamoo
Associate Professor
Biochemistry and Cell Biology

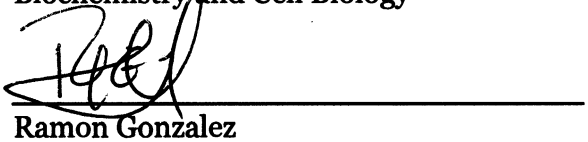

Ramon Gonzalez
Assistant Professor
Chemical and Biomolecular Engineering

HOUSTON, TEXAS
MARCH 2011

ABSTRACT

The Role of Alpha-Hemoglobin Stabilizing Protein in Human Hemoglobin Assembly

by

Todd L. Mollan

Hemoglobin biosynthesis in erythrocyte precursors involves several steps. The correct ratios and concentrations of normal alpha (α) and beta (β) globin proteins must be expressed, apoproteins must be folded correctly, heme must be synthesized and incorporated into these globins, and the resulting α and β subunits must be rapidly and correctly assembled into heterotetramers. These events occur on a large scale in vivo, and dysregulation causes serious clinical disorders such as thalassemia syndromes. Recent work has implicated a conserved erythroid protein known as Alpha-Hemoglobin Stabilizing Protein (AHSP) as a participant in these events. Current evidence suggests that AHSP enhances α subunit stability and diminishes its participation in harmful redox chemistry. There is also evidence that AHSP facilitates one or more early-stage post-translational hemoglobin biosynthetic events. In this work, the rate constants associated with AHSP binding to and dissociation from native ferric and ferrous human α subunits have been determined, along with the binding and dissociation equilibrium constants. Also, several mutant AHSP proteins were used to better define the cis-trans peptidyl-prolyl isomerization events that AHSP is known to undergo, and several naturally occurring human α subunit missense mutants were used to probe AHSP function. Additionally, several post-binding events regarding AHSP:α-subunit interactions were investigated, such as

autooxidation, heme uptake, hemin loss, effects on ligand binding, and secondary structure acquisition. Finally, AHSP was co-expressed with α and β subunits in transgenic *Escherichia coli* as a way of probing the effects of AHSP on hemoglobin production. Collectively, these data support the model that AHSP rapidly binds α subunits, stabilizes them, and then is displaced by β subunits during hemoglobin production.

Acknowledgments

John S. Olson has been a superb advisor and mentor. His greatness as an intellectual and decency as a person stand out even against a backdrop of excellence. I have been made speechless many times by his superiority and intellect, and feel privileged to have been in his company for the last several years.

Kathleen M. Beckingham, George N. Bennett, and Yousif Shamoo have been excellent scientific mentors. Undoubtedly, this work would not have been possible without their support and help, and I am grateful for their efforts.

Kevin R. MacKenzie has been a great help, scientifically and otherwise. His sharpness, generosity, and kindness have left me appreciably indebted to him, and he has expanded my understanding of quality and excellence.

M. Susan Cates has selflessly gone out of her way to help me again and again, and Mitchell J. Weiss has been a great collaborator. Dara L. Wegman-Geedey and Heidi Storl have taught me many important lessons. The current and past members of the John S. Olson Laboratory have been significantly assistive, particularly Angela N. Hvitved and Mallory D. Salter, as well as these people: Faiza Hussain, Philip C. Lisius, Nicholas R. Clayton, Andrew J. Hobbs, Alexander S. Garbe, Christopher J. Alesandrini, Thomas W. Flannigan, Ivan A. Birukou, George C. Blouin, Loren J. Stagg, Sarah E. Ratzel, Marian Fabian, Arindam Sarkar, Michael Perham, Jonathan M. Choe, Mary L. Harrison, Abdu Alayash, Robert P. Strobo, Christian T. Laden, Eileen W. Singleton, Jayashree Soman,

Cornelius L. Varnado, Timothy J. O'Dell, Damian E. Dalle Nogare, and Phil E. Graves.

Terrence P. Mollan, Cheryl A. Mollan, Courtney M. Kohlstedt, and Lindsay L. Mollan have also made this work possible in indescribable ways.

This work could not have been completed without the financial and other support of the National Institutes of Health, Department of Health and Human Services, United States of America.

Thank you.

Table of Contents

Abstract ii

Acknowledgements iv

List of Figures viii

List of Tables x

List of Abbreviations, Conventions, Symbols xi

Hemoglobin, Oxidation State Nomenclature xiv

Chapter 1: Introduction 1

Significance 1

Hypothesis and Specific Aims 3

Types, Occurrence, Overview of Human Hemoglobin 3

Post-Translational Pathways of HbA Biosynthesis 8

Heterologous Expression of Recombinant HbA 14

Overview of AHSP 17

The Role of AHSP During HbA Biosynthesis 27

Medical Relevance of AHSP 30

Chapter 2: Materials, Methods, Instruments 34

Human AHSP Expression, Purification 34

Native Wild-Type Adult Human Hemoglobin Purification 40

Alpha, Beta Subunit Isolation 41

Heme Extraction from Isolated Subunits 44

Recombinant HbA and HbF Production, Mutagenesis 45

Mass Spectrometry 49

Instrumentation, Materials 49

Chapter 3: AHSP Binding to and Dissociation from Human Alpha Chains 51

AHSP, Alpha Chain Association 51
AHSP, Alpha Chain Dissociation 66
AHSP Affinity for (O_2), (CO), (met)Alpha Chains 71
Chapter 4: Changes in α^H Chain Properties Following Binding to AHSP 75
AHSP and Alpha Chain Oxidation, Hemichrome Formation 75
AHSP and Alpha Chain Hemin Loss and CO-Heme Binding 82
AHSP and Alpha Chain O_2, CO Binding 85
AHSP and Alpha Chain Secondary Structure 87
Chapter 5: Hemoglobin Turriff (αK99E) as a Probe of AHSP Function 90
Alpha Chain Mutants for Probing AHSP Function 90
Significance of Hb Turriff 95
Binding of Hb Turriff α^H Chains to AHSP, β^H Chains 97
Interactions Between Hb Turriff α^H Chains and Wild-Type, Revertant AHSP 101
Chapter 6: Co-Expression of AHSP with Recombinant HbA 108
Expression System Construction 108
Co-Expression of AHSP with rHb 110
Chapter 7: Characterization of HbF Toms River 114
Background, Case Information 114
Functional Studies of Hemoglobin Toms River 116
Chapter 8: Summary of Findings 121
References Cited 123

List of Figures

Figure 1-1. Structure of HbA 5

Figure 1-2. Structure of HbF 7

Figure 1-3. Prosthetic group binding to HbA and its subunits 10

Figure 1-4. Pathways of folding, heme insertion, subunit assembly 12

Figure 1-5. Inter-subunit interactions 14

Figure 1-6. Human AHSP sequence information 19

Figure 1-7. Cis and trans structural conformers of human AHSP 23

Figure 1-8. X-ray crystallographic structures of AHSP:α^H-chain complexes 25

Figure 1-9. Proposed functional roles of AHSP 31

Figure 2-1. AHSP purification stages 38

Figure 2-2. Boyer titration, subunit purity determination 44

Figure 3-1. Intrinsic fluorescence emission of AHSP, α^H chains, β^H chains 53

Figure 3-2. AHSP association with α^H chains 57

Figure 3-3. AHSP, α^H chain association rates unders pseudo-first order conditions 60

Figure 3-4. Mechanism of AHSP, α^H chain association reaction 61

Figure 3-5. Mutant AHSP association with α^H chains 64

Figure 3-6. Rate constants for mutant AHSP, α^H chain association 66

Figure 3-7. AHSP, β^H chain competition for free α^H chains 67

Figure 3-8. Displacement reaction concentration dependence 68

Figure 3-9. Wild-type and mutant AHSP, α^H chain displacement reactions 69

Figure 3-10. Kinetics of AHSP binding to and dissociation from (O_2)-, (CO)-, and (met)-α^H-chains 72

Figure 4-1. Autooxidation of AHSP:α^H-chain complexes 78

Figure 4-2. AHSP-induced α^H chain hemichrome formation 79

Figure 4-3. Reversibility of AHSP-induced α^H chain hemichromes 81

Figure 4-4. Effects of AHSP on α^H chain on hemin loss rates..... 84

Figure 4-5. Effects of AHSP on α^O globin CO-heme binding rates 85

Figure 4-6. AHSP influence on α chain secondary structure 88

Figure 5-1. Clinically significant α^H chain residues 92

Figure 5-2. Wild-type, mutant AHSP:α^H-chain binding interfaces 96

Figure 5-3 Electrophoresis of wild-type, mutant subunits..... 98

Figure 5-4. (K99E)α^H chain association with β^H chains..... 99

Figure 5-5. Intrinsic fluorescence emission of AHSP, (K99E)α^H chains 100

Figure 5-6. $AHSP^{Q25K}$, $AHSP^{D29R}$ binding to Hb Turriff α^H chains 102

Figure 5-7. $AHSP^{Q25K}$, $AHSP^{D29R}$ binding to wild-type α^H chains..... 104

Figure 5-8. (K99E)α^H chain, AHSP revertant displacement reactions..... 105

Figure 6-1. AHSP, rHb co-expression vectors 110

Figure 6-2. Co-expression of AHSP with rHb in E. coli 112

Figure 7-1. Wild-type HbF, HbF Toms River Structures..... 117

Figure 7-2. Autooxidation of wild-type, mutant HbF..... 119

List of Tables

Table 3-1. Kinetic parameters for wild-type and mutant AHSP, α^H chain dissociation 70

Table 3-2. Kinetic parameters for AHSP binding to and dissociation from (O_2), (CO), and (met)-α^H chains 73

Table 4-1. AHSP:α^H-chain ligand binding kinetic parameters 86

Table 5-1. Summary of mutant α^H chain synthesis, binding evidence 94

Table 5-2. Kinetic parameters for α^H chain, AHSP revertant interactions 106

Table 7-1. Kinetic parameters for ligand binding to wild-type, mutant HbF 119

List of Abbreviations, Conventions, Symbols

α ..... alpha

α^H ..... alpha with heme or hemin; holoalpha

α^O ..... alpha lacking heme or hemin; apoalpha

AU ..... arbitrary units

AHSP ..... Alpha-Hemoglobin Stabilizing Protein

amu ..... atomic mass unit

β ..... beta

β^H ..... beta with heme or hemin; holobeta

β^O ..... beta lacking heme or hemin; apobeta

BLAST ..... Basic Local Alignment Search Tool

BPG ..... 2,3-bisphosphoglyceric acid

BME ..... β-mercaptoethanol

CAE ..... cellulose acetate electrophoresis

CD ..... circular dichroism

CN^- ..... cyanide

CO..... carbon monoxide

CO_2 ..... carbon dioxide

DT ..... sodium dithionite

CPK ..... Corey-Pauling-Koltun

E. coli ..... *Escherichia coli*

EDTA ..... ethylenediaminetetraacetic acid

EPR ..... electron paramagnetic resonance

ExPASy ..... Expert Protein Analysis System

F^- ..... fluoride ion

Fe ..... iron

FPLC ..... fast protein liquid chromatography

GST ..... glutathione-S-transferase

g ..... gram

H^+ ..... hydrogen ion

Hb ..... hemoglobin

HbA ..... Hemoglobin A

HbF ..... Fetal Hemoglobin

HBOC ..... hemoglobin-based oxygen carrier

HP ..... high performance

IPTG ..... isopropyl β-D-1-thiogalactopyranoside

kg ..... kilogram

kDa ..... kilodalton

λ ..... lambda

L ..... liter

LB ..... Luria-Bertani

LC ..... liquid chromatography

M ..... molar

MALDI-TOF ..... matrix-assisted laser desorption/ionization time of flight

mL ..... milliliter

ms ..... milliseconds

MS ..... mass spectrometry

N_3^- ..... azide ion

NCBI ..... National Center for Biotechnology Information

NMR ..... nuclear magnetic resonance

NO ..... nitric oxide

O_2 ..... dioxygen

O_2^- ..... superoxide radical

OH^- ..... hydoxide

PBS ..... phosphate buffered saline

PCR ..... polymerase chain reaction

PDB ..... Protein Data Bank

PMB ..... ρ-hydroxymercuribenzoate

PPIase ..... peptidyl-prolyl isomerase

PRBCs ..... packed red blood cells

RPM ..... revolutions per minute

ROS ..... reactive oxygen species

rHb ..... recombinant Hb

rHBOC ..... recombinant hemoglobin-based oxygen carrier

SDS-PAGE ..... sodium dodecyl sulfate polyacrylamide gel electrophoresis

SIB ..... Swiss Institute of Bioinformatics

SNP ..... single nucleotide polymorphism

TB ..... terrific broth

TF ..... transcription factor

TSE ..... transmissible spongiform encephalopathy

wt ..... wild-type

Hemoglobin, Oxidation State Nomenclature

Bis-histidyl ..... heme/hemin iron hexacoordination between His E7 and His F8

Hemin ..... protoporphyrin IX ring bearing a Fe^{3+} atom

Heme ..... protoporphyrin IX ring bearing a Fe^{2+} atom

Hemichrome ..... bis-histidyl coordination with ferric iron

Hemochrome ..... bis-histidyl coordination with ferrous iron

Ferric ..... Fe^{3+} atom

Ferrous ..... Fe^{2+} atom

Ferryl ..... Fe^{4+} atom

Met, as in methemoglobin and (met)α^{H}-chains ..... indicates the ferric state

The use of roman typeface refers to proteins, and the use of italicized typeface refers to genes. “Chains” and “subunits” refer to hemoglobin monomers irrespective of the presence or absence of heme or hemin, and “globin” specifically denotes the absence of heme or hemin. Concentrations will be given on a per heme basis unless otherwise noted. For example, a hemoglobin concentration of 5 millimolar (mM) will be reported as 20 mM, because hemoglobin is a tetramer with four heme prosthetic groups.

Chapter 1: Introduction

*Much of the prose, figures, and references that appear in this chapter were taken from Mollan et al. (*1*). The portions reproduced here were those that were composed by the first author of that publication, and quotation marks and further references to this work have been omitted to avoid redundancy.

Significance

In recent years, over 14 million units of allogeneic whole blood and red blood cells have been transfused annually into patients in the United States (*2*). These transfusions are often life-saving (*3-5*) and seldom cause adverse events (*6-11*). Unfortunately, U.S. hospitals have recently reported blood shortages that are predicted to worsen as the population ages (*2*, *12-16*). Costly diagnostics and handling regulations, increasingly stringent donor deferral criteria, and diminishing rates of blood donation partly explain this problem (*17-21*). However, other issues such as emergent pathogens, natural disasters, wars, and adverse reactions from mistransfusions are also of concern (*6*, *17*, *22-31*). These and other factors have led to a "cost explosion" in the industry (*6*), with the price of one unit of packed red blood cells (PRBCs) significantly increasing in recent years (*32-34*).

Many of these concerns can be addressed with recombinant hemoglobin-based oxygen carriers (rHBOCs). These therapeutics consist of concentrated solutions of acellular human Hemoglobin A (HbA) which has been expressed in and isolated from transgenic organisms (*35-39*). They are similar to non-recombinant HBOCs, which are a more well-studied class of therapeutics that are derived from animal erythrocytes or outdated units of human blood (reviewed in *6*, *40-61*). In principle, rHBOCs can be transfused in place of

PRBCs to facilitate dioxygen (O_2) transport while offering the following advantages: (1) decreased immunopathology, (2) longer shelf-life, (3) diminished risk of disease transmission, (4) enhanced oxygen delivery, (5) controllable rheological and osmotic properties, (6) improved uniformity in composition, (7) higher purity, (8) more reliable availability, (9) fewer transfusion-induced adverse events, and (10) availability to patients who cannot receive conventional blood transfusions for personal, geographical, religious, or clinical reasons (*50-52*, *62*, *63*). Despite these advantages, regulatory approval has been limited thus far (presently, only one HBOC has been approved for human use in South Africa, with another being approved for veterinary use in the United States of America)(*58*, *60*, *64*). One of the main reasons for the lack of an approved HBOC is that transfusions of current-generation products has in some cases led to adverse cardiovascular, cerebrovascular, and other harmful events (*65*). Another reason is that recombinant HBOCs which have been rationally designed to mitigate these adverse events are costly to investigate due to technological issues associated with their production.

The main objective of this thesis has been to address several problems in HBOC research by obtaining a more thorough understanding of the post-translational events associated with HbA production. This knowledge should put researchers in a better position to optimize the production of candidate rHBOCs which can then be evaluated as alternatives to PRBCs. Because the cost of recombinant HbA expression is currently a significant impediment to commercial development, overcoming this issue would be a major advance.

A second objective has been to generate a better understanding of the relationship between certain hematological disorders and HbA production. Although a great deal is known about normal and aberrant HbA production, our understanding of this process is incomplete, and work in this area is expected to inform treatment options and research regarding some of these disorders. Lastly, the determination of HbA assembly mechanisms will help expand our understanding of how other biologically important, multi-subunit proteins are produced in vivo.

Hypothesis and Specific Aims

The hypothesis for this work is that a putative molecular chaperone known as Alpha-Hemoglobin Stabilizing Protein (AHSP) assists with human HbA biosynthesis in vivo. The specific aims were: (a) to characterize the impact of this protein on HbA subunit assembly and to better define its function, and (b) to ascertain whether this protein can be used in rHBOC production to enhance heterologous expression yields of recombinant hemoglobin (rHb) in *Escherichia coli* (*E. coli*).

Types, Occurrence, Overview of Human Hemoglobin

Normal adult human blood contains approximately 12 to 15 grams (g) of hemoglobin (Hb) per 100 milliliters (mL) of fluid (*66-68*). This amounts to more than 600 g of Hb per person, assuming that the person is healthy and possesses a normal blood volume of approximately 5 liters (L)(*67*, *68*). About 92% of this abundant protein is a subtype of Hb that has been designated

Hemoglobin A (HbA)(*66*). HbA belongs to a class of highly conserved and functionally diverse proteins whose evolution can be traced back for at least 1.8 billion years (reviewed in *69-82*). In humans, this protein has been shown to be responsible for O_2 transport (reviewed in *83-86*). It has also been shown to play a role in carbon dioxide (CO_2) transport, blood pH and redox chemistry regulation, and vasoregulation through chemical reactions involving nitric oxide (NO)(reviewed in *66*, *87-102*).

Structurally, HbA is a 64,500 ± 100 Dalton (Da) tetrameric protein which consists of two alpha (α^H) chains and two beta (β^H) chains (Figure 1-1A) (*103*). Each chain consists of helical and non-helical sections, with α^H chains possessing seven α helices and β^H chains possessing eight (*104-107*). The helices within each chain are referred to by convention using the letters A through H, with α^H chains lacking a D helix (Figure 1-1B, C)(*107*). Within each chain, there is a single, iron-containing protoporphyrin IX group ("heme" in the case of ferrous (II) iron; "hemin" in the case of ferric (III) iron)(*66*, *107*). These groups are held in place by numerous interactions with the globin chain, including a covalent bond between the heme iron and the imidazole nitrogen of conserved histidines within each chain (*66*). This bonding occurs with His87 in α^H chains and His92 in β^H chains, both of which are referred to as the proximal histidines (Figure 1-1)(*66*, *107*). The opposite face of each heme group (the distal side) is responsible for binding ligands such as alkyl isocyanides, carbon monoxide (CO), NO, and O_2, as well as azide (N_3^-), cyanide (CN^-), fluoride (F^-), hydroxide (OH^-), NO, and water (H_2O) when the heme iron is oxidized to the ferric state (*66*, *108-112*).

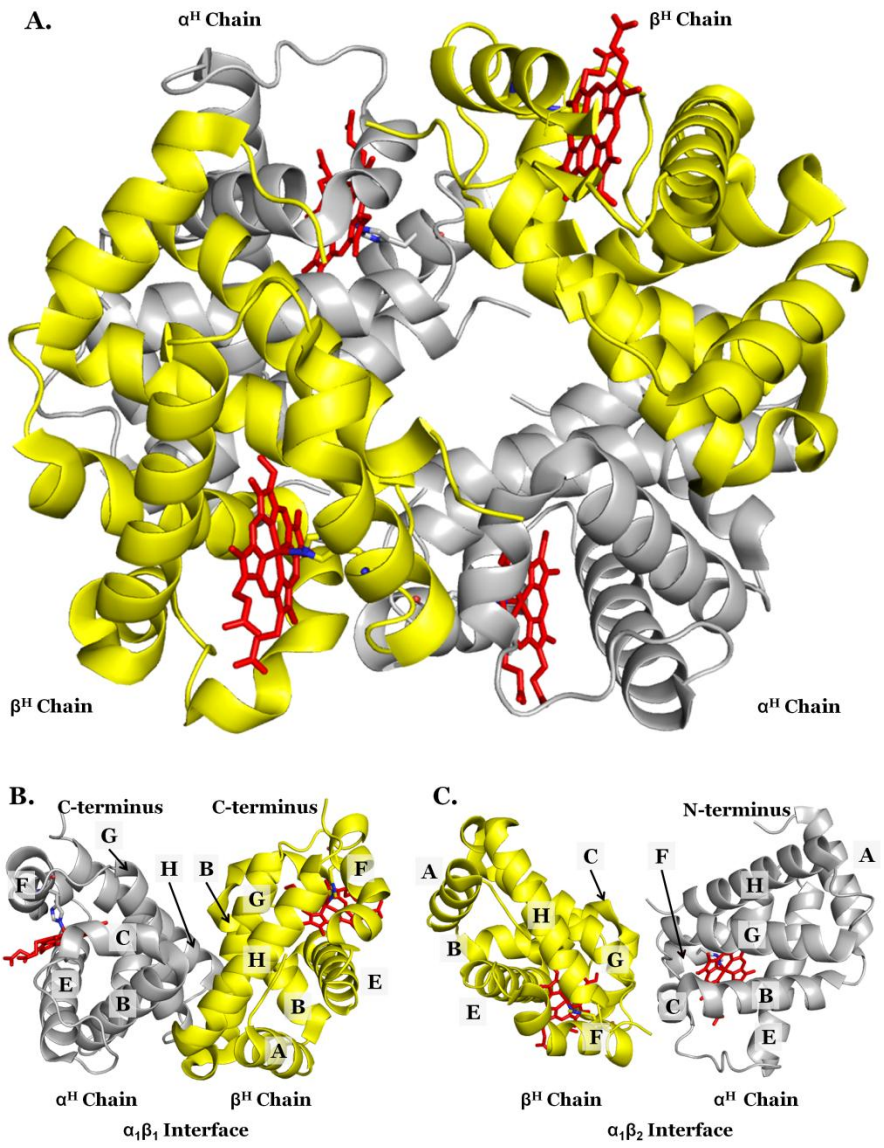

Figure 1-1. Structure of HbA
Heme groups are shown as red stick structures, α^H chains in gray ribbon structures, and β^H chains in yellow ribbon structures. Proximal histidines are depicted using stick structures with Corey-Pauling-Koltun (CPK) coloring. HbA is shown in *Panel A*, the $\alpha_1\beta_1$ (or $\alpha_2\beta_2$) interface in *Panel B*, and the $\alpha_1\beta_2$ (or $\alpha_2\beta_1$) interface in Panel C. The nature and extent of inter-subunit contacts change depending on whether the subunits are deoxygenated or have O_2 bound. Figure generated using PyMOL Molecular Graphics System and PDB 1LFL (DeLano Scientific, Palo Alto, California, US)(*113*).

The chains of each tetramer are held together through a series of non-covalent bonds, mostly apolar, which make up two types of inter-subunit

interfaces (*107*). Those involving the B, G, and H helices and the GH corner from each subunit are called $\alpha_1\beta_1$ (or $\alpha_2\beta_2$) interfaces (Figure 1-1B)(*107*). Those involving the C and G helices and the FG corner from each subunit are called $\alpha_1\beta_2$ (or $\alpha_2\beta_1$) interfaces (Figure 1-1C)(*107*). Within each HbA tetramer, there are a total of four interfaces: (1) $\alpha_1\beta_2$, (2) $\alpha_2\beta_1$, (3) $\alpha_1\beta_1$, and (4) $\alpha_2\beta_2$. There is little, if any, direct α-α or β-β chain contact within HbA tetramers (*105*, *107*).

In humans, HbA is produced from three genes: two *α globin* genes and one *β globin* gene per haploid genome (*HBA1* and *HBA2* on Chromosome 16, NCBI Accession NM_000558.3 and NM_000517.4*;* and *HBB* on Chromosome 11, NCBI Accession NM_000518.4)(*114*, *115*). *HBA1* and *HBA2* each code for the same α globin protein, which is 141 residues long and has a molecular mass of 15,126.7 ± 1.4 Da without its heme group (NCBI Accession NP_000549.1, NP_000508.1)(*114*, *116*). *HBB* encodes β globin, which is a 146-residue-long protein with a molecular mass of 15,867.4 ± 0.7 Da without heme (NCBI Accession NP_000509.1)(*114*, *116*). The molecular genetics and regulatory programs coordinating the expression of these genes are complex (reviewed in *117-127*). Moreover, there are over 1,000 mutations which are known to affect the expression and/or functional properties of these genes and their products (*128*).

HBA1, *HBA2*, and *HBB* are situated within a cluster of other *globin* genes which are differentially expressed as part of a developmental process called globin switching (reviewed in *117*, *119*, *129-132*). Part of this work involves the study of human fetal Hb (HbF), which is a type of Hb that is produced during this process. HbF is present in small amounts in healthy

human adults (<1% of the total Hb in circulating erythrocytes) and in large amounts in embryos and fetuses beginning at about six weeks post-fertilization (>75% of total Hb)(*66*, *131*). By about 18 weeks post-birth, HbF expression is appreciably diminished (*66*, *131*).

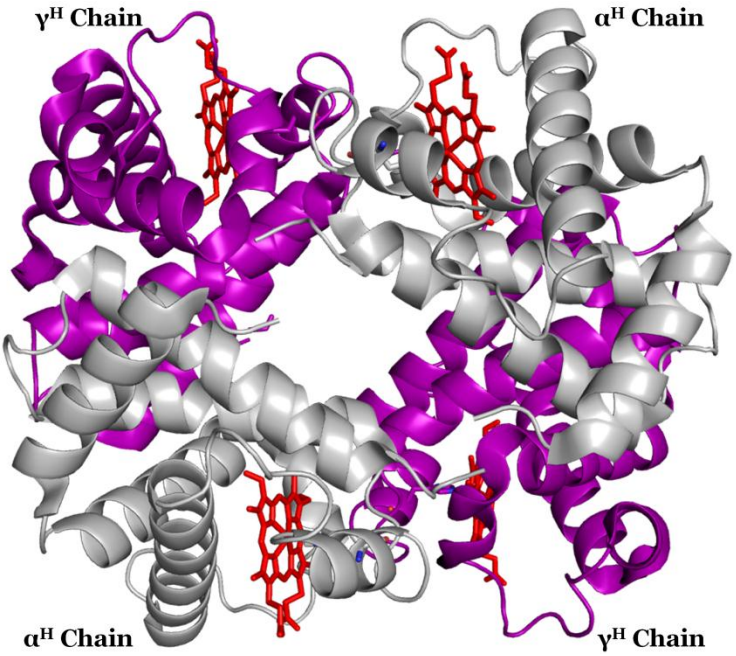

Figure 1-2. Structure of HbF
The color scheme, ribbon and stick forms used in this figure are the same as those used in Figure 1-1, except that γ^H chains appear in purple. Figure generated using PyMOL Molecular Graphics System and PDB 1FDH (DeLano Scientific, Palo Alto, California, US)(*133*).

Like HbA, HbF is a tetramer, with each subunit bearing a single heme or hemin group (Figure 1-2)(*133*). HbF is functionally very similar to HbA, and it is thought to act primarily as an O_2 transport protein that is adapted for O_2 uptake in the placenta (*66*, *134*). The major difference is that instead of possessing two α^H and two β^H chains, HbF possesses two α^H and two gamma (γ^H) chains (Figure 1-2). The primary amino acid sequence of γ^H chains differs

from that of β^H chains at 36 positions (*66*). Also, there are two *γ globin* genes on Chromosome 11, designated $^A\gamma$ and $^G\gamma$ *globin*, which code for 146-residue-long proteins that differ at position 136 of their primary sequences (*HBG1* and *HBG2*, NCBI Accession NM_000559.2, NM_000184.2, P69891.2, NP_000175.1)(*114*, *115*).

Post-Translational Pathways of HbA Biosynthesis

A great deal of information is known about the structural biology and physiology of HbA and its various mutants (*66*, *107*, *135*, *136*). However, much less is known about certain post-translational events that occur during HbA production in vivo. These events include HbA subunit folding, heme or hemin binding, and assembly into functional heterotetramers. Previous work on these processes has left many open questions regarding how they fit together in vivo, and several alternate pathways for HbA production may co-exist in mammalian pre-erythroid cells.

The first steps of HbA production involve *HBA1*, *HBA2*, and *HBB* gene translation, which takes place on the order of a few minutes per subunit (*137-141*). Given that α helices and certain other structural features are capable of forming spontaneously and in less than a few microseconds (*142-145*), it is plausible to conclude that α and β chains acquire at least some of their secondary and tertiary structure co-translationally. Several studies using cell-free protein expression systems have supported this idea, and have further indicated that heme or hemin insertion is also a co-translational process (*136*, *146*, *147*). However, not everyone agrees on the timing of these events, and

several researchers have reported that heme- or hemin-free α and β globins (α^O or β^O globins) only acquire their prosthetic groups after first dissociating from ribosomes (*148-151*).

In vitro work suggests that the rate constants associated with prosthetic group binding to and dissociation from α and β chains are nonequivalent (*152-157*). These values are dependent not only on which amino acids line the globin binding pockets, but also on whether the globins are monomeric or oligomeric, and whether they are in complex with heme-containing or heme-free subunits (*152-163*). The reaction of reduced CO-heme with heme-free αβ dimers ($\alpha^O\beta^O$ dimers; apodimers; apoglobin) is rapid and spontaneous, occurring with rate constants on the order of 10^7 to 10^8 $M^{-1}s^{-1}$ (*164-167*). The rates for hemin binding are less well defined, most likely because free hemin aggregates in solution and complicates kinetic analyses (*153*, *164*, *168*, *169*). In contrast, heme loss occurs at almost immeasurably slow rates (*156*, *170*). These rates increase upon oxidation of the iron to the ferric state, and the observed rates range from 0.3 and 40 hr^{-1} in pH 7.0 buffer at 37 ^OC, depending on the particular subunit and quaternary state under investigation (*155*).

Figure 1-3 provides an overview of heme and hemin binding to and dissociation from HbA and its subunits. Although the equilibrium constants associated with these events are not known with certainty, it is clear that HbA and its subunits have a higher affinity for heme than for hemin. Moreover, heme binding has been linked to helicity increases (18% to 65% in α chains; 51% to 65% in β chains)(*171*), and inter-subunit association events cause increases in both secondary and quaternary structure (*155*, *171-175*).

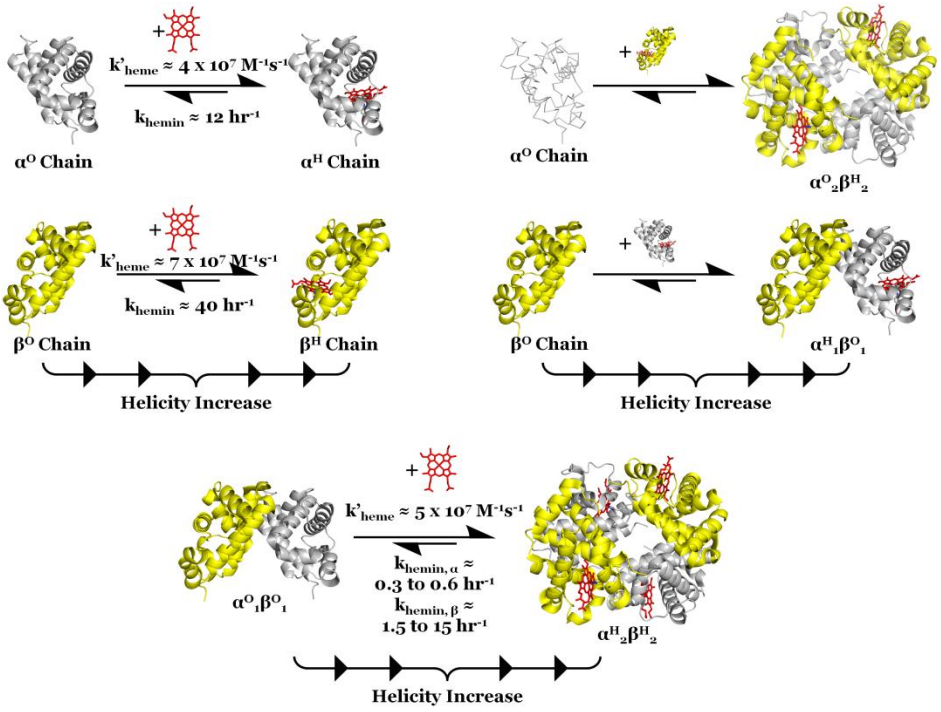

Figure 1-3. Prosthetic group binding to HbA and its subunits

Heme insertion rates were measured in 50 mM Tris, 50 mM NaCl, pH 8.0 at 20 ^{O}C, and hemin loss rates in 150 mM potassium phosphate buffer with 450 mM sucrose, pH 7.0 at 37 ^{O}C. Colors, ribbons, and stick forms are the same as in Figure 1-1. Figure generated using PyMOL Molecular Graphics System and PDB entry 1LFL (DeLano Scientific, Palo Alto, California, US)(*113*, *153*, *155*, *156*, *164*, *171-173*).

In vitro reconstitution studies of HbA suggest that its formation occurs through a series of monomeric, dimeric, and tetrameric intermediates that are partially saturated with heme (*175-178*). Some workers have suggested that α^{H} chains drive heme insertion into β^{O} globins following $\alpha^{H}\beta^{O}$ dimer formation (*161*, *179*, *180*). Consistent with this hypothesis, α^{O} chains have been shown to have a higher affinity for heme than β^{O} chains (*152*, *160*, *164*, *174*, *175*, *177*, *178*, *181*). Also, both α^{O} and α^{H} chains have been reported in their monomeric forms in vivo, and free β^{H} chains tend to be absent except in cases of severe α thalassemia (*161*). Although these observations are consistent with the idea that

α^H chains are the primary drivers of HbA formation, several other plausible models exist.

Isolated β^O chains are known to possess more well-defined structural features than α^O chains (*182*, *183*), and β_4^H tetramers can form once heme binding occurs (*184*, *185*). This evidence supports the observation that isolated β chains are more stable than isolated α chains in solution (*186*), and suggests an assembly model in which β^H chains self-chaperone and drive heme insertion into and folding of α^O chains. Alternatively, the assembly of partially folded α^O and β^O subunits into more fully folded $\alpha^O\beta^O$ globin dimers could drive heme uptake into both subunits. In support of this idea, the removal of heme from HbA results in $\alpha^O\beta^O$ globin dimers, and dissociation into monomeric α^O and β^O subunits leads to the immediate precipitation of both subunits at temperatures above 5° C (*171-173*). Although isolated and partially unfolded α^O and β^O subunits do not readily recombine to form $\alpha^O\beta^O$ globin dimers in vitro (*171*, *172*), indirect in vivo evidence for the existence of this dimeric species has been reported in some studies (*148-150*).

Figure 1-4 depicts several plausible pathways regarding these events. Although there are a great deal of data, there is presently little consensus regarding the exact sequence of in vivo events.

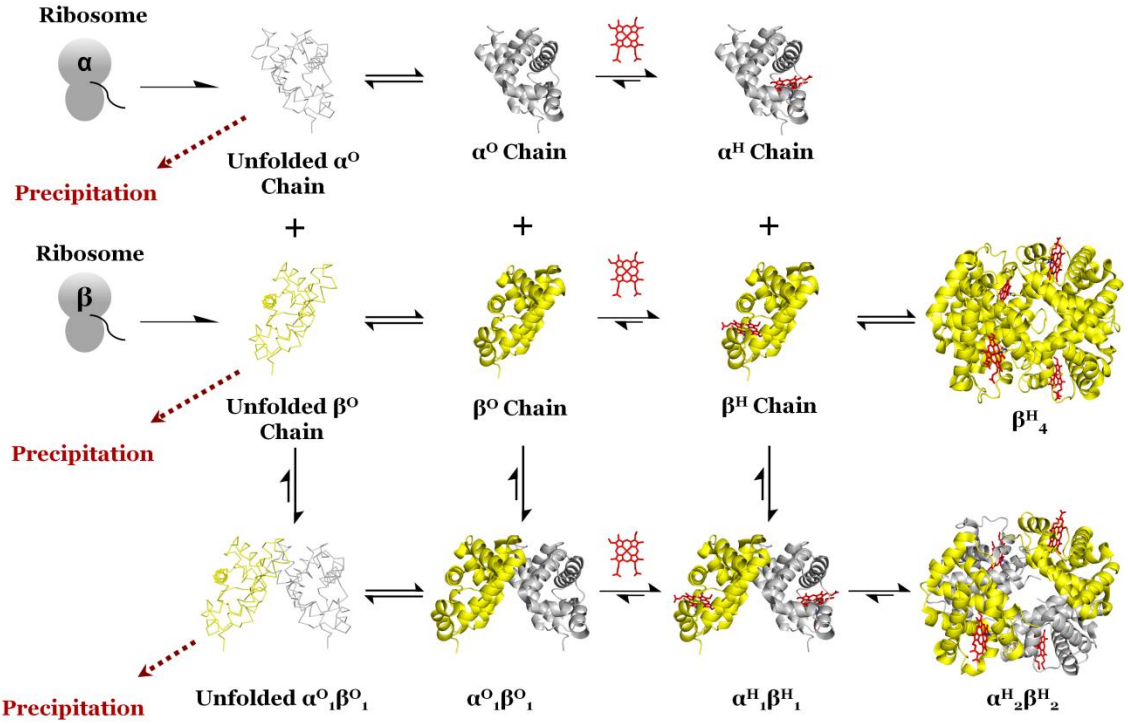

Figure 1-4. Pathways of folding, heme insertion, subunit assembly
The most likely pathways for HbA production are summarized in this figure. Not depicted is the role of AHSP, which is discussed later. Also not shown is the possibility that heme insertion into one chain drives other events, or that any of these events might occur co-translationally. Colors, ribbons, and stick forms are the same as in Figure 1-1, except the use of thin lines and ribbons for the backbone structures indicates unfolded and folded states, respectively. Figure generated using PyMOL Molecular Graphics System and PDB entries 1CBM and 1LFL (DeLano Scientific, Palo Alto, California, US)(*187*, *188*).

In contrast to folding and heme insertion events, the association of isolated α^H and β^H chains to form intact tetramers in solution has been studied extensively and presents a clearer picture (*150*, *165*, *166*, *171-173*, *184*, *185*, *189-205*). When mixed together in vitro and at low concentrations (<10 μM), α^H and β^H chains spontaneously associate with each other to form HbA as part of a two-step process. First, monomeric α^H and β^H chains associate to form $\alpha^H{}_1\beta^H{}_1$ dimers, then two of these dimers associate to form tetrameric HbA (*190*, *191*, *200*, *201*, *206*). The observed bimolecular association rate constants for both of

these steps are approximately 5 x 10^5 $M^{-1}s^{-1}$ for deoxygenated subunits (*190*, *193*, *201*). Because of similarities between the deoxy-, carbonmonoxy-, and oxy-states of HbA at the $\alpha^H_1\beta^H_1$ interface, the rate constants for $\alpha_1\beta_1$ (or $\alpha_2\beta_2$) bond formation are likely to be independent of ligand state (*196*, *205*). The same cannot be said of the $\alpha_1\beta_2$ and $\alpha_2\beta_1$ interfaces, which exhibit significant alterations depending on whether they have ligands bound (*196*, *205*). It has been shown that in the absence of O_2, for example, tetramer dissociation into $\alpha^H_1\beta^H_1$ dimers is several orders of magnitude slower than when O_2 is bound (*196*, *197*, *204*).

An additional detail regarding subunit assembly is that isolated β^H chains readily form homotetramers (β^H_4) at subunit concentrations ≥10 μM (K_D ≈ 10^{-15} to 10^{-17} M^3)(*184*, *185*), whereas α^H chains remain monomeric at subunit concentrations ≤100 μM (K_D ≈ 10^{-4} M)(*184*, *194*). Thus, the assembly of HbA involves three steps when subunit concentrations are high. First, β^H_4 tetramers dissociate into β^H chain monomers, which occurs with rate constants of approximately 0.25 s^{-1} to 0.001 s^{-1}, depending on the concentration of inorganic or organic phosphates present (*201*). Then, the two association events to form HbA tetramers occur (*190*, *200*, *201*, *206*).

Figure 1-5 contains a summary of rate constants for these events. It is important to note that the overall reaction sequence described here is the same for oxygenated and deoxygenated subunits (*200*), but that recorded values suggest that the rate of flux through these pathways is ligand-modulated. Also, in the first bimolecular associative step, it is important to note that α and β subunits combine to form the $\alpha_1\beta_1$ interface, which involves extensive

hydrophobic and some electrostatic interactions between the B, G, and H helices and the GH corner from each subunit (Figure 1-1B). Then, these dimers associate in the second bimolecular step to form two new interfaces, the $\alpha_1\beta_2$ and $\alpha_2\beta_1$ interfaces, which are less extensive and involve more polar interactions (Figure 1-1C)(*66*, *104*, *105*, *107*, *206*, *207*).

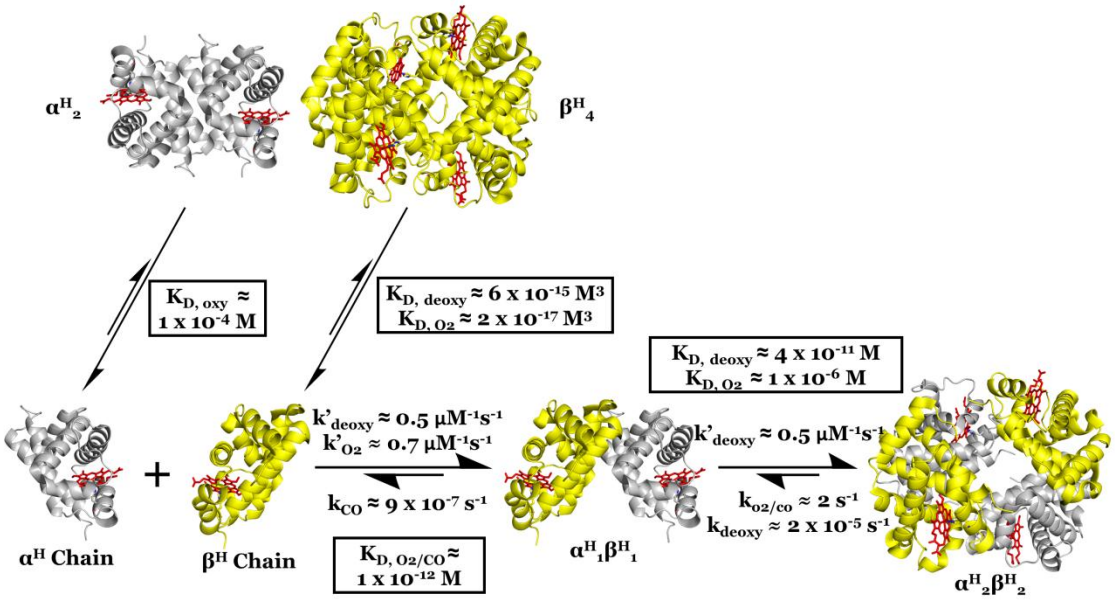

Figure 1-5. Inter-subunit interactions
Rate constants were measured using comparable buffer conditions (pH ~7 at ~22 ^{O}C, buffered by 50 to 150 mM phosphate, with excess sodium dithionite). Colors, ribbons, and stick forms are the same as those used in Figure 1-1. Figure generated using PyMOL Molecular Graphics System and PDB entries 1LFL and 1CBM (DeLano Scientific, Palo Alto, California, US)(*113*, *184*, *185*, *188*, *196-199*, *201-205*).

Heterologous Expression of Recombinant HbA

Experiments dealing with the heterologous expression of recombinant HbA using transgenic organisms first began in the 1980s. Transgene overexpression in *E. coli* and *S. cerevisiae* was accomplished with expression levels exceeding ~5% of total cellular protein content (*208-214*). Subsequent developments in animals led to the development of transgenic pigs which expressed up to 32 grams of human hemoglobin per liter of whole blood

hemolysate, amounting to ~24% of the total Hb content in the pig erythrocytes (*215*). Although rHb production has now been achieved in numerous organisms, including mice, tobacco plants, and insect cells, most work has focused on expression in *E. coli* (*39*, *179*, *208-210*, *212-214*, *216*, *217*, *217*, *218*, *218-223*, *223-251*). Many significant advancements have been made in this system during the last two decades (reviewed in *247-276*).

In the early 1980s, it was shown that β subunits from human HbA could be expressed in and isolated from bacteria (*277-279*). Subsequent work revealed that these recombinant β subunits could be reconstituted with native α^H subunits to produce functional tetrameric rHb (*277*, *280*). Individual apoglobin expression was later accomplished for α subunits (*228*, *281-283*). These early efforts utilized a cleavable lambda (λ) phage leader sequence designed to inhibit bacterial proteolysis and increase expression levels. Protocols involved preparative protein refolding of insoluble aggregates in the presence of heme, as well as leader sequence cleavage and removal prior to subunit recombination to form HbA. Investigators subsequently developed more refined methods which did not involve all these steps (*211*, *213*, *216*, *217*, *225*, *226*, *250*, *251*, *284-287*). In recent years, several groups have begun exploring the use of non-human Hbs as an rHBOC source material. For example, Hbs from Bos taurus and Arenicola marina are being investigated for this purpose (*288-295*).

In the 1990s, significant commercialization efforts culminated in the development of two rHBOCs which reached late stage-clinical trials before their development was halted due to costs associated with conducing further necessary research (rHb 1.1 and rHb 2.0; Somatogen Incorporated,

subsequently acquired by Baxter International Incorporated)(*58*, *64*). At that time, significant efforts were underway to understand the side effects associated with transfusing unmodified acelluar HbA into humans. These side effects include: (1) nephrotoxicity with complex underlying causes (*50*, *296-313*), (2) rapid clearance by the kidneys, reticuloendothelial system, and other mechanisms ($t_{1/2}$ < ~1 hour)(*187*, *299*, *314-331*), (3) significantly altered O_2 affinity and offloading characteristics (*54*, *55*, *332-355*), and (4) side effects such as adverse immune reactions, vasoconstriction, gastrointestinal distress, neurotoxicity, perturbed retinal morphology, reduced cardiac output, increased systemic and pulmonary vascular resistance, coagulation events, redox dysregulation, and other events that appear to be associated with interference with NO signaling in smooth muscle (*42*, *296*, *306*, *356-406*). Other problems include issues related to colloid osmotic pressure and viscosity differentials between PRBCs and acellular HbA (*306*, *407-433*).

Another key problem is rHBOC production efficiency. The most up-to-date expression systems require about 750 L of log-phase bacterial culture to produce one unit of blood (*56*). Moreover, "… 2 units of [recombinant Hb] at $700 to $1000 per unit have a similar Hb content to a single unit of donated blood at $200" (*62*), and trauma care patients often each require an excess of 10 units of PRBCs following acute and severe injuries (*434*, *435*). Animal-derived Hb might seem like a more cost-effective rHBOC source material, given that one cow can be killed to provide 40 units of blood (*61*). However, it is expensive and time-consuming to produce transgenic livestock, and making genetic changes to rHbs in these systems requires developing entirely new lines

of animals, as opposed to simply mutagenizing a bacterial plasmid. At present, the greatest need is to inexpensively produce mid-sized batches of rationally designed rHBOCs which can be utilized in pre-clinical animal studies to address toxicity issues.

The most advanced *E. coli*-based rHb expression systems involve one- or two-plasmid ensembles which co-express codon-optimized *α* and *β globin* genes along with other proteins such methionine aminopeptidase (MAP) and, in some cases, hemin transporters (*39*, *211*, *216*, *436-439*). An additional approach to bolstering rHb expression yields is to use the putative molecular chaperone AHSP (*440-442*). However, in order to assess the usefulness of this approach, AHSP must first be well characterized and its role as a chaperone established quantitatively.

Overview of AHSP

Several individuals examining AHSP have suggested that this protein is a molecular chaperone which participates in HbA production (*442-445*). A molecular chaperone is a protein "… that binds to and stabilizes an otherwise unstable conformer of another protein—and by controlled binding and release of the substrate protein, facilitates its correct fate in vivo: be it folding, oligomeric assembly, transport to a particular subcellular compartment, or controlled switching between active/inactive conformations" (*446*). This class of proteins is large, diverse, and well-studied (*447-454*). Although AHSP is conserved among diverse vertebrates, it shares no sequence motifs with any

other known proteins, chaperones or otherwise (*443*). Figure 1-6 contains primary sequence information regarding AHSP.

AHSP was discovered from experiments on transmissible spongiform encephalopathies (TSEs)(*455*, *456*). TSEs are serious neurological diseases caused by "epigenetic templated protein misfolding" (*457*), and were initially identified in the early 1980s (reviewed in *458*). In 2001, a study was published in which researchers sought to identify molecular markers useful for diagnosing these diseases and AHSP was discovered (*456*). The *ahsp* gene codes for a 102-residue-long protein that was initially named Erythroid Differentiation Related-Factor (EDRF) because it was found in erythroblasts and bone marrow (another designation for AHSP is Erythroid-Associated Factor (ERAF))(*455*, *456*). Concurrent work directed by Mitchell J. Weiss at the University of Pennsylvania resulted in the independent discovery of this protein, which has subsequently become known as AHSP on the basis of its apparent function (*443*, *444*).

The characterization of AHSP began following a screen for downstream targets of GATA-1 (*443*). GATA-1 is a member of the highly-conserved GATA family of zinc-finger transcription factors (TFs) (reviewed in *459-461*). As "… one of the primary determinants of the erythroid lineage" (*462*), GATA-1 has specifically been shown to be critical to erythropoiesis (*463*, citing *464*). Due to the complexity of signaling pathways involving this TF, Weiss and co-workers hypothesized that there may be unknown GATA-1 targets (*443*). Using

A.

```
   atggctcttcttaaggccaataaggatctcatttccgcaggattgaaggagttcagcgttctgctgaatcagcaggtcttc
 1 M  A  L  L  K  A  N  K  D  L  I  S  A  G  L  K  E  F  S  V  L  L  N  Q  Q  V  F
   aatgatcctctcgtctctgaagaagacatggtgactgtggtggaggactggatgaacttctacatcaactattacaggcag
28 N  D  P  L  V  S  E  E  D  M  V  T  V  V  E  D  W  M  N  F  Y  I  N  Y  Y  R  Q
   caggtgacaggggagccccaagagcgagacaaggctctgcaggagcttcggcaagagctgaacactctggccaacccttc
55 Q  V  T  G  E  P  Q  E  R  D  K  A  L  Q  E  L  R  Q  E  L  N  T  L  A  N  P  F
   ctggccaagtacagggacttcctgaagtctcatgagctcccgagtcacccaccgccctcctcctag
82 L  A  K  Y  R  D  F  L  K  S  H  E  L  P  S  H  P  P  P  S  S 102
```

Aromatic Residues α Helical Segments

B. **Organisms with Sequence Evidence of AHSP Protein**

Ailuropoda melanoleuca (panda)	Homo sapiens (human)	Oryctolagus cuniculus (rabbit)
Bos taurus (cattle)	Loxodonta africa (elephant)	Otolemur garnetti (galago)
Callithrix Jacchus (marmoset)	Macaca mulatta (rhesus macaque)	Ovis aries (sheep)
Canis familiaris (dog)	Macropus eugenii (wallaby)	Pan troglodytes (chimpanzee)
Cavia porcellus (guinea pig)	Microcebus murinus (mouse lemur)	Pongo abelii (orangutan)
Choloepus hoffmanni (sloth)	Monodelphis domestica (opossum)	Procavia capensis (rock hyrax)
Dasypus novemcinctus (armadillo)	Mus musculus (mouse)	Pteropus vampyrus (megabat)
Equus Caballus (horse)	Mustela putorius (ferret)	Rattus norvegicus (rat)
Erinaceus europaeus (hedgehog)	Myotis lucifugus (brown bat)	Sus scrofa (pig)
Felis catus (domestic cat)	Ochotona princeps (pika)	Tarsius syrichta (tarsier)
Gorilla gorilla (gorilla)	Ornithorhynchus anatinus (platypus)	Tupaia belangeri (tree shrew)

Figure 1-6. Human AHSP sequence information
Panel A depicts the human *ahsp* gene cDNA and its translated product (NCBI Accession NM_016633.2)(*114*). Aromatic residues which give rise to the spectral properties discussed in Chapter 3 are highlighted in yellow, and the three α helices of this protein are highlighted in blue. *Panel B* lists other organisms whose genomes indicate the existence of AHSP protein. Searches using *ahsp* mRNA, cDNA, and translated protein sequences using different algorithms, parameters, and databases suggest that AHSP homologs are absent from known arthropod, invertebrate, fungal, and microbial genomes (bacterial, archaeal, eukaryotic microbes). Sequence translation and analysis was performed using tools available from the ExPASy (Expert Protein Analysis System) proteomics server at the Swiss Institute of Bioinformatics (SIB), available http://expasy.org/tools/, accessed January 6, 2011. Genome searches were performed using data and the Basic Local Alignment Search Tool (BLAST), both available at NCBI, http://blast.ncbi.nlm.nih.gov/, accessed January 6, 2011.

subtractive hybridization and a GATA-1 null mutant erythroid cell line (*465-467*), they identified AHSP as a novel GATA-1 target that is expressed in hematopoietic tissues (*443*).

Glutathione-S-transferase (GST) pulldown and cellulose acetate electrophoresis revealed that AHSP associates with α^H chains, but not β^H chains

or HbA (*443*). Also, HbA forms as β^H chains are titrated into solutions of AHSP and α^H chains, and Western blotting showed that AHSP does not remain bound to the HbA complexes following the titration (*443*). Gel filtration elution profiles reported in another study corroborate these findings by showing that AHSP elutes independently from α^H and β^H chains in solutions containing all three components (*444*). Also, Wright-Giemsa and crystal violet staining of murine cells suggested that AHSP inhibits Hb inclusion body formation in vivo (*443*).

Weiss and co-workers initially reported that AHSP expression increases incrementally during HbA biosynthesis in erythroid precursor cells (*443*), a finding which was subsequently confirmed by real-time quantitative PCR (*468*). To further investigate AHSP function, $AHSP^{-/-}$ and $AHSP^{+/-}$ mutant mice were generated and compared to wild-type animals (*469*). All three genotypes were indistinguishable by gross examination at birth (*469*). However, many null mutant mice had morphologically atypical and anemic erythrocytes, and some showed elevated reticulocyte counts (*469*). There were also inclusion and Heinz bodies (denatured globin chains) in the mutant mice erythrocytes (*469*). Although there was no evidence of HbA subunit precipitation in wild-type animals, $AHSP^{+/-}$ mice showed α^H chain precipitation, and $AHSP^{-/-}$ mice showed both α^H and β^H chain precipitation (*469*). This latter finding was unexpected because previous work suggested that AHSP does not interact with β^H chains (*469*). It was hypothesized that homozygotic disruption of AHSP creates a surplus of monomeric α^H chains which then catalyze oxidative reactions that lead to HbA and α^H and β^H chain precipitation (*469*).

Extensive erythrophagocytosis and a diminished circulation half-life of erythrocytes were also observed in mutant mice (*469*). Mutants also exhibited enlarged spleens and preerythroid hyperplasia in both splenic and bone marrow tissues (*469*). Cell surface markers unique to specific developmental stages and flow cytometry revealed an abnormally high ratio of immature to mature erythrocytes in mutant mice (*469*). There was also elevated apoptosis in mutant animal hematopoietic tissues (*469*). On the basis of these findings, Weiss and co-workers concluded that abrogation of AHSP is harmful to both immature and mature erythrocytes, even though AHSP exists in lower concentrations in the latter cells (*443*, *469*).

Mackay and co-workers at the University of Sydney utilized circular dichroism (CD) spectroscopy, analytical ultracentrifugation, and analytical size-exclusion gel filtration chromatography to study several biophysical properties of AHSP (*444*). CD spectra strongly suggested that AHSP consists principally of α helices, and analytical ultracentrifugation indicated that it exhibits an apparent molecular weight in the 11,200-11,800 range and exists as a monomer in solution (*444*). The stoichiometry of the association of AHSP with α^H chains was studied by mixing different ratios of these proteins together and analyzing the resulting solutions by gel filtration chromatography (*444*). These experiments demonstrated a 1:1 stoichiometry between AHSP and α^H chains, and indicated that AHSP is also capable of binding α^O globins (*444*). They also suggested tight binding, which was confirmed by isothermal titration calorimetry (the association equilibrium constant was measured to be 1.0×10^7 M^{-1} at 20 ^OC)(*444*).

In 2004, Santiveri et al. (*470*) determined the structure of AHSP using nuclear magnetic resonance (NMR) spectroscopy. This structure is shown in Figure 1-7. Initial data suggested that AHSP exhibits conformational heterogeneity as a result of cis-trans isomerization about the Asp29-Pro30 peptide bond (*470*). To further investigate this point, a P30A mutant of AHSP was constructed to prevent isomerization (*470*). This mutant facilitated a determination of the three-dimensional solution structures for both (cis)AHSP and (trans)AHSP. It was found that the wild-type protein occupies only one conformation upon binding to α^H chains, but in the absence of α^H chains it exists in roughly equal populations of cis and trans conformers (*470*). Also, AHSP helices 1, 2, and the loop separating them constitute the binding interface in AHSP:α^H-chain complexes (*470*). According to Santiveri et al., the three antiparallel α helices of AHSP are abnormally long and are arranged in a "right-handed twist" that has only been observed in one other protein, a prokaryotic ribosome recycling factor (*470*).

These findings were extended in a subsequent study by Feng et al. (*445*), who determined the first crystal structure of AHSP by X-ray diffraction. The crystal structure was for a complex consisting of AHSP and (oxy)α^H chains at 2.8 Å resolution (*445*). In this structure, the G and H helices of α^H chains were bound to AHSP helices 1 and 2 and the intervening loop. According to Feng et al.(*445*), the binding interface for these two proteins is similar to the $\alpha^H{}_1\beta^H{}_1$ and

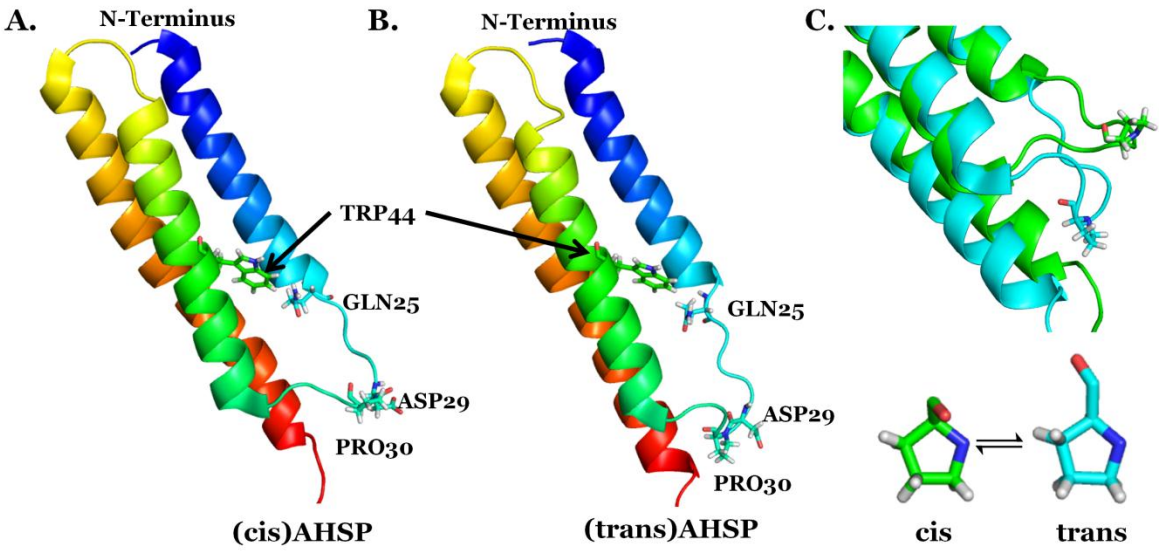

Figure 1-7. Cis and trans structural conformers of human AHSP
Human AHSP is depicted in ribbon form with several residues of interest in stick form using CPK coloring. The import of these residues is explained in Chapters 3 and 5. *Panel A* depicts (cis)AHSP, *Panel B* depicts (trans)AHSP, and Panel C depicts the two conformers which proline adopts in AHSP (bottom), as well as an overlay of the two structures after their α carbons were aligned using the built-in PyMol alignment function (Top). Most structural differences between the two conformers exist in the loop separating helices 1 and 2, and in the C-termini of each conformer. Drawings were produced using the PyMol Molecular Graphics System and PDB entries 1W0A and 1W09 (DeLano Scientific, Palo Alto, California, US)(*470*).

$\alpha^{H}_{2}\beta^{H}_{2}$ interfaces within HbA, except that $\alpha^{H}_{1}\beta^{H}_{1}$ and $\alpha^{H}_{2}\beta^{H}_{2}$ binding involves more extensive hydrogen bonding and shorter van der Waals distances than are present in AHSP:α^{H}-chain complexes (*445*). These observations support the conclusion that the binding interface for AHSP:α^{H}-chain complexes is "nonoptimal" (*445*), as well as the initial observation by Kihm et al. (*443*) that β^{H} chains appear to displace AHSP from α^{H} chains in solution when all three proteins are co-incubated.

Feng et al. (*445*) also compared the heme pockets of α^{H} chains in HbA with those in complex with AHSP, and discovered that the heme iron in

AHSP:α^H-chain complexes is coordinated by His58 instead of His87. This is unusual because in HbA, His58 (the distal histidine) is not bound to the heme at all, and ligands such as O_2 bind to iron on this side of the heme group (*107*). In the modified conformation of the crystal structure, however, ligands must bind to the opposite side of the heme if they bind at all. This alteration, along with several other changes within the binding pocket, were predicted to increase the heme group's exposure to solvent (*445*). Figure 1-8A depicts the structures reported by Feng et al. (*445*).

Feng et al. (*445*) also showed that AHSP binding induces rapid oxidation of the heme iron of (oxy)α^H chains. This finding was unexpected in light of previous work indicating that AHSP reduces the formation of reactive oxygen species (ROS) in vivo (*445*, *469*). This apparent contradiction is resolved if AHSP drives the α^H chain heme iron into a low-spin ferric state that does not permit further participation in oxidative reactions (*445*). Support for this idea was found in studies comparing absorbance and Raman spectra of α^H chains and α^H chains bound to AHSP. This work led to the hypothesis that AHSP locks α^H chains "… into an oxidized but fully liganded low-spin, non-reactive state" (*445*). Thus, according to the model presented by Feng et al. (*445*), the crystal structure of (oxy)α^H chains complexed with AHSP represents a transition state that exists before the formation of a hexacoordinated, low-spin species that is unable to participate in ROS generation (*445*).

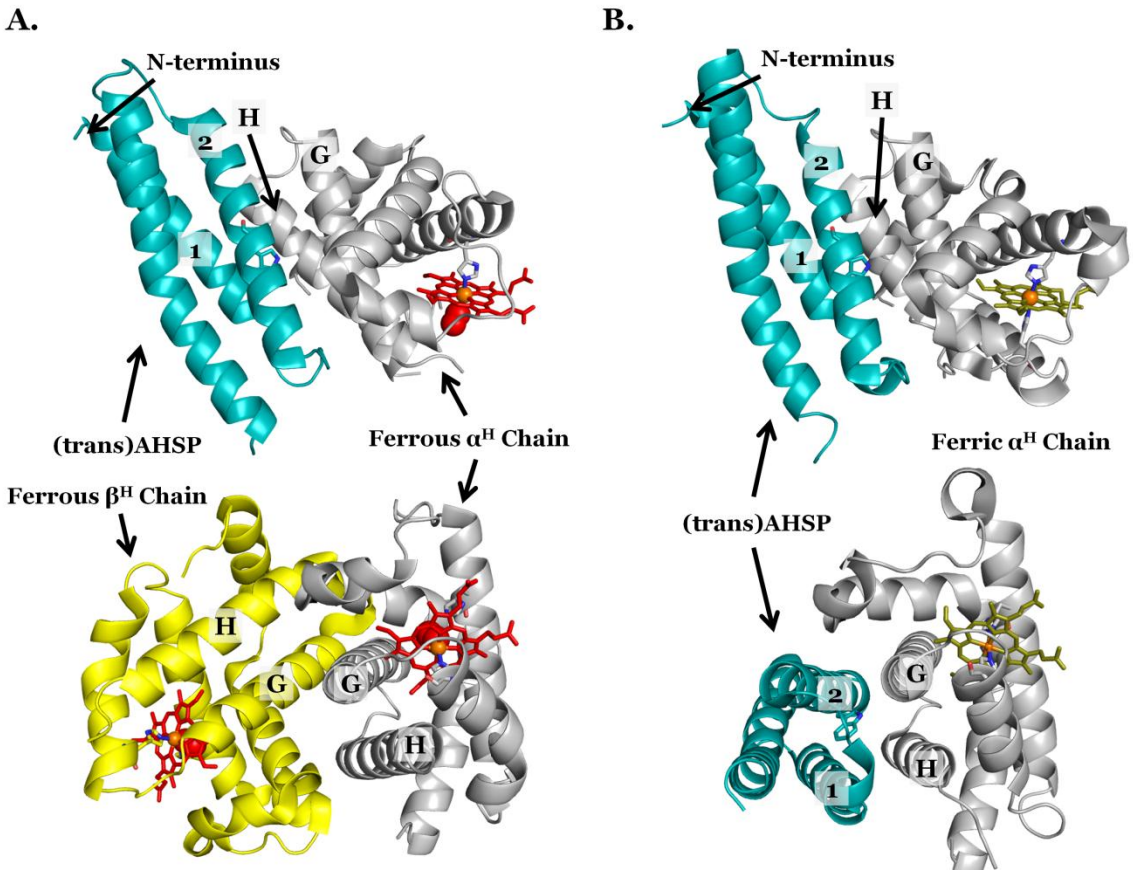

Figure 1-8. X-ray crystallographic structures of AHSP:α^H-chain complexes
Ferrous and ferric α^H chains are shown in complex with either AHSP or β^H chains. *Panel A* shows ferrous α^H chains in complex with AHSP (top) and in complex with ferrous β^H chains as part of the $\alpha^H{}_1\beta^H{}_1$ interface (bottom). Note that the F-helix is disordered in the AHSP complex and that the distal histidine is bound to the heme iron instead of the proximal histidine (top). *Panel B* shows ferric AHSP:α^H-chain complexes in two different orientations. Note that the hemin is coordinated by both the proximal and distal histidines in this state. AHSP appears in teal and hemin in olive, and the other colors, ribbon, and stick forms are the same as those used in Figure 1-1. The AHSP in these studies contained the P30A mutation, as well as a C-terminal truncation of 11 residues. Drawings were produced using the PyMol Molecular Graphics System and PDB entries 1Y01, 1Z8U, 1GZX (DeLano Scientific, Palo Alto, California, US)(*445*, *471*, *472*).

Seven months after the publication of the first crystal structure, another crystal structure was reported by these same investigators, along with several follow-up experiments (*471*). This report contained the structure of AHSP in complex with oxidized (that is, ferric) α^H chains instead of ferrous α^H chains

(*471*). Unlike the crystal structure of the oxygenated species, the ferric complex possessed a hexacoordinated hemin iron which was coordinated to both His58 and His87 (a hemichrome, or bis-histidyl conformation)(Figure 1-8)(*471*). This hexacoordination involves significant structural alterations attributable to the secondary structures surrounding the hemin group, particularly the B, C, E, F, and H helices (*471*). These findings are consistent with the investigators' previous idea that such a hexacoordinated hemin might represent a "biochemically inert state" (*445*), because this conformation inhibits hemin-H_2O_2 interactions (*471*). The hexacoordinated state of oxidized α^H chains bound to AHSP was also confirmed by electron paramagnetic resonance (EPR) spectroscopy in a more recent paper, which also provided evidence that the formation of this structure occurs spontaneously under physiological conditions (*473*).

Feng et al. (*471*) also assayed heme group sensitivity to oxidant damage by analyzing the decrease in Soret absorbance following exposure to H_2O_2. Also, tetramethyl-p-phenylenediamine (TMPD) and hydrogen peroxide were used to probe for redox reactions (*471*). Thus, both the impact of oxidants on the heme group and the impact of the heme group on oxidative reactions were observed as a function of heme iron coordination state. It was found that AHSP appears to diminish further heme iron oxidation by H_2O_2 and subsequent generation of oxidants. Also, it was shown by native gel electrophoresis that tetrameric hemoglobin can be formed using ferric AHSP:α^H-chain complexes as precursors (*471*).

The Role of AHSP During HbA Biosynthesis

There have been several studies of the impact of AHSP on rHb expression in *E. coli*-based heterologous protein production systems. One of the earliest efforts was reported by Marden and co-workers (*441*). They constructed a co-expression system which enables expression of either genetically fused GST-α^H-chains alone or in conjunction with GST-AHSP (*441*). Biochemical analyses indicated that the α^H chains purified using this system have properties almost identical to those of native α^H chains (*441*). Using this system, AHSP was found to significantly enhance soluble α^H chain production when the two proteins were co-expressed simultaneously in the presence of exogenously added hemin (*441*). When GST-α^H-chains were expressed alone, exposing the cell lysates to GST-AHSP during cell disruption did not recover any insoluble α^H chains that may have accumulated throughout the growth (*441*). The authors suggested that AHSP facilitates α^H chain production by binding newly synthesized globin and facilitating folding and heme uptake (*441*). Their study demonstrates that AHSP acts to prevent α^H chain aggregation, precipitation, and/or degradation, which is consistent with a molecular chaperone function.

Weiss and co-workers subsequently provided further evidence for AHSP chaperone activity by investigating the adverse effects of *ahsp* gene disruption in mice (*442*). Given that a small pool of free α^H chains is known to exist in erythroblasts (*148*, *474-479*), it was hypothesized that the ill effects caused by *ahsp* gene disruption might be mitigated by lowering *α globin* gene dosage (*442*). This change would reduce or eliminate the pool of free α^H chains that are unescorted by AHSP, and consequently might lessen the severity of the *ahsp*

knockout phenotype (*442*). The following strains of mutant mice were constructed to investigate this hypothesis: (a) mice lacking 1 of 4 *α globin* alleles (*α globin*$^{*\alpha/\,\alpha\alpha}$), (b) homozygous null *ahsp* mice (*ahsp*$^{-/-}$), and (c) *ahsp*$^{-/-}$, *α-globin*$^{*\alpha/\,\alpha\alpha}$ double mutants (*442*).

Surprisingly, the *α globin*$^{*\alpha/\,\alpha\alpha}$ mutation did not rescue the *ahsp*$^{-/-}$ phenotype, and the *ahsp*$^{-/-}$, *α-globin*$^{*\alpha/\,\alpha\alpha}$ mice instead exhibited more severe phenotypes than mice carrying either mutation alone (*442*). Also, the mice possessing both mutations exhibited significant amounts of β^H chain precipitation (*442*). As part of this work, Yu et al. (*442*) conducted a series of in vitro assays using recombinant AHSP. These assays showed that AHSP renders α^H chains more resistant to trypsin digestion, and that it enhances HbA production yields in an in vitro wheat-germ transcription and translation system, possibly by facilitating α^H chain folding (*442*). These findings suggest that AHSP is more than just a stabilizer of excess free α^H chains and may be an active participant in HbA production.

In a subsequent study, Dos Santos et al. (*480*) discovered that human *ahsp* gene expression is affected by the presence and absence of iron. They showed that the 3'-end of *ahsp* mRNA contains a stretch of non-coding nucleotides that are predicted to form a stem-loop structure in solution (*480*). This sequence is similar to known iron responsive elements (IREs), and the investigators hypothesized that this stem-loop might interact with iron regulatory proteins (IRPs) in a way that makes *ahsp* gene expression iron dependent (*480*). Upon investigation, IRP-IRE interactions were confirmed, and it was shown that iron disrupts these interactions and results in the

destabilization of *ahsp* mRNA (*480*). By contrast, iron depletion using the chelator desferrioxamine had the opposite effect (*480*). These data strongly suggest that *ahsp* gene expression is upregulated when iron is scarce and downregulated when iron is abundant (*480*). These findings support the idea that AHSP stabilizes free α^{O} globins which are known to build up when iron and heme are in short supply (*480*). Conversely, when intracellular iron and heme are abundant, there are fewer free α chains and therefore less of a need for AHSP, explaining IRE-mediated downregulation (*480*).

Recently, Faggiano et al. (*289*) constructed an *E. coli*-based expression system which co-expresses AHSP with a human-bovine hybrid Hb (Hb Polytaur). Hb Polytaur is a ~500 kDa Hb consisting of human α^{H} chains and bovine β^{H} chains, both of which possess mutations designed to facilitate spontaneous self-polymerization by disulfide linkages (*289*). Interestingly, co-expressing equal amounts of AHSP with this Hb results in decreased Hb expression yields (0.2 mg of Hb per L of medium, as opposed to 48 mg/L)(*289*). This finding seems inconsistent with previous data regarding AHSP function. However, the authors note that "…since Hb Polytaur is a hybrid globin, the contacts at the α-β interfaces are not as tight as they would be in the naturally occurring hemoglobins, resulting in a less effective ability of the β bovine chains to replace AHSP after binding to α human chains" (*289*).

Figure 1-9 contains a summary of what is known about AHSP function. Yu et al. (*442*) have suggested that AHSP may play a role in α^{H} chain folding and heme uptake. Such a role would be consistent with the observation that AHSP causes significant structural changes upon binding, particularly in the

area of the heme binding pocket. It is plausible that AHSP modulates the rates and affinities for heme or hemin binding to α chains. Alternatively, AHSP might ensure that heme is inserted in the correct orientation or that iron-free protoporphyrin IX is excluded from the binding pocket. Notably, AHSP and β^H chains bind to α^H chains at the same interface, making their interactions mutually exclusive, and AHSP must dissociate from α^H chains before β^H chains can bind. Thus, it appears that AHSP does not participate in the events that are downstream of $\alpha^H_1\beta^H_1$ dimer formation, but instead acts as a competitive inhibitor of HbA assembly starting from isolated α^H and β^H subunits.

Medical Relevance of AHSP

The participation of AHSP in HbA biosynthesis prompted early speculation that AHSP dysregulation may play a causative role in certain diseases (*443*). The relationships between AHSP and various thalassemia syndromes have been of particular interest. Viprakasit et al. (*481*) investigated whether variations in the apparent clinical severity of HbE β thalassemia could be explained by the presence of mutant *ahsp* alleles among affected individuals. Several single nucleotide polymorphisms (SNPs) were identified, but none of them were found to correlate with the severity of the thalassemic phenotype (*481*). Other work has shown that both healthy and thalassemic individuals may

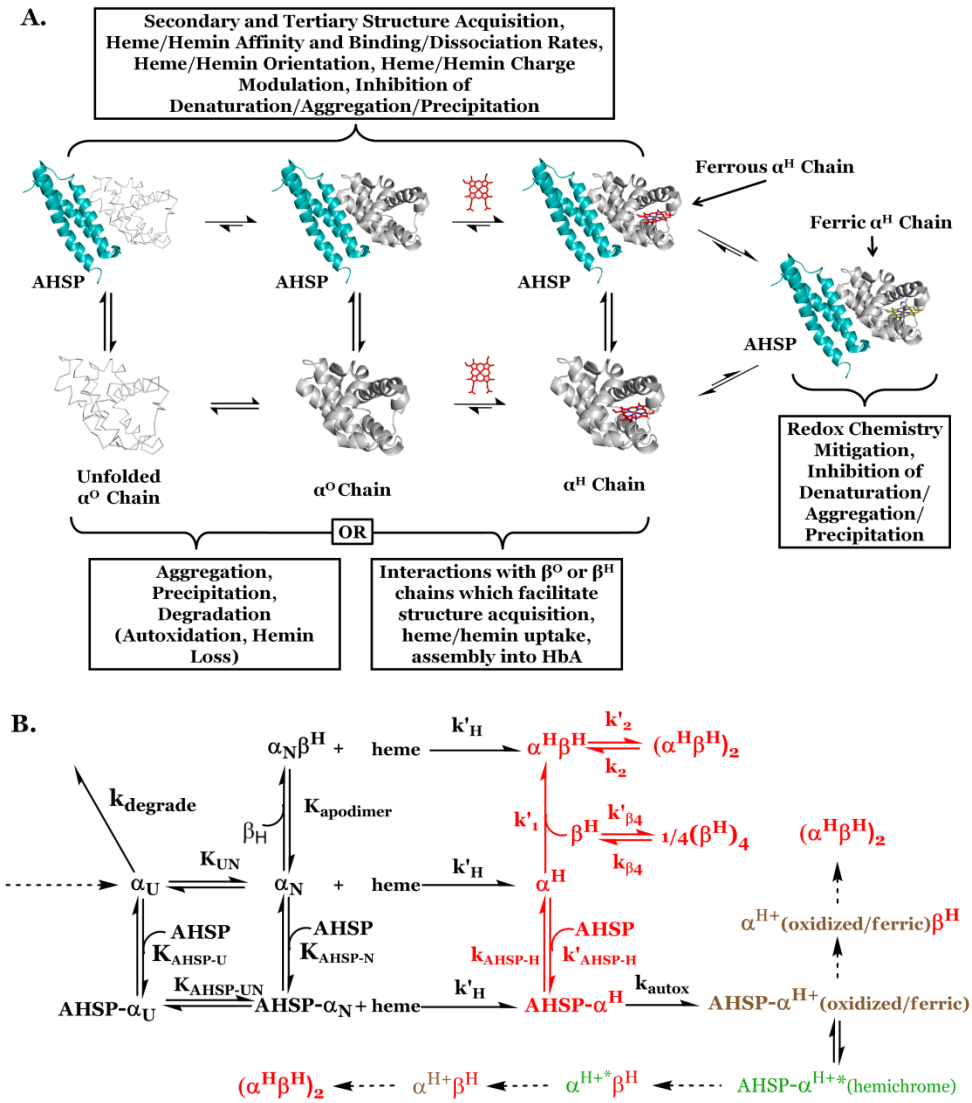

Figure 1-9. Proposed functional roles of AHSP
Panel A depicts the different roles that AHSP occupies during α^H chain biosynthesis. *Panel B* depicts a scheme which situates these events as part of the larger process of HbA biosynthesis. Colors, ribbon, and stick forms are the same as those utilized in Figure 1-8. *Panel A* was produced using the PyMol Molecular Graphics System and PDB entry 1Z8U (DeLano Scientific, Palo Alto, California, US)(*471*). *Panel B* was produced using ChemDraw Pro with significant assistance from John S. Olson.

possess an uncommon missense mutation that results in AHSP with an isoleucine at position 75 instead of an asparagine (N75I)(*470*, *482*, *483*). This mutation does not occur at the AHSP:α^H-chain interface, but initial work suggests that it may nonetheless be functionally important (*470*, *482*, *483*).

In another study, Lai et al. (*484*) have shown that *ahsp* mRNA levels in reticulocytes vary considerably in healthy individuals, and several sequence variants have been identified which affect *ahsp* transcription levels and may be linked to the phenotypic discordance observed in certain types of β thalassemia. Also, a variant in *ahsp* intron 1 has been associated with altered AHSP expression levels and occurs commonly in healthy individuals (*483*). Interestingly, certain *ahsp* alleles bearing SNPs that are thought to result in diminished AHSP expression have been linked to Heinz body-, drug-, and infection-induced hemolytic anemia (*485*). Thus, *ahsp* gene expression levels and function appear to be relevant in a variety of clinical contexts, and ongoing work in this area is likely to be informative.

Marden and co-workers have suggested that AHSP:α^H-chain interactions are impeded by a proline to serine mutation at position 119 of α^H chains (P119S; Hb Groene Hart), which results in an α thalassemia phenotype (*486*). Another α^H chain mutation, F117S (Hb Foggia), also results in a phenotype typical of α thalassemia (*487*). This mutation is predicted to disrupt favorable interactions with AHSP (*445*, *487*), and several investigators have recently looked directly at these issues by evaluating a set of clinically relevant α^H chain mutations which might exhibit impaired AHSP interactions: H103L (Bronovo), C104Y (Sallanches), C104S (Oegstgeest), T108N (Bleuland), L109R (Suan Dok), L109Q, F117S (Foggia), P119S (Groene Hart), P119L (Diamant), and L129P (Utrecht)(*440*).

Vasseur et al. (*440*) co-expressed GST-tagged wild-type AHSP with the GST-tagged mutant α^H chains listed above in *E. coli* and quantified expression

levels of these α^H chain mutants. The detection of variable amounts of soluble α^H chains demonstrates that the selected amino acid replacements may have significant effects on the stability of the AHSP:α^H-chain interface (*440*). However, the mutations selected occur in a region of the α^H chains that is part of the shared interface for binding to both AHSP and β^H chains. Thus, these results are ambiguous, and it is unclear which disrupted interactions, AHSP:α^H-chain or $\alpha^H{}_1\beta^H{}_1$, give rise to the observed phenotypes. Most recently, this group has reported the discovery and characterization of a novel AHSP mutant, V56G, which has been linked to thalassemia syndrome (*488*).

In Chapters 3 through 6, the rate constants associated with AHSP binding to and dissociation from native ferric and ferrous human α subunits are reported, along with the binding and dissociation equilibrium constants. Also, several mutant AHSP proteins were used to better define the cis-trans peptidyl-prolyl isomerization events that AHSP is known to undergo, and several naturally occurring human α subunit missense mutants were used to probe AHSP function. Additionally, several post-binding events regarding AHSP:α-subunit interactions were investigated, such as autooxidation, heme uptake, hemin loss, effects on ligand binding, and secondary structure acquisition. Finally, AHSP was co-expressed with α and β subunits in transgenic *E. coli* as a way of probing the effects of AHSP on hemoglobin production. Collectively, these investigations were undertaken to better define AHSP function in vivo.

Chapter 2: Materials, Methods, Instruments

Human AHSP Expression, Purification

AHSP was obtained using the bacterial expression vector pGEX-2T that had the human *ahsp* gene inserted into its multiple cloning site (NCBI Accession NM_016633.2 for AHSP and U13850.1 for empty vector)(*114*). This empty vector was manufactured by GE Healthcare Bio-Sciences Corporation (Piscataway, New Jersey, US). This plasmid, which will be referred to as pGEX2T-AHSP, was provided by and constructed in the Laboratory of Mitchell J. Weiss at the University of Pennsylvania (*443*, *444*). The coding regions were sequenced upon receipt using sequencing primers that were designed by the manufacturer and synthesized by Integrated DNA Technologies, Inc. (Coralville, Iowa, US) (5'-CCG GGA GCT GCA TGT GTC AGA GG-3' and 5'-GGG CTG GCA AGC CAC GTT TGG TG-3'). The human *ahsp* gene in this vector was not optimized for *E. coli* codon bias. Sequencing reactions for these and other reactions were performed by Lone Star Laboratories, Incorporated (Houston, Texas, US). Glycerol stocks of DH5α cells were prepared to maintain pGEX2T-AHSP and other plasmids using the methods outlined in Sambrook et al. (*489*). The cells purchased from Invitrogen Corporation (Carlsbad, California, US). Unless otherwise noted, the molecular biology protocols set forth in Sambrook et al. (*489*) were used throughout this work.

The pGEX2T-AHSP vector consists of *ahsp* that had been cloned downstream and in the correct reading frame of the S. japonicum *glutathione S-transferase* (*gst*) gene (NCBI Accession U13850.1, region 258..956)(*114*). The AHSP protein produced from this vector has GST protein appended to its N-

terminus. The theoretical molecular masses of these proteins are 26,986.32 Da in the case of GST and 11,840.42 Da in the case of AHSP, giving GST-AHSP a total molecular mass of ~38,826.74 Da according to the ExPASy Proteomics Server and known protein sequences (http://expasy.org/tools/ pi_tool.html; NCBI Accession U13850.1 and NM_016633.2)(*114*). GST can be freed from AHSP using thrombin protease, although this leaves a gly-ser dipeptide appended to the N-terminus of the resulting AHSP protein due to the protease recognition site. This vector contains a pBR322 origin of replication, confers ampicillin resistance upon its host, and expresses GST-AHSP under the control of a tac promoter. It is approximately 5,200 base pairs in length with the *ahsp* insert.

Several components of this work involved the use of recombinant AHSP mutants. These mutants were generated using the QuikChange II Site-Directed Mutagenesis Kit (Stratagene Corporation, La Jolla, California, US, later acquired by Agilent Technologies, Incorporated, Santa Clara, California, US)(*490*). $AHSP^{P30A}$ was generated using the following mutagenic primers (emboldened codons indicate the region of mutation): 5'-CTG AAT CAG CAG GTC TTC AAT GAT **GCG** CTC GTC TCT GAA GAA GAC-3' and 5'-GTC TTC TTC AGA GAC GAG **CGC** ATC ATT GAA GAC CTG CTG ATT CAG-3'. $AHSP^{P30W}$ was generated using these primers: 5'-GTC TTC TTC AGA GAC GAG **CCA** ATC ATT GAA GAC CTG CTG ATT CAG -3' and 5'-CTG AAT CAG CAG GTC TTC AAT GAT **TGG** CTC GTC TCT GAA GAA GAC-3'. $AHSP^{D29R}$ was generated using these primers: 5'-AAT CAG CAG GTC TTC AAT **CGT** CCT CTC GTC TCT GAA GAA G-3' and 5'- C TTC TTC AGA GAC GAG AGG **ACG** ATT GAA GAC CTG

CTG ATT-3'. AHSP^{Q25K} was generated using these primers: 5'-C AGC GTT CTG CTG AAT CAG **AAG** GTC TTC AAT GAT CCT CTC-3' and 5'-GAG AGG ATC ATT GAA GAC **CTT** CTG ATT CAG CAG AAC GCT G-3'. Site-directed mutagenesis reactions were carried out in accordance with instructions provided by the manufacturer (*490*), and sequences were verified and glycerol stocks prepared using the methods described above.

AHSP expression was performed in *E. coli* BL21 cells using protocols initially developed in the Laboratory of Mitchell J. Weiss. This protocol is summarized as follows.

BL21 cells were purchased from Agilent Technologies, Incorporated (Santa Clara, California, US). Chemically competent BL21 cells were first transformed with pGEX2T-AHSP in accordance with vendor transformation guidelines (*491*). After transformation, cells were plated on Luria-Bertani (LB) agar plates with 100 μg/mL of ampicillin and incubated overnight at 37 ^{O}C. Following overnight incubation, a single colony was used to inoculate a 1 L Erlenmeyer flask containing 250 mL of sterile 2x YT medium containing 100 μg/mL of ampicillin. This culture was grown at 37 ^{O}C with shaking at 225 revolutions per minute (RPM) overnight before being evenly and aseptically distributed into six, 4 L Erlenmeyer flasks, each of which contained 1 L of sterile 2X YT medium with 100 μg/mL of ampicillin.

Cultures were grown at 37 ^{O}C at 225 RPM until the optical absorbance at 600 nm reached 0.8 to 1.0, at which time the culture temperatures were dropped to 32 ^{O}C and were induced with 1.0 mM isopropyl β-D-1-thiogalactopyranoside (IPTG) for 6 hours before harvesting by centrifugation at

10,000 x g for 40 minutes at 4 ^{O}C. The cells were resuspended in approximately 200 mL of ice cold phosphate buffered saline (PBS) solution (140 mM NaCl, 3 mM KCl, 10 mM Na_2HPO_4, 2 mM KH_2PO_4, pH 7.4 at 20 ^{O}C), and were disrupted using an Emulsiflex-C5 high pressure homogenizer (Avestin, Ottowa, Ontario, Canada). The lysate was then centrifuged to remove cell debris, and the supernatant was passed through a 0.2 μm filter (Fisher Scientific, Pittsburgh, Pennsylvania, US).

The soluble GST-AHSP present in the supernatant was captured using approximately 50 mL of Glutathione Sepharose High Performance (HP) resin in accordance with manufacturer instructions (GE Healthcare Bio-Sciences Corporation, Piscataway, New Jersey, US). During this process, PBS was used as a binding and wash buffer, and 50 mM Tris-HCL with 10 mM reduced glutathione, pH 8.0 at 4 ^{O}C, was used as an elution buffer. This step of the purification was performed using either a gravity-fed column or one that was equipped with a Masterflex peristaltic pump (Cole Parmer, Vernon Hills, Illinois, US). Clarified lysate was applied to the column and washed until the optical absorbance of the flow-through in the middle ultraviolet (UV) range (200-300 nm) matched that of the binding and wash buffer. Then, elution of AHSP was followed by monitoring light absorbance at 280 nm of various fractions of the flow-through.

Without concentrating or buffer exchanging the eluate, GST was cleaved from AHSP using 500 units of thrombin in an overnight incubation at room temperature with mild agitation. The thrombin was obtained from GE Healthcare Bio-Sciences Corporation (Piscataway, New Jersey, US), and

manufacturer literature defines one unit of thrombin as capable of digesting >90% of 100 μg of test fusion protein in 16 hours at 22 ^{O}C (*492*). Following digestion, the reduced glutathione, free GST, thrombin, and untagged AHSP were dialyzed exhaustively against PBS buffer at 4 ^{O}C to remove the reduced glutathione. Then, the solution was again passed through the Glutathione Sepharose HP resin to remove as much free GST and uncleaved GST-AHSP as possible. Lastly, thrombin, residual GST, residual GST-AHSP, and un-tagged AHSP were resolved by size exclusion chromatography using a preparative grade Superdex 75 prepacked column and an ÄKTA fast protein liquid chromatography (FPLC) system (GE Healthcare Bio-Sciences Corporation, Piscataway, New Jersey, US). A representative sodium dodecyl sulfate polyacrylamide gel electrophoresis (SDS-PAGE) gel of the various purification fractions are show in Figure 2-1.

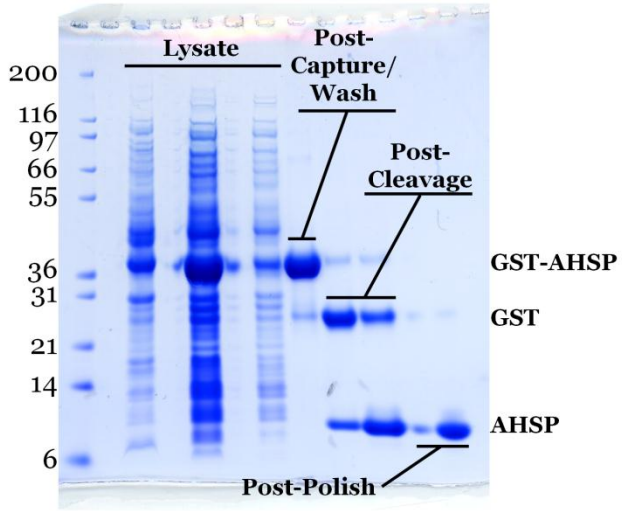

Figure 2-1. AHSP purification stages
The materials used in the preparation of this SDS-PAGE gel were obtained from Invitrogen Corporation (Carlsbad, California, US). The numbers listed on the left side of the gel are molecular masses in kDa. This marker was Mark 12 Unstained Standard, and the gel was a pre-cast NuPAGE 4-12% bis-tris gel that was run in MES running buffer and stained with Coomassie stain.

All solutions and buffers were maintained at 4 ^{O}C throughout the purification. Approximately 6 L of bacterial culture yielded approximately 100 mg of fusion protein. AHSP was remarkably stable throughout all purification steps, and protein was stored at -80 ^{O}C in PBS buffer.

The experimentally determined molar extinction coefficients used to determine the concentrations of wild-type AHSP were 10,825 M^{-1} cm^{-1} at 280 nm in 6 M guanidinium HCl, and 12,300 M^{-1} cm^{-1} at 280 nm in H_2O (provided by David Gell at the University of Sydney, personal correspondence). The mutant AHSP protein molar extinction coefficients were calculated using the ExPASy Proteomics Server (http://expasy.org/tools/ protparam.html). This tool revealed that $AHSP^{WT}$, $AHSP^{P30A}$, $AHSP^{D29R}$, and $AHSP^{Q25K}$ all are predicted to share the same extinction coefficient of 11,460 M^{-1} cm^{-1} at 280 nm in H_2O. Since the value provided by David Gell was experimentally determined, it was used over the theoretical value for concentration determinations for wild-type AHSP and these mutants. However, the presence of an extra tryptophan in $AHSP^{P30W}$ resulted in an increased theoretical molar extinction coefficient of 16,960 M^{-1} cm^{-1} at 280 nm in H_2O. This value was used in this work rather than an experimentally determined one.

To clone the *ahsp* gene into pBAD33, the pGEM-T Vector System was utilized (Promega Corporation, Madison, Wisconsin, US). Additionally, the following primers were used: 5' TAT GGT ACC AGG AGG AAT TCA CCA TGG CTC TTC TTA AGG CC 3' and 5' GGC ATG CGA TAA GCT TCT AGG AGG AGG GCG GTG G 3'. Co-transformations were accomplished using the Z-Competent

E. coli Transformation Kit that was purchased from Zymo Research Corporation (Irvine, California, US).

Native Wild-Type Adult Human Hemoglobin Purification

HbA was obtained from expired units of human blood or PRBCs that were purchased from the Gulf Coast Regional Blood Center (Houston, Texas, US). HbA was purified using established methods (*493*). Briefly, erythrocytes from PRBCs were washed several times with a solution of 0.9% NaCl and resuspended in an equal volume of cold, deionized water that had been saturated with CO prior to its use. The suspension was incubated at 4 ^{O}C overnight to induce osmotic lysis. The NaCl concentration of the solution was then increased to 3% (w/v), after which it was clarified by centrifugation at 10,000 x g for 60 minutes at 4°C. The supernatant was then dialyzed exhaustively against 30 mM Na_2HPO_4 at 4 ^{O}C. Bound 2,3-bisphosphoglyceric acid (BPG) was removed from the HbA by buffer exchanging the solution into 10 mM Tris-HCL, 100 mM NaCl, pH 8.0 using a Sephadex G-25 column. HbA was stored in liquid N_2 in the CO-bound form in 100 mM sodium or potassium phosphate buffer, pH 7.4 at 4 ^{O}C, when it was not being used.

To convert CO-bound HbA to O_2-bound HbA, solutions of Hb were placed in a round bottom flask, which was rotated and partially submerged in an ice water bath while being exposed to a strong light source and pure O_2 gas. Periodically the absorbance spectrum of the sample was monitored to follow the conversion to the O_2-bound form. To deoxygenate the protein, a concentrated solution of O_2-bound HbA was diluted into a buffer that had been thoroughly

bubbled with pure argon or nitrogen gas. Then, excess sodium dithionite (DT) was added to the solution and optical absorption spectroscopy was used to verify that the protein was completely deoxygenated. To oxidize the protein, equimolar amounts of potassium ferricyanide were added to CO- or O_2-bound HbA or isolated subunits, and optical absorbance was again used to monitor the transition to the ferric state. Alternatively, vast excess amounts of potassium ferricyanide were added to a sample, after which it was incubated at 4 ^{O}C for 20 to 30 minutes before using a Sephadex G-25 column to remove the excess potassium ferricyanide. Known molar extinction coefficients and optical absorbance maxima and minima in the visible and ultraviolet ranges were used to determine HbA, α^{H} chain, and β^{H} chain concentrations and ligand binding and oxidation state (*494-496*).

Alpha, Beta Subunit Isolation

HbA subunits were also isolated using previously developed methods which will be summarized here (*194*, *195*, *497*). CO-bound HbA was first buffer exchanged into 10 mM KH_2PO_4, 80 mM NaCl buffer at 4 ^{O}C. Then, the protein was concentrated to approximately 1.6 mM HbA on a per tetramer basis. In a separate solution, enough ρ-hydroxymercuribenzoate (PMB) was dissolved in 1 mL of 0.1 N NaOH to give at least a six fold molar excess of PMB over HbA. For approximately 10 mL of a 1.6 mM HbA solution, this amounts to approximately 35 mg of PMB. Then, small amounts of 1 M acetic acid were added to the PMB solution with vigorous agitation until the formation of a very small amount of white precipitate was observed. The entirety of this solution was then added to

the 10 mL HbA solution, and the pH of the resulting mixture was adjusted to 6.2 using 1 M acetic acid. This solution was allowed to stand at 4 ^{O}C overnight in a stoppered Erlenmeyer flask whose headspace was filled with CO. This amount of PMB causes the HbA cysteines, which occur at the inter-subunit interfaces, to react with PMB and split the HbA into individual subunits.

The next morning, the solution was passed through a gravity fed Sephadex G-25 column to exchange the solution into 10 mM potassium phosphate buffer, pH 8.0 at 4 ^{O}C. The resulting solution was then concentrated to a small volume (<15 mL) and applied to a diethylaminoethyl (DEAE) column that was previously equilibrated with the same buffer. The α^{H} chains elute from this column under these buffer conditions, whereas the β^{H} chains and tetrameric HbA are retained by the resin. HbA was subsequently eluted by transitioning the buffer to 20 mM potassium phosphate buffer, pH 7.5 at 4 ^{O}C, and then the β^{H} chains were eluted from the resin by again transitioning to 100 mM potassium phosphate, pH 7.0 at 4 ^{O}C. The HbA fraction was discarded, and the α^{H} and β^{H} chain fractions were then buffer exchanged into 20 mM potassium phosphate buffer, pH 7.4 at 4 ^{O}C. All these purification steps were performed at 4 ^{O}C using buffers that were saturated with CO prior to use in order to diminish heme iron oxidation.

The α^{H} and β^{H} chains produced using this procedure have PMB reacted with their cysteine groups at the end of the protocol, and it was necessary to remove the PMB groups so that subunit re-assembly events could be studied in vitro. Removal was accomplished using a modified version of the method reported by Geraci et al. (*195*). Briefly, the isolated chains were incubated with a

10-fold molar excess of β-mercaptoethanol (BME) on ice for approximately 30 minutes. Then, the solutions were buffer exchanged into 100 mM potassium phosphate buffer, pH 7.4 at 4 ^{O}C, using a gravity fed Sephadex G-25 column. Depending on the results of the assay described in the next paragraph, this procedure was repeated several times in order to ensure the complete removal of all PMB groups from the chains.

To confirm the removal of the PMB groups, a Boyer titration was performed (*498*). This method involves titrating sub-stoichiometric amounts of PMB into dilute solutions of either α^{H} or β^{H} chains of a known concentration and monitoring optical absorbance spectral changes at 255 nm (*498*). Changes at this wavelength report on mercaptide bond formation between cysteines and PMB (*498*). Alpha chains have one cysteine and β^{H} chains have two cysteines, and incrementally increasing the titer of PMB up until the point of equimolarity results in absorbance increases at 255 nm. Once cysteine:PMB equimolarity is reached, no further increases in absorbance are observed. After PMB removal was established using this method, the purities of the isolated α^{H} and β^{H} chains were verified by cellulose acetate electrophoresis (CAE). This method separates α^{H} and β^{H} chains on the basis of charge. Because isolated chains are approximately the same molecular mass, this method is more suitable than SDS-PAGE gel analysis. Figure 2-2 contains representative data for a Boyer titration and a CAE analysis.

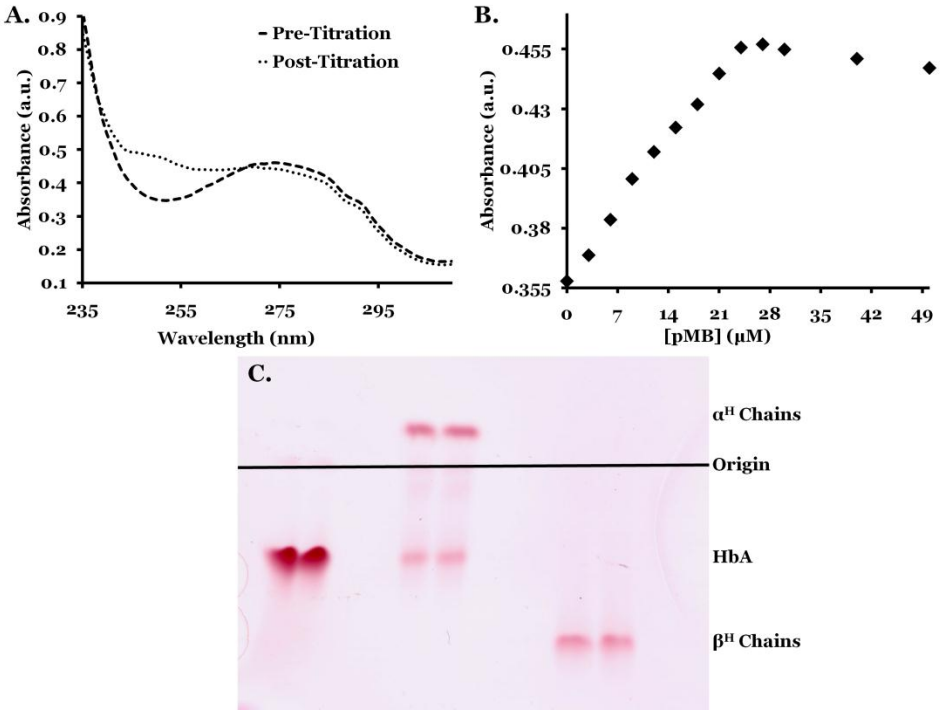

Figure 2-2. Boyer titration, subunit purity determination
Panel A, spectra of β^H chains before and after Boyer titration. *Panel B*, absorbance changes at 255 nm plotted against PMB concentration. In *Panel B*, β^H chain concentration was 12 μM, giving cysteine concentration of 24 μM. Panel C, CAE membrane. The slight HbA contamination in the α^H chain sample indicated that re-purification was necessary. Materials, buffers and apparatus for the CAE membrane were obtained from Helena Laboratories, Incorporated (Beaumont, Texas, US). Proteins were stained with Ponceau S stain. Plots were generated using Microsoft Excel (Microsoft Corporation, Redmond, Washington, US).

Heme Extraction from Isolated Subunits

Preparation of α^O and β^O chains was done using the acid-acetone method that is described elsewhere (*172*, *173*, *192*, *499*). Samples containing 5 mL of 1 mM ferric chains were exhaustively dialyzed against cold water. Care was taken during this step to prevent rupture of the dialysis bags due to the large osmotic pressure differential between the initial contents of the dialysis bag and pure water. Although desalting columns were attempted, the total absence of salt

caused the protein to interact with the gel filtration resin, leading to appreciable band spreading during sample migration through the column. After all salts were removed, the ferric Hb solution was then added dropwise to a 200 mL volume of acetone containing 5 mM HCl which was previously been cooled to at least -20 ^{O}C using a dry ice-ethanol bath. Following the addition of the protein, hemin remained in solution while globin formed a white precipitate. The solution was then centrifuged at 5,000 RPM at -20 ^{O}C for 30 minutes using glass centrifuge tubes to collect the precipitate. The hemin-containing solution was then removed and the precipitate resuspended in a small volume of cold water. This solution was then dialyzed into 50 mM potassium phosphate buffer, pH 7.4 at 4 ^{O}C. Precipitation usually occurred at this stage, often to an appreciable extent, and these aggregates were removed prior to storage by brief centrifugation using an Eppendorf centrifuge (Hamburg, DE) at 4 ^{O}C. Both α^{O} and β^{O} chains are highly unstable at temperatures above 5 to 7 ^{O}C in most dilute aqueous buffers. Occasionally, the above steps needed to be repeated to remove residual hemin.

Recombinant HbA and HbF Production, Mutagenesis

Recombinant HbA and HbF were produced using an expression system developed by Shen (*213*, *216*) and Hoffman (*211*). In this system, JM109 cells are transformed with an Hb-expression plasmid, either pHE2 for HbA or pHE9 for HbF (pHE2 was provided by C. Ho and T-J. Shen, Carnegie Mellon University, Pittsburgh, Pennsylvania, US; and pHE9 was provided by K. Adachi, The Children's Hospital of Philadelphia, Philadelphia, Pennsylvania, US). These

plasmids are very similar to each other, and each contains a single globin expression cassette which bears codon-optimized sequences which encode α and β globin proteins for HbA expression, and α and γ globin proteins for HbF expression. Individual globins are expressed as separate polypeptides from a single transcript under the control of a tac promoter. These vectors confer ampicillin resistance upon their host. They also express methionine amino peptidase (MAP), which cleaves the N-terminal methionine residue from each globin chain to produce recombinant Hb that is "essentially identical" to native Hb (*213*, *216*).

Several mutants were prepared using the same methods as described above for AHSP. Specifically, $HbA^{\alpha K99E}$ was produced using the primers: 5'-CCG GTT AAC TTC **GAA** CTG CTG TCT CAC TGC C-3' and 5'- GGC AGT GAG ACA GCA **GTT** CGA AGT TAA CCG G-3'. Also, $HbF^{\gamma V67M}$ was produced using the primers: 5'- GTC AAG GCA CAT GGC AAG AAG **ATG** CTG ACT TCC TTG GGA GAT GCC-3' and 5'-GGC ATC TCC CAA GGA AGT CAG **CAT** CTT CTT GCC ATG TGC CTT GAC-3'.

Both HbA and HbF expression were performed by flask fermentation using a protocol that was provided to the Olson Laboratory by Nancy Ho from the Department of Biological Sciences at Carnegie Mellon University (personal correspondence between Jayashree Soman and Nancy Ho). According to this protocol, following the transformation of pHE2 or pHE9 into JM109 cells that were purchased from Agilent Technologies, Incorporated (Santa Clara, California, US), a single colony was used to inoculate a 5 mL pre-culture consisting of LB media with 100 μg/mL ampicillin. After approximately eight

hours of growth at 32 ^{O}C, 225 RPM, the entirety of this pre-culture was used to inoculate two, 1 L flasks, each containing 250 mL of sterile terrific broth (TB) media with 100 μg/mL ampicillin (2.5 mL of pre-culture per flask). These cultures were grown overnight at 32 ^{O}C at 225 RPM, and the next morning they were split aseptically into six, 4 L Erlenmeyer flasks, each of which contained 500 mL of sterile TB media with 100 μg/mL ampicillin. For inoculation at this stage, 50 mL of culture were utilized per each 4 L flask, giving an initial optical absorbance at 600 nm of approximately 0.6-1.0 arbitrary absorbance units (a.u.). These cultures were grown under the same conditions for approximately 6 hours post inoculation before protein expression was induced with 50 mg/mL IPTG. At the time of induction, the temperature was dropped to 32 ^{O}C, and 50 mg/L hemin was added to the media. Harvesting by centrifugation at 10,000 x g for 45 minutes at 4 ^{O}C occurred approximately four hours post-induction.

Purification of HbF and HbA was also performed using methods which were developed by others (*500*, *501*). This method will be summarized briefly here. After harvesting, the cell pellet was resuspended in approximately 100 mL of 40 mM Tris-HCL, pH 8.6 at 4 ^{O}C, with 1 mM benzamidine, and then the cells were disrupted using an Emulsiflex-C5 high pressure homogenizer (Avestin, Ottowa, Ontario, Canada). The lysate was then placed in an Erlenmeyer flask, and the headspace of this flask was gassed with CO and stoppered. The flask was allowed to stand overnight at 30 ^{O}C with no agitation to facilitate contaminant precipitation. The next morning, the lysate was clarified by centrifugation at 10,000 x g for 40 minutes at 4 ^{O}C and passed through a 0.2 μm filter (Fisher Scientific, Pittsburgh, Pennsylvania, US). This clarified lysate

was then applied to an immobilized metal ion affinity chelating (IMAC) column equipped with a Masterflex peristaltic pump (Cole Parmer, Vernon Hills, Illinois, US). The column had been packed with Chelating Sepharose HP media and was charged with zinc acetate and equilibrated in accordance with manufacturer instructions before use. All buffers were bubbled with CO prior to their use and this and subsequent steps of the purification were all performed at 4 ^{O}C.

During and following the application of the clarified lysate to the column, the flow rates utilized were consistently near the upper limits of those that were recommended by the manufacturer. The dark red protein bound to the resin, and the following wash steps were performed: (1) 3 column volumes of 20 mM Tris-HCL, 500 mM NaCl, pH 8.5 at 4 ^{O}C, (2) 2 column volumes of 200 mM Tris-HCL, pH 8.5 at 4 ^{O}C, and (3) 3 column volumes of 20 mM Tris-HCL, pH 8.5 at 4 ^{O}C. Then, the HbA or HbF was eluted using 20 mM Tris-HCL, 15 mM EDTA, pH 8.5 at 4 ^{O}C. Each successive wash removed impurities which were discarded.

Although the HbA and HbF was generally >90% pure following the completion of these steps, two more columns were routinely utilized to remove residual contaminants, a SOURCE 15Q and a SOURCE 15S column. These columns were successively used in accordance with the methods described by Hoffman et al. (*211*).

Mass Spectrometry

Following wild-type and mutant AHSP purification, an AHSP SDS-PAGE gel band was cut out and sent for liquid chromatography-mass spectrometry analysis (LC-MS/MS) at ProTech, Inc. (Norristown, Pennsylvania, US). This technique, along with matrix-assisted laser desorption/ionization time of flight (MALDI-TOF) mass spectrometry experiments performed on campus, confirmed the identity of AHSP. Also, HbF, mutated HbF, α^{H} and β^{H} chain identity and purity was assayed by MALDI-TOF mass spectrometry as well.

Instrumentation, Materials

Manual mixing spectrophotometry was done using either a Cary 50Bio (Varian, Incorporated, Palo Alto, California, US) or a UV2401PC spectrophotometer (Shimadzu, Incorporated, Columbia, Maryland, US) using cuvettes purchased from Starna Cells (Atascadero, California, US). CD spectropolarimetry was measured in a Jasco J-810 spectropolarimeter. Stopped-flow spectrophotometry was done using either a modified Durrum Model D-110 (Palo Alto, California, US) or an Applied Photophysics PiStar CD and fluorescence stopped-flow spectrophotometer (Leatherhead, Surrey, UK). Glass syringes were used whenever possible in the stopped-flow experiments to prevent atmospheric gas contamination (Cadence Science, Lincoln, Rhode Island, US), and all buffers, salts, and media components used for these experiments were obtained from either Sigma-Aldrich (St. Louis, Missouri, US) or Fisher Scientific (Pittsburgh, Pennsylvania, US). During the fluorescence stopped-flow experiments, a 302 nm cutoff filter was utilized to monitor total

fluorescence upon excitation at 280 nm. Unless otherwise noted, the resins utilized in the purifications described above were obtained from GE Healthcare Bio-Sciences Corporation (Piscataway, New Jersey, US).

Chapter 3: AHSP Binding to and Dissociation from Human Alpha Chains

Although two previously reported studies have examined the rates and equilibria of α^H chain binding to and dissociation from AHSP (*1, 488*), neither of these studies were comprehensive in terms of detailed mechanisms. It is important to fully characterize these reactions because doing so will inform our understanding as to which pathways are the dominant routes for HbA subunit assembly (Figure 1-9B). In the experiments presented in this chapter, various forms of α^H chains were mixed with AHSP to measure bimolecular association rate constants, and AHSP:α^H-chain complexes were mixed with excess β^H chains to measure the rate constants for AHSP:α^H-chain dissociation.

AHSP, Alpha Chain Association

Wild-type human AHSP exhibits intrinsic fluorescence in solution due to the presence of one tryptophan and four tyrosines, several of which are located at the AHSP:α^H-chain binding interface (*502*). Although individual α^H and β^H chains contain numerous aromatic residues (48 per HbA tetramer, with 1.5 tryptophans per subunit), neither of these subunits exhibit strong intrinsic fluorescence due to highly efficient energy transfer between their aromatic residues and the heme prosthetic groups (fluorescence quenching has been estimated at >99% for α^H chains and ~98% for β^H chains)(*503, 504*). When AHSP is bound to an α^H chain, this energy transfer quenches intrinsic AHSP fluorescence (*502*). The key residue is AHSP Trp44 (*502*), which occurs in helix

2, is solvent-exposed in unbound AHSP, but becomes buried when this protein binds to an α^H chain (Figures 1-6, 1-7, and 1-8)(*445*).

Figure 3-1 depicts several experiments which expand on the early work of Baudin-Creuza et al. (*502*) on intrinsic AHSP fluorescence. Figures 3-1A and 3-1B show that upon excitation with light at 280 nm, AHSP fluoresces in solution, whereas α^H and β^H chains do not. These panels also show that adding an equimolar amount of α^H chains to a solution of AHSP greatly diminishes the apparent intrinsic fluorescence of AHSP (Panel A). To a lesser extent, β^H chains exert the same effect (Panel B), which in this case is probably not due to direct binding but to an inner filter effect as a result of the β^H chains absorbing some of the exciting light. Panel C shows the fluorescence intensity of AHSP as it is titrated into the following solutions: (1) buffer alone, (2) buffer containing 15 μM α^H chains, and (3) buffer containing 15 μM β^H chains. As AHSP is titrated into solutions of α^H chains, its intrinsic fluorescence signal is silenced up to the point of AHSP and α^H chain equimolarity. Then, further increases in AHSP concentration result in a linear increase in fluorescence emission intensity. By contrast, this initial fluorescence signal silencing is completely absent in the titration involving β^H chains, and there is a linear signal increase throughout the titration as AHSP is added to the β^H chain solution.

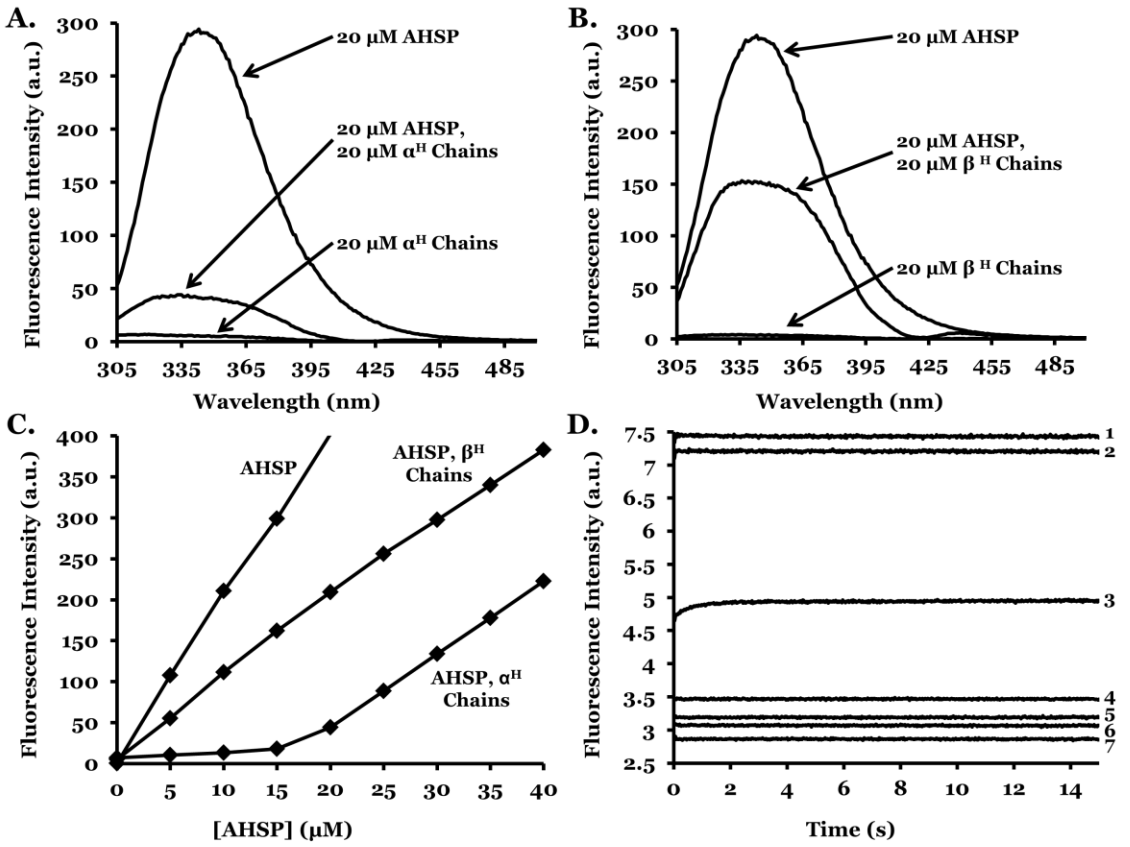

Figure 3-1. Intrinsic fluorescence emission of AHSP, α^H chains, β^H chains
The buffer utilized for these experiments was 50 mM potassium phosphate, pH 7.0 at 21 ^{O}C, which had been saturated with CO prior to use. For *Panels A-C*, the entrance and exit slits on the instrument were both set to 5 nm, and each scan was recorded over the course of less than one minute to avoid photobleaching. A Cary Eclipse scanning fluorescence spectrophotometer was used to collect these data using default settings unless otherwise noted (Agilent Technologies Inc., Santa Clara, California, US). *Panel C* plots emission intensity maxima at 350 nm and not total integrated values. *Panel D* documents the following reactions: (1) 250 nM AHSP + 250 nM β^H chains, (2) 250 nM AHSP + buffer, (3) 250 nM AHSP with 250 nM α^H chains + buffer, (4) 250 nM α^H chains + 250 nM β^H chains, (5) 250 nM α^H chains + buffer, (6) 250 nM β^H chains + buffer, and (7) buffer + buffer. The fluorescence increase observed in trace (3) is due to a small amount of dissociation of the AHSP:α^H-chain complex following rapid dilution. Excitation for all experiments occurred at 280 nm. Concentrations listed here are post-mixing values. For stopped-flow experiments, instrument slits were set to 5 nm, entrance and exit, and 1000 to 3000 data points were collected during symmetric mixing mode using a total shot volume of 150 µL. Plots were generated using Microsoft Excel and PowerPoint (Microsoft Corporation, Redmond, Washington, US).

Baudin-Creuza et al. (2004) were the first investigators to report that fluorescence quenching during co-incubation of AHSP with α^H chains is due to

the formation of a complex between the two proteins (*502*). They proposed a simple bimolecular binding mechanism

$$AHSP^{*} + \alpha^{H}\ Chain^{\varnothing} \rightleftharpoons AHSP{:}\alpha^{H}\text{-}Chain^{\varnothing} \qquad \text{(Scheme 3-1)}$$

where (*) indicates fluorescence emission and ($^{\varnothing}$) indicates the absence of a fluorescence signal.

Fluorescence quenching is a useful method of studying protein-protein binding (*505*), particularly when one of the partners is a heme protein. For example, the binding of haptoglobin to $\alpha^{H}_{1}\beta^{H}_{1}$ dimers results in a strong quenching of intrinsic haptoglobin fluorescence (*506*, *507*). Also, fluorescence quenching has been shown to report on the binding of a fluorescent 2,3-bisphosphoglyceric acid (BPG) analog to HbA (*506*, *507*). Based on how heme groups quench fluorescence emissions (*503*), it seems clear that the loss of AHSP fluorescence signal observed in Figure 3-1A corresponds to a binding event.

This idea is confirmed by the data in Panel C, which show that the AHSP fluorescence signal loss caused by α^{H} chains only appears to occur when AHSP is present in equal or sub-stoichiometric amounts. Because AHSP and α^{H} chains associate with each other in a one-to-one stoichiometry (*443*, *444*), the signal increases observed when AHSP is in excess are likely due to the fluorescence of free, unbound AHSP.

Based on comparisons of just Panels A and B of Figure 3-1, it is plausible that β^{H} chains could also bind to AHSP. The lack of complete fluorescence

signal silencing in Panel B could mean that β^H chains might have a lower affinity for AHSP, or that AHSP:β^H-chain complexes are capable of greater intrinsic fluorescence than AHSP:α^H-chain complexes. However, previous electrophoresis and gel filtration studies have consistently indicated that β^H chains do not bind to AHSP (*443*, *444*), and the titration data in Panel C support these studies.

The cause of the apparent loss in fluorescence signal in Figure 3-1B is due to the absorbance of incident excitation light by β^H chains (an inner filter effect). This conclusion is supported by the slopes of the lines in Panel C. The titration of free AHSP into solution by itself results in larger fluorescence signals than the titration of AHSP into the solution of β^H chains. The linear nature of these fluorescence increases suggest that the β^H chains do not interact with AHSP, but rather mask AHSP intrinsic fluorescence by absorbing incident light. If these two proteins were interacting, the initial part of the titration curve involving β^H chains would be expected to exhibit no fluorescence or at least a smaller slope, as was observed with the titration involving α^H chains. Thus, these fluorescence data support previous data (*443*, *444*) which suggest that β^H chains and AHSP are non-interacting species.

Figure 3-1D shows the results of several preliminary fluorescence emission stopped-flow mixing reactions which were undertaken to determine rates of α^H chain binding to AHSP. Equal volumes of AHSP and α^H chains, β^H chains, or solvent were mixed together rapidly and the total fluorescence emission signal of the mixture was recorded as a function of time. Multiple controls were examined to confirm that AHSP, α^H chains, and β^H chains do not

denature, aggregate, precipitate, oxidize, lose their prosthetic groups, photobleach, and/or otherwise react in a way which gives rise to fluorescence signal changes that could be misinterpreted as binding events following their rapid dilution in solvent. These dilution controls were essential to provide evidence that the observed fluorescence changes recorded on mixing AHSP with α^H chains are due to binding and not denaturation and light scattering.

The data in Figure 3-1D, are consistent with the fluorescence properties that are shown in Panels A-C of this figure. They show using rapid mixing instrumentation that α^H and β^H chains do not exhibit intrinsic fluorescence in solution, either following dilution or when mixed together. They also show that AHSP stably fluoresces in solution following rapid dilution, and that mixing various combinations of AHSP and β^H chains does not result in detectible fluorescence changes on millisecond to second time scales. The only exception is the reaction of the AHSP:α^H-chain complexes with buffer (Figure 3-1D, reaction 3), which shows an intermediate fluorescence signal and a small increase in fluorescence in the 2 to 4 seconds following mixing. This small increase reflects a small amount of α^H chain dissociation from AHSP due to dilution of the complex.

In contrast to these control reactions, a large quenching of the AHSP fluorescence signal is observed on time scales of less than 100 seconds when α^H chains are mixed with AHSP. As shown in Figures 3-2A and 3-2B, the observed traces for the reaction of α^H chains with AHSP are biphasic. The large fast phase shows a rate which is linearly dependent on α^H chain concentration, and the small slow phase shows a rate which is concentration-independent and equal to

approximately 0.04 ± 0.01 s^{-1}. In addition, the slow phase is not observed when the concentrations of α^H chains are less than that of AHSP.

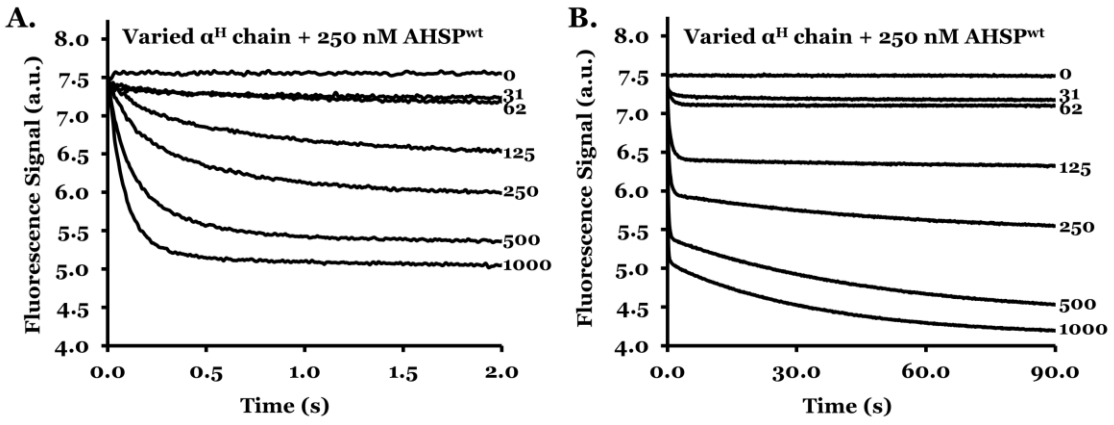

Figure 3-2. AHSP association with α^H chains
The buffer utilized in this stopped-flow experiment was 50 mM potassium phosphate, pH 7.0 at 21 ^{O}C, which had been saturated with CO prior to use. Data were collected using the same instrument and configuration as in Figure 3-1D. The post-mixing AHSP concentration was fixed at 250 nM, with the concentration of α^H chains being varied with post-mixing values listed in the right margins of each panel in units of nM. Plots were generated using Microsoft Excel and PowerPoint (Microsoft Corporation, Redmond, Washington, US).

There are at least two plausible mechanistic explanations for the two phases observed when α^H chains are mixed with wild-type AHSP. First, the fast phase could correspond to AHSP:α^H-chain complex formation, followed by a slow phase that is due to structural rearrangements within AHSP and/or the α^H chains. For example, alterations which affect the orientation and local environment of the AHSP Trp44 side chain, or its distance from the heme group, could cause slow additional fluorescence quenching following the large initial decrease in fluorescence due to bimolecular binding. A second possibility is that one of the proteins exists in two sub-populations, a fast-reacting population and a slow-reacting population. If each of the two populations bind

at different rates, their sequential depletion would give rise to biphasic fluorescence quenching.

Most of the evidence argues against the first model. Although AHSP binding has been shown to induce structural rearrangements in oxygenated α^H chains after binding, including those that are related to autooxidation and hemichrome formation (*442*, *445*, *471*, *473*, *508*), these rearrangements take hours at 20 ^oC to complete (see Chapter 4) and not seconds as depicted in Figures 3-2A and 3-2B. In addition, the experiments in Figure 3-2 used CO-bound α^H chains, which do not readily autooxidize or undergo heme pocket rearrangements. These experiments were also conducted at α^H chain concentrations that were more than 100-fold lower than the dissociation equilibrium constant for α^H chain self-dimerization. Thus, the slow phase cannot be attributed to a rate-limiting α^H_2 dimer dissociation event. Similarly, AHSP has been shown to remain monomeric in solution at much higher concentrations than the ones utilized in these experiments (*444*).

The observed slow phases are only present when AHSP is mixed with equimolar or excess α^H chains (Figure 3-2B). This kinetic pattern suggests that it is AHSP which exists in populations of fast- and slow-reacting species. If α^H chain concentrations are lower than those of AHSP, the fast-binding population of AHSP is preferentially depleted before any slow-binding AHSP is able to react. Under these conditions, no second phase is observed because the slow-binding population of AHSP has no free α^H chain binding partners with which to interact. In contrast, when equimolar or excess α^H chains are mixed with limiting AHSP, all of the free AHSP reacts, including the slow-reacting

population which gives rise to a second fluorescence quenching phase. If α^H chains existed in fast- and slow-reacting populations, the opposite pattern would be predicted (that is, two phases would be observed when AHSP is present is in excess, with the abrogation of one phase when AHSP is limiting). Similarly, if the slow phase were being caused by structural rearrangements, this phase would also be predicted to occur with excess AHSP, although its rate might be affected. Thus, the two-conformation model for wild-type AHSP is consistent with the observed kinetic data.

Further analysis of the kinetic titration shown in Figures 3-2A and 3-2B suggests that the fast phase corresponds to a simple bimolecular association reaction (Scheme 3-1). The association rate constant for AHSP binding (k'_{AHSP}) in this model can be obtained by plotting the observed rate constants for the fast phases versus the free α^H chain concentration under pseudo first-order conditions where α^H chains are in excess (Figure 3-3). Fitting data from four experiments gives an apparent association rate constant for AHSP binding of $8.5 \pm 2.1\ \mu M^{-1}s^{-1}$. This is approximately 17-fold greater than the association rate constant for α^H chain binding to β^H chains, which occurs at a rate of approximately $0.5\ \mu M^{-1}s^{-1}$, irrespective of the ligand bound (See Figure 1-5)(*198*, *201*).

As discussed in Chapter 1, wild-type AHSP is known to exhibit cis and trans conformations about the Asp29-Pro30 peptide bond. The binding of α^H

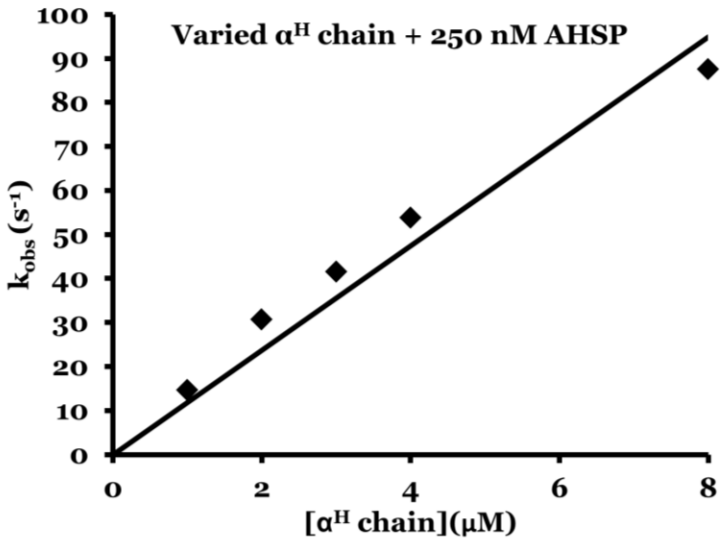

Figure 3-3. AHSP, α^H chain association rates unders pseudo-first order conditions
Buffer conditions and experimental configuration are the same as those in Figure 3-2. Concentrations are listed as post-mixing values. Observed traces were fit to a single exponential equation, and the observed rate constants were plotted against α^H chain concentration. The line represents a linear fit whose slope equals k'_{AHSP}. Figure generated using Microsoft Excel and PowerPoint (Microsoft Corporation, Redmond, Washington, US).

chains quenches this conformational heterogeneity, and the initial work of Santiveri et al. (*470*) and Feng et al. (*445*) suggested that AHSP occupies the trans conformer upon binding. Santiveri et al. (*470*) estimated that the populations of cis and trans AHSP in the unbound form are roughly equal at room temperature, and their NMR chemical shift data indicate that the two species interconvert slowly in solution, with the interconversion occurring with a lifetime of ≥0.1 seconds (*470*).

These initial NMR data and the time courses in Figure 3-2 suggested that the observed fast phase corresponds to the formation of (trans)AHSP:α^H-chain complexes which occurs in less than a few seconds following mixing. The

observed slow phase would then correspond to a rate-limiting conversion of (cis)AHSP to (trans)AHSP, which then rapidly binds to free α^H chains to form the final (trans)AHSP:α^H-chain complex. This mechanism is depicted in Figure 3-4.

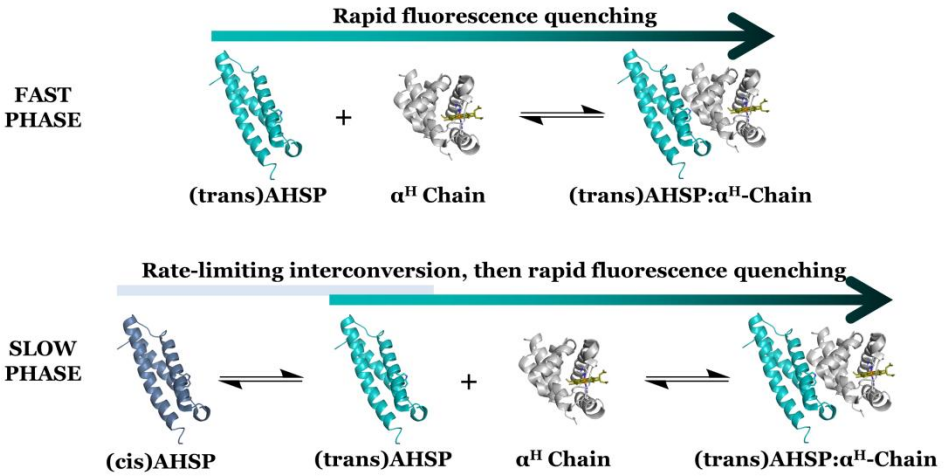

Figure 3-4. Mechanism of AHSP, α^H chain association reaction
Colors, ribbons, and stick forms are the same as those used in Figure 1-8, except (cis)AHSP is depicted in purple in this figure. Figure generated using Microsoft PowerPoint (Microsoft Corporation, Redmond, Washington, US) and the PyMol Molecular Graphics System and PDB entry 1Z8u (DeLano Scientific, Palo Alto, California, US)(*471*).

More recent work by Gell et al. (*508*), however, suggests an alternate model. Their NMR and X-ray crystallographic data indicate that AHSP exclusively occupies the cis conformation in bound AHSP:α^H-chain complexes. If true, then α^H chain binding to (cis)AHSP is rapid and followed by a rate-limiting interconversion of (trans)AHSP to (cis)AHSP before the remaining AHSP binds. Although this model contradicts the conclusions of Santiveri et al. (*470*), data from both research groups are consistent in indicating that only one peptidyl-prolyl conformation of AHSP exists in bound AHSP:α^H-chain

complexes (*470*, *508*). The data presented here indicate the presence of both proline isomers, although it is unclear which one is the fast-reacting species.

Based on the relative amplitudes of each kinetic phase, it appears that 20-30% of AHSP occupies one Pro30 peptidyl-prolyl conformation while 70-80% occupies another at equilibrium (50 mM potassium phosphate buffer, pH 7.3 at 20 ^{O}C). Although this estimate differs from the 50/50 mixture that Santiveri et al. (*470*) reported, it is consistent with other studies which show that at equilibrium, 60-90% of model oligopeptides occupy the trans peptidyl-prolyl conformation and 10-40% the cis conformation (*509*). Additionally, the observed rate of the slow phase (0.04 ± 0.01 s^{-1}) in Figure 3-2 is consistent both with the rate assignment of Santiveri et al. (*470*) and with other studies which show that cis/trans interconversion occurs spontaneously with time constants of 10 to 100 seconds at 25 ^{O}C (*509*). Also, the observations that the rate of the slow phase is (1) concentration-independent and (2) completely eliminated when α^{H} chains are limiting are also supportive of a model involving AHSP binding that is rate-limited by cis/trans conformational interconversion.

Several peptidyl-prolyl isomerases (PPIases) were obtained to further investigate these ideas. Based on personal correspondence with Christopher M. Dobson (University of Cambridge, Cambridge, UK), Hiram F. Gilbert (Baylor College of Medicine, Houston, Texas, US), and Franz X. Schmid (Universität Bayreuth, Bayreuth, Bavaria, DE), it was hypothesized that adding a PPIase to the solutions of AHSP prior to mixing them with α^{H} chains might alter the rate, amplitude, and/or presence of the observed slow phase. If this were the case, this phase could be more directly attributed to AHSP cis-trans peptidyl-prolyl

isomerization. Human recombinant Cyclophilin-A and FK506 Binding Protein 4 were selected for this purpose and obtained from Prospec Protein Specialists (East Brunswick, New Jersey, US). When AHSP was pre-incubated with either of the enzymes and then mixed with α^H chains there was no change in the rate or amplitude of the slow phase. Most likely, the active sites of these PPIases have regio- and stereo-specificities that preclude interaction with Pro30 in the folded loop between helices 1 and 2 of AHSP.

Another approach was to mutate the proline at position 30 in AHSP to an alanine residue ($AHSP^{P30A}$). This mutation was previously shown by NMR spectroscopy to quench AHSP conformational heterogeneity in favor of the conformation observed for the trans Pro30 form (*445*, *470*). The proline at position 30 was also mutated to a tryptophan ($AHSP^{P30W}$), because this mutation was expected to have the same effect while conferring greater intrinsic fluorescence due to the presence of an extra tryptophan. Additionally, $AHSP^{P30W}$ was reported to have a different affinity for α^H chains than wild-type AHSP (personal communications, Mitchell J. Weiss, University of Pennsylvania, Philadelphia, Pennsylvania, US).

In stopped-flow experiments in which α^H chains were mixed with these mutants, no slow phases were observed at any α^H chain concentration examined. Representative kinetic traces are shown in Figure 3-5, and in these experiments the concentration of α^H chains was increased to 8000 nM to look for slow phases.

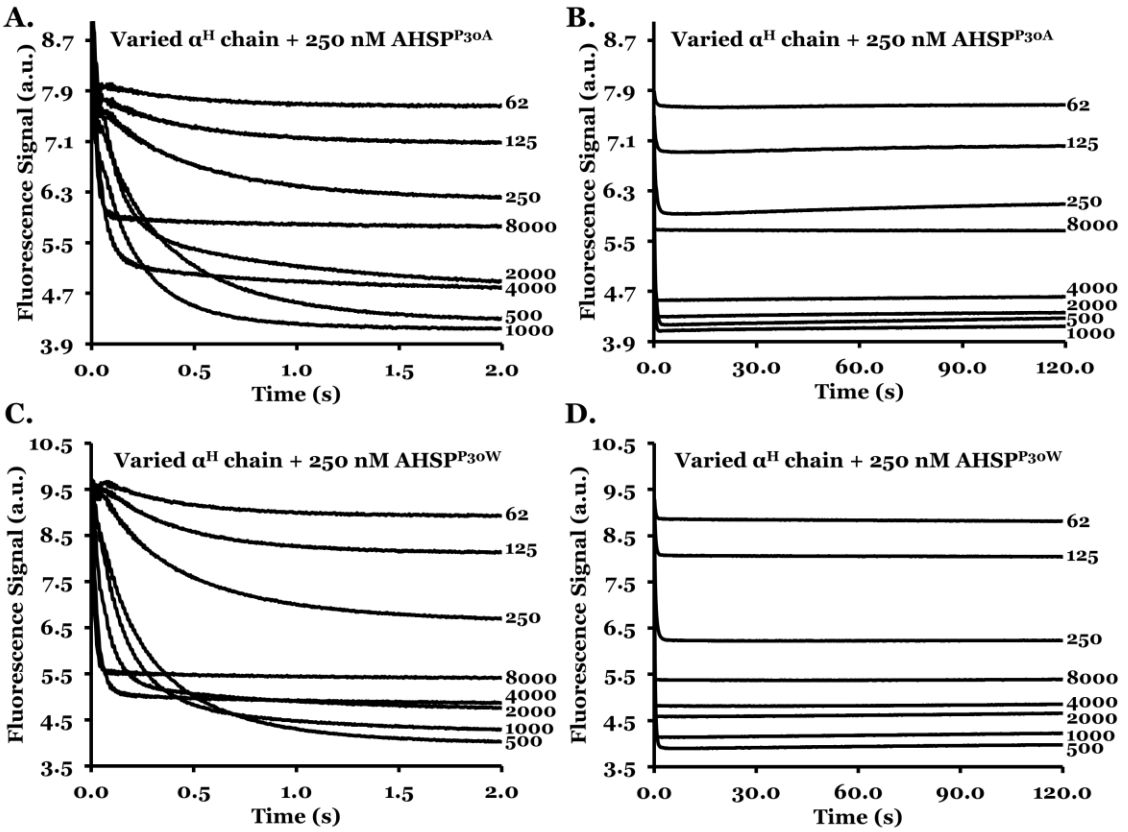

Figure 3-5. Mutant AHSP association with α^H chains
The buffer utilized in this stopped-flow experiment was 100 mM potassium phosphate, pH 7.3 at 21 ^{O}C, which had been saturated with CO prior to use. Data were collected using the same instrument and configuration as in Figure 3-1, Panel D. The post-mixing AHSP concentration was fixed at 250 nM, with the concentration of α^H chains being varied with post-mixing values listed in the right margin of each panel in units of nM. Plots were generated using Microsoft Excel and PowerPoint (Microsoft Corporation, Redmond, Washington, US).

As these data show, the concentration of α^H chains affects not only the observed rates of the reactions, but also the apparent intensity of the fluorescence signal changes of each kinetic trace. For example, there is a clear upward shifting of the fluorescence traces observed in Figure 3-5 at α^H chain concentrations higher than 500 nM. This same effect was observed in the experiments mixing wild-type AHSP with α^H chains (not shown) and is a result of significant absorbance of both excitation and emitted light by the α^H chains. In addition, at higher α^H chain concentrations, significant light scattering

occurs due to small amounts of denatured protein which increases the background fluorescence of each affected trace. Consistent with this explanation, the traces in Figure 3-1D show that mixing 250 nM α^H chains with 250 nM β^H chains results in a larger apparent fluorescence signal than mixing either subunit with buffer alone (compare traces 4 through 7). Similar phenomena have previously been documented in other studies of hemoglobin solutions (*510*, *511*), and these issues complicate the appearance of the time courses at high α^H chain concentrations but not the kinetic analyses. Note that no slow phases are observed with these mutants despite the changes in intensities of the absolute fluorescence signals (Figure 3-5B and 3-5D).

The time courses for the reactions involving $AHSP^{P30A}$ and $AHSP^{P30W}$ are all monophasic, with concentration dependences similar to the wild-type AHSP mixing reactions. The bimolecular rates of complex formation were calculated using the same method that was used for wild-type AHSP association with α^H chains (Figure 3-3), and the association rate constants for $AHSP^{P30A}$ and $AHSP^{P30W}$ are 7.0 $\mu M^{-1}s^{-1}$ and 10.4 $\mu M^{-1}s^{-1}$, respectively, and nearly identical to that for wild-type AHSP. The plots of the observed rate constants versus α^H chain concentration under pseudo first-order conditions where α^H chains are in excess are shown in Figure 3-6.

These data confirm that AHSP binding to α^H chains is a rapid reaction that can be followed by fluorescence quenching. Additionally, they are consistent with a two-conformation model of AHSP structure.

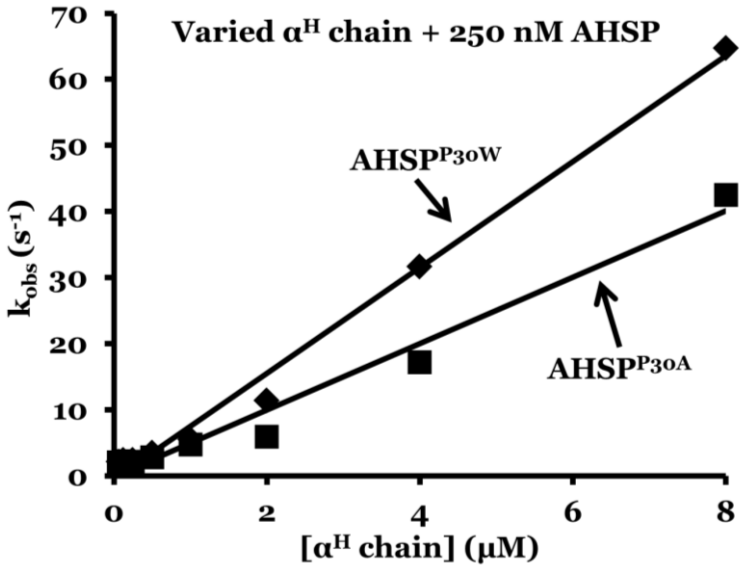

Figure 3-6. Rate constants for mutant AHSP, α^H chain association
Buffer conditions and experimental configuration are the same as those in Figure 3-2. Concentrations are listed as post-mixing values. Observed traces were fit to a single exponential equation, and the observed rate constants were plotted against α^H chain concentration. The line represents a linear fit whose slope equals k'_{AHSP}. Figure generated using Microsoft Excel and PowerPoint (Microsoft Corporation, Redmond, Washington, US).

AHSP, Alpha Chain Dissociation

It has been shown by size exclusion gel filtration chromatography and electrophoretic mobility shift assays that β^H chains are capable of competitively displacing α^H chains from AHSP:α^H-chain complexes to form intact HbA (*443*, *444*, *471*). Formation of HbA occurs because: (1) α^H chains have a much higher affinity for β^H chains than they do for AHSP (*197*, *201*, *202*, *205*, *444*), and (2) α^H chains cannot simultaneously bind to AHSP and β^H chains because both of these interactions involve the same set of α^H chain helices at the complex interfaces (*445*, *471*, *502*). This displacement mechanism is depicted in Figure 3-7.

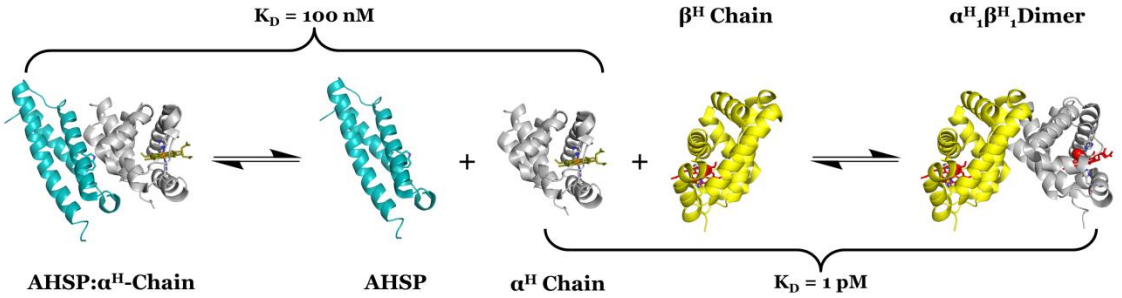

Figure 3-7. AHSP, β^H chain competition for free α^H chains
Equilibrium constants were measured using comparable buffer conditions (pH ~7 at ~22 ^{O}C, buffered by 50 to 150 mM phosphate buffer). Colors, ribbons, and stick forms are the same as those used in Figures 1-1 and 1-9. Figure generated using the PyMol Molecular Graphics System and PDB entries 1Z8u and 1GZX (DeLano Scientific, Palo Alto, California, US)(*196*, *201-203*, *205*, *444*, *471*, *472*).

The only species in Figure 3-7 which exhibits strong intrinsic fluorescence in solution is AHSP that is not complexed with α^H chains (*502*). Consequently, when AHSP:α^H-chain complexes are mixed with β^H chains, the displacement of α^H chains from AHSP by β^H chains results in an increase in fluorescence emission as free AHSP is generated (*502*). The rate at which this process occurs can be studied using the same fluorescence emission stopped-flow device that was used to measure bimolecular binding. Preliminary studies using this approach have been reported by Brillet et al. (*488*) and Mollan et al. (*1*).

At high AHSP and β^H chain concentrations, the amount of free α^H chains is small and in a steady-state during the displacement reaction. Under these conditions, the rate of the displacement reaction is given by:

$$r_{obs} = \frac{(k_{AHSP})(k'_{\alpha\beta})[\beta^H\ Chain]}{(k'_{\alpha\beta})[\beta^H\ Chain]+(k'_{AHSP})[AHSP]} \qquad \text{(Equation 3-1)}$$

where k_{AHSP} is the rate constant for dissociation of the AHSP:α^H-chain complex, k'_{AHSP} is the association rate constant for AHSP:α^H-chain complex formation,

and $k'_{\alpha\beta}$ is the association rate constant for $\alpha^{H}_{1}\beta^{H}_{1}$ dimer formation (*1*, *512*, *513*). By conducting displacement reactions at varied concentrations of β^{H} chains and measuring the r_{obs} values for these reactions, Equation 3-1 can be used to obtain values for k_{AHSP} and the ratio of k'_{AHSP} to $k'_{\alpha\beta}$ (*1*). Expressions of this general form have previously been used to study the rates of ligand replacement for HbA and myoglobin (Mb)(*512*, *513*).

Representative traces for a set of displacement reactions are shown in Figure 3-8. As this figure shows, mixing β^{H} chains with AHSP:α^{H}-chain complexes results in an increase in the fluorescence emission of the resulting solution. The magnitudes of the fluorescence changes for these reactions are consistent with the AHSP displacement mechanism that is depicted in Figure 3-7, and the observed time courses are monophasic at these concentrations.

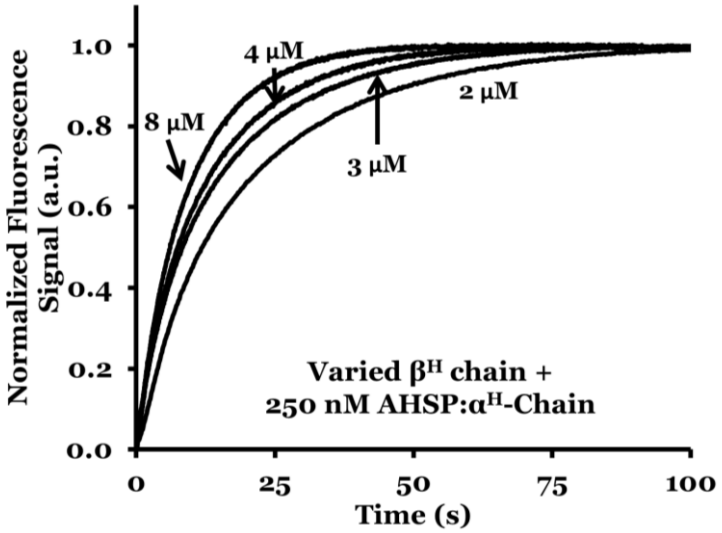

Figure 3-8. Displacement reaction concentration dependence
Data were collected using 50 mM potassium phosphate buffer, pH 7.3 at 22 ^{O}C. The instrumental configuration was the same as in Figure 3-1D. Plots were generated using Microsoft Excel and PowerPoint (Microsoft Corporation, Redmond, Washington, US).

Because high concentrations of AHSP result in strong background fluorescence, these studies require the mixing of low concentrations of AHSP:α^H-chain complexes with five-fold or greater concentrations of β^H chains. This departure from pseudo-first-order conditions results in a varying concentration of free AHSP throughout the course of the reactions. In the analyses, the concentrations of free AHSP were fixed to 50% of their post-mixing start values (125 nM). Additionally, because β^H chains readily self-associate to form homotetramers in solution, an upper limit of 8.0 μM β^H chains (post-mixing value) was used to prevent the appearance of a slow phase due to $\beta^H{}_4$ tetramer dissociation (*201*).

As Figure 3-9A shows, the displacement reaction involving AHSP^{P30W} is dramatically slower than the reactions involving wild-type AHSP and AHSP^{P30A}. Figure 3-9B shows the experimentally measured rates of replacement for these

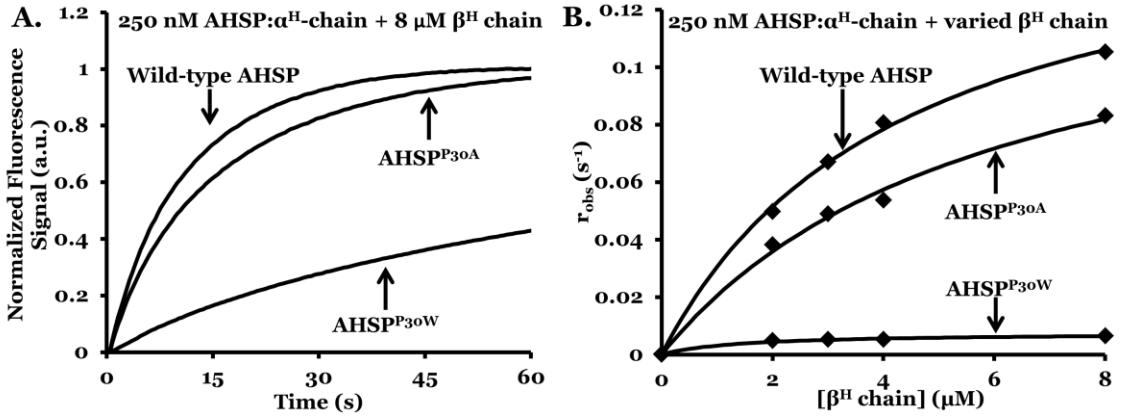

Figure 3-9. Wild-type and mutant AHSP, α^H chain displacement reactions
Panel A, plots of the displacement reactions for wild-type AHSP, AHSP^{P30A}, and AHSP^{P30W}. *Panel B*, theoretical replacement reaction curves plotted along with measured replacement rates for each protein. The data were collected using the same instrumental configuration as described in Figure 3-1D. Plots were constructed using Microsoft Excel and Microsoft PowerPoint (Microsoft Corporation, Redmond, Washington, US).

three proteins at varying concentrations of β^H chains, as well as fitted replacement reaction rate curves generated using Equation 3-1.

To obtain values for k_{AHSP} and $k'_{\alpha\beta}$, k'_{AHSP} was fixed to the values determined from the bimolecular association reactions described in the preceding section. The values which give the best fits to Equation 3-1 are shown in Table 3-1. These values were then used to estimate the equilibrium dissociation constants for AHSP:α^H-chain complex dissociation for all three AHSP proteins, which are also listed in this figure.

	k_{AHSP} (s^{-1})	k'_{AHSP} ($\mu M^{-1}s^{-1}$)	$k'_{\alpha\beta}$ ($\mu M^{-1}s^{-1}$)	$K_{D,\,AHSP}$ (nM)
Wild-Type AHSP	0.19 ± 0.02	8.5 ± 2.1	0.17 ± 0.07	22 ± 7.7
$AHSP^{P30A}$	0.086	7.0	0.28	12
$AHSP^{P30W}$	0.0078	10	0.82	0.78

Table 3-1. Kinetic parameters for wild-type and mutant AHSP, α^H chain dissociation
The data used in these calculations were collected using the same instrumental configuration as described in Figure 3-1D. Rate constants were calculated by fitting r_{obs} values from experiments like the one depicted in Figure 3-8 to Equation 3-1. The reactions involving $AHSP^{P30A}$ and $AHSP^{P30W}$ were repeated twice, and the numbers presented here constitute the average of the two calculated values. The reaction involving wild-type AHSP was repeated three times, and the numbers reported in the table are the mean values plus or minus (±) the standard deviation of the mean. The equilibrium dissociation constant was calculated by dividing k_{AHSP} by k'_{AHSP}. Calculations were done using Microsoft Excel and the table was constructed using Microsoft PowerPoint (Microsoft Corporation, Redmond, Washington, US).

The fitted values for $k'_{\alpha\beta}$ roughly agree with those which were reported by McGovern et al. (*201*) and Kawamura and Nakamura (*198*)(0.5 $\mu M^{-1}s^{-1}$ and 0.75 $\mu M^{-1}s^{-1}$, respectively). Also, the fitted values for k'_{AHSP} and k_{AHSP} for wild-type AHSP are similar to those that were independently determined by Brillet et

al. (*488*)(20 $\mu M^{-1}s^{-1}$ and 0.5 s^{-1} at 37 ^{O}C, respectively). Together, these data suggest a ~5-fold lower dissociation equilibrium constant for AHSP:α^{H}-chain complexes than previous reports indicated (Gell et al. (*444*) reported a K_D of 100 nM at 20 ^{O}C).

Two key results from this work are that: (1) the mutation of proline 30 to alanine in AHSP abolishes the slow association phase but with α^{H} chain kinetic parameters that are equivalent to those of the rapidly-reacting conformer of wild-type AHSP, and (2) the Pro30Trp mutation causes a >25-fold increase in affinity for α^{H} chains due to a >20-fold decrease in the AHSP:α^{H}-chain dissociation rate constant. This increase in affinity for $AHSP^{P30W}$ was recently confirmed by Gell et al. (*508*), who reported a dissociation equilibrium constant for this protein of 7.7 ± 2.3 nM at 20 ^{O}C. Gell et al. (*508*) have also recently reported an affinity constant for $AHSP^{P30A}$ binding which is similar to the value determined in this work (33.0 ± 3.0 nM at 20 ^{O}C).

AHSP Affinity for (O_2), (CO), (met)Alpha Chains

Feng et al. (*445*, *471*) showed that AHSP binding induces structural rearrangements in α^{H} chains, particularly in the area of the heme or hemin binding pocket. Because these alterations have been shown to affect α^{H} chain oxidation chemistry and O_2 binding (*471*, *473*), it was hypothesized that the affinity of AHSP might be nonequivalent for α^{H} chains with different oxidation states or bound ligands.

To investigate this hypothesis, AHSP and α^{H} chain association and dissociation reactions were studied using α^{H} chains that were liganded with O_2

and CO, as well as α^H chains that had been oxidized to the ferric state using potassium ferricyanide ((met)α^H chains). Using the previously described methods, bimolecular association reactions were measured to determine k'_{AHSP}. Once obtained, displacement reactions using (CO)β^H chains were performed to obtain values for k_{AHSP} and $k'_{\alpha\beta}$. The plots that were used to obtain k'_{AHSP} are shown in Figure 3-10A, and the theoretical replacement reaction rate curves are shown in Figure 3-10B. As was done in previous calculations, the values for k'_{AHSP} that had been determined from the bimolecular association reactions were fixed for determinations of k_{AHSP} and $k'_{\alpha\beta}$.

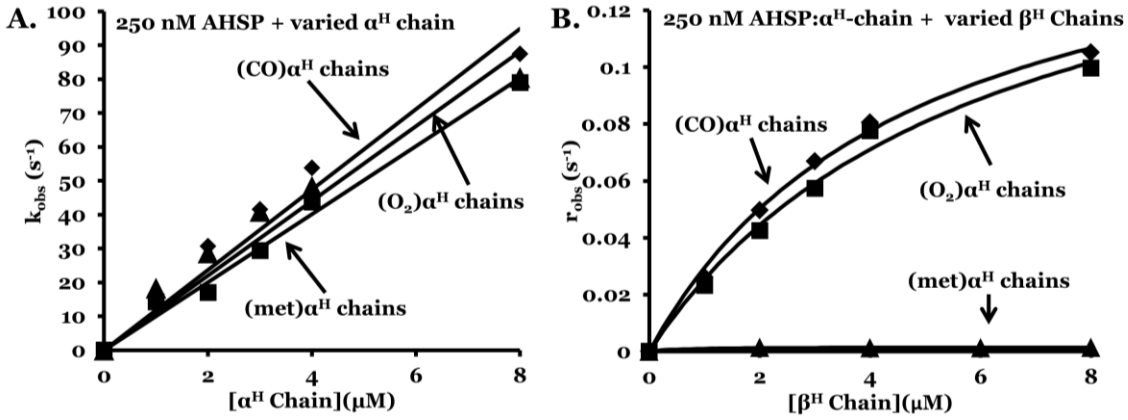

Figure 3-10. Kinetics of AHSP binding to and dissociation from (O_2)-, (CO)-, and (met)-α^H-chains
Panel A, plot depicting the rates of bimolecular association. *Panel B*, theoretical replacement reaction curves plotted along with measured replacement rates for each sample set. Plots were constructed using Microsoft Excel and Microsoft PowerPoint (Microsoft Corporation, Redmond, Washington, US).

The rate constants obtained from these studies are set forth in Table 3-2. As these data indicate, there is a dramatic difference between the rates of displacement of (met)α^H chains as compared to the reduced liganded complexes. Because the values for k'_{AHSP} are approximately equivalent for all three types of α^H chains, this result indicates that AHSP has a much higher

affinity for (met)α^H chains than it does for the other forms. There are several functional implications relating this finding.

	k_{AHSP} (s^{-1})	k'_{AHSP} ($\mu M^{-1}s^{-1}$)	$k'_{\alpha\beta}$ ($\mu M^{-1}s^{-1}$)	$K_{D, AHSP}$ (nM)
$(O_2)\alpha^H$-Chain	0.18	11.0	0.23	16.0
$(CO)\alpha^H$-Chain	0.19 ± 0.02	8.5 ± 2.1	0.17 ± 0.07	22 ± 7.7
(met)α^H-Chain	0.0018	10.0	0.84	0.18

Table 3-2. Kinetic parameters for AHSP binding to and dissociation from (O_2), (CO), and (met)-α^H chains
The data used in these calculations were collected using the same experimental conditions as was described in Figure 3-9. The experiments involving (O_2)- and (met)-α^H-chains were not done in duplicate, though various methods of oxidizing AHSP:α^H-chains complexes were used to investigate and confirm the apparent slow rate of (met)α^H-chain dissociation. The equilibrium dissociation constant was calculated by dividing k_{AHSP} by k'_{AHSP}. The reactions involving (met)α^H-chains are preliminary, though they have been reproduced in a series of slightly different assays. Calculations were done using Microsoft Excel and the table was constructed using Microsoft PowerPoint (Microsoft Corporation, Redmond, Washington, US).

Isolated subunits and HbA in the met or ferric oxidation state are known to be less stable than their ferrous counterparts. One reason is that hemin loss is normally much faster from ferric heme proteins than from the reduced forms (*153-157*, *159*, *170*, *514*, *515*), resulting in apoprotein that rapidly denatures, aggregates, and precipitates (*171-173*). In vitro studies have shown that oxidation to the ferric state occurs spontaneously in the presence of O_2 (autooxidation)(*41*, *90*, *516-523*), but erythrocytes possess reductases which rapidly re-reduce these proteins to their more stable ferrous states in vivo (*66*, *524*, *525*). Because AHSP has been shown to stabilize α^H chains following binding (*442*, *443*, *445*, *469*, *469*, *471*, *473*, *526*), the finding that AHSP binds to

(met)α^H chains with a higher affinity than the other forms of α^H chains suggests that it preferentially stabilizes subunits which are more in need of stabilization. Additionally, these affinity constants suggest that AHSP impedes the incorporation of oxidized α^H chains into HbA tetramers, thereby contributing to a more stable end state population of reduced HbA following subunit assembly. If endogenous reductases are able to reduce AHSP:(met)α^H-chain complexes in vivo, as the data in Chapter 4 will suggest, then the affinity of AHSP is modulated, and reduced α^H chains can readily be displaced by β^H chains. Although AHSP redox reactions have been studied by others (*445*, *471*, *473*), this specific process has not been directly examined before this work.

The data presented in this chapter indicate that AHSP is capable of binding to α^H chains faster than β^H chains can bind, and that AHSP has a higher affinity for (met)α^H chains than ferrous α^H chains. Both of these findings are consistent with the previously proposed molecular chaperone activity of AHSP.

Chapter 4: Changes in α^H Chain Properties Following Binding to AHSP

Several studies have focused on the post-binding effects of AHSP on α^H chains (*442*, *443*, *445*, *471*, *473*, *502*, *508*). These effects include increasing α^H chain resistance to denaturation, aggregation, and precipitation (*443*), as well as structural rearrangements which have been linked to altered α^H chain redox chemistry and α^O globin folding (*445*, *471*, *508*, *527*). These studies have been continued and expanded because the mechanisms underlying these effects are incompletely understood, and the results are presented in this chapter.

AHSP and Alpha Chain Oxidation, Hemichrome Formation

Autooxidation of human HbA is a spontaneous process in which O_2 bound to ferrous heme spontaneously dissociates superoxide ($^{\bullet}O_2^-$), leaving the iron in the ferric state (*518*). In vitro studies indicate that this process results in the formation of a hemin iron which is coordinated on one side by a histidine (the proximal or F8 histidine) and on the other by weakly bound H_2O or OH^-, depending on buffer pH (*528*, *529*). Once the protein is in this oxidized or ferric form, the hemin iron can coordinate an additional histidine (the distal, or E7 histidine) that is located on the opposite side of the heme as the proximal histidine (*528*, *529*). This can occur when hemoglobin structure is perturbed or partially unfolded (*530*). These "bis-histidyl" adducts are called hemichromes, and the hemin iron is said to exist in a hexacoordinated state (*528*, *529*). In cases involving a reduced or ferrous heme iron, this bis-histidyl hexacoordinated state is referred to as a hemochrome. The ferrous and ferric forms of pentacoordinate HbA with or without weakly bound water exhibit

unique optical absorbance spectral properties (*496*), as do hemichromes and hemochromes (*528*, *529*).

It has been shown that autooxidation and hemichrome formation can occur spontaneously in HbA, particularly under denaturing conditions, and that isolated α^H and β^H subunits undergo these processes at faster rates than tetrameric Hbs (*186*, *531-533*). Hemichrome formation is often thought of as a detrimental process which precedes protein precipitation in vivo (*531*). However, other roles for hemichrome formation have recently been suggested (*528*, *529*). For example, recent work has shown that these conformations are intermediates in globin folding pathways (*530*).

Although previous studies have made it clear that AHSP appreciably accelerates both autooxidation and hemichrome formation in isolated α^H chains (*1*, *445*, *471*, *473*), questions as to the reversibility of these processes remain unanswered. For example, can α^H chains be readily re-reduced following AHSP-induced oxidation to the ferric bis-histidyl (hemichrome) state? Does re-reduction result in (1) ferrous bis-histidyl adducts (hemochromes), (2) simple, pentacoordinate, and native deoxy ferrous α^H chains, or (3) other conformations? Is the AHSP-induced ferric bis-histidyl conformation a folding intermediate, or is it part of an α^H chain degradative pathway as some have suggested (*444*)? These are important questions to answer because the changes which AHSP induces render α^H chains incapable of O_2 transport. Thus, the question as to whether or not the redox changes are reversible has a direct bearing on the in vivo function of AHSP.

Previous findings regarding autooxidation and hemichrome formation were first verified using wild-type AHSP, and were then extended by assaying the effects of $AHSP^{P30A}$ and $AHSP^{P30W}$. As shown in Figure 4-1A, incubating solutions of isolated, $(O_2)\alpha^H$-chains with AHSP results in prominent spectral changes. The 541 and 577 nm peaks for $(O_2)\alpha^H$ chains transition into peaks at 535 and 565 nm, which represent the hemichrome form of $(met)\alpha^H$-chains (Fe^{3+}, bis-histidyl conformation)(*528*). The observed rates for these transitions were measured to be 0.98 hr^{-1}, 0.30 hr^{-1}, and 0.23 hr^{-1}, respectively, for AHSP:α^H-chain complexes, $AHSP^{P30A}$:α^H-chain complexes, and $AHSP^{P30W}$:α^H-chain complexes in 100 mM potassium phosphate buffer, pH 7.0 at 37 ^OC. These rates are all significantly faster than the rate of autooxidation of α^H chains alone (~0.078 hr^{-1} in 100 mM MES buffer, pH 6.5 at 35 ^OC (*534*)). Gell et al. (*508*) have recently reported similar rates for these AHSP mutants, and have suggested that the smaller rates observed with the mutants as compared to wild-type AHSP are related to the elimination of the cis peptidyl-prolyl conformation at position 30 of AHSP (*508*).

This work was extended by investigating the reversibility of AHSP-induced hemichrome formation. Spectra were recorded of ferrous α^H chains before and after the addition of excess potassium ferricyanide. This reagent rapidly oxidizes α^H chains to the ferric state (*66*), and allows the processes of oxidation and hemichrome formation to be studied as separate events.

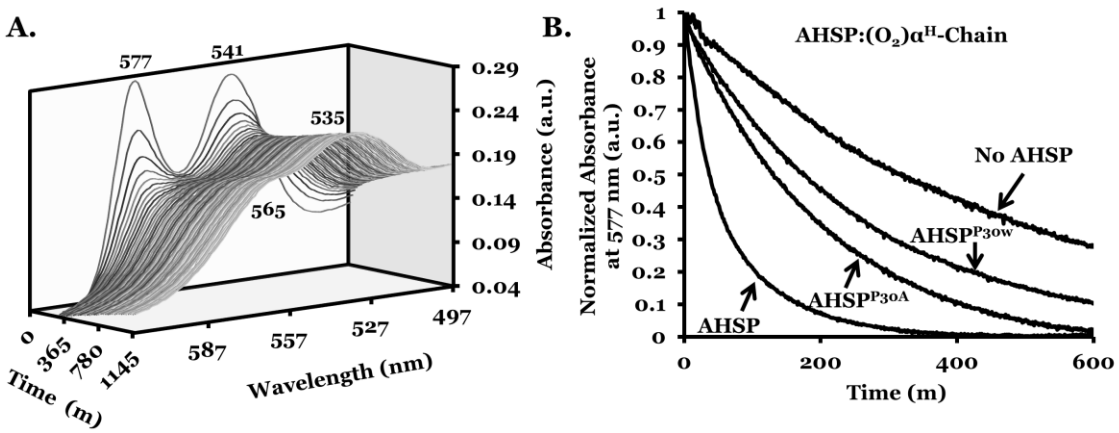

Figure 4-1. Autooxidation of AHSP:α^H-chain complexes
Panel A, Plot of AHSP:α^H-chain autooxidation absorbance spectra as a function of time. *Panel B*, absorbance changes at 577 nm for α^H chains, AHSP:α^H-chain complexes, $AHSP^{P30A}$:α^H-chain complexes, and $AHSP^{P30W}$:α^H-chain complexes. AHSP:α^H-chain concentrations were fixed at 20 μM in 100 mM potassium phosphate buffer, pH 7.0 at 37 ^{O}C. Scans were taken every minute for approximately 24 hours. Plots were generated using Microsoft PowerPoint and Excel (Microsoft Corporation, Redmond, Washington, US).

The spectral differences between $(O_2)\alpha^H$ chains and $(met)\alpha^H$-chains are presented in Figure 4-2, with $(O_2)\alpha^H$ chains exhibiting strong absorption peaks at 541 and 576 nm and $(met)\alpha^H$-chains exhibiting less intense peaks at 500 and 635 nm (*495*, *496*). In the $(met)\alpha^H$-chain spectrum, the minor peaks at 540 and 575 nm suggest a small amount of OH^- binding to the ferric hemin iron (*496*). Equimolar amounts of AHSP were manually added to this solution of $(met)\alpha^H$-chains, and peaks at 535 and 565 nm were immediately observed along with the disappearance of the 500 and 635 nm peaks. This finding indicates that AHSP rapidly induces hemichrome formation $(met)\alpha^H$-chains. The rate of this transition was investigated using a stopped-flow device in which absorbance changes at 565 nm were followed. Upon mixing 10 μM $(met)\alpha^H$ chains with 10 μM AHSP, a transition with an apparent rate of 50 to 100 s^{-1} was observed (Figure 4-2, inset). This rate is roughly what would be expected for a simple

bimolecular binding of (met)α^H-chains to AHSP, which is discussed in Chapter 3 (that is, $k_{obs} \approx k'_{AHSP}$*[AHSP], which means that (10 $\mu M^{-1}s^{-1}$)*(10 μM) = 100 s^{-1}).

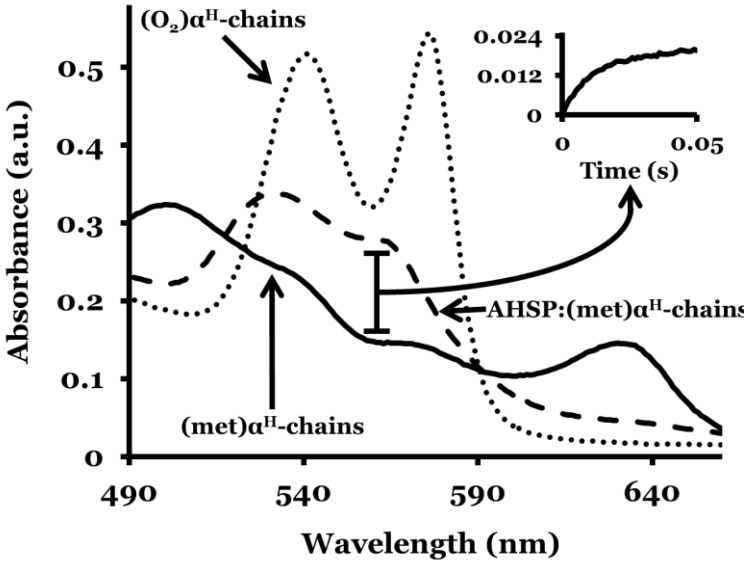

Figure 4-2. AHSP-induced α^H chain hemichrome formation
The buffer used to record these spectra was 50 mM potassium phosphate, pH 7.2 at 22 ^oC. After preparing 35 μM α^H chains in this buffer and recording the spectrum, a two-fold excess of potassium ferricyanide was added, followed by the addition of 35 μM wild-type AHSP. The Y-axis of the kinetic trace shown in the inset represents the change in absorbance following mixing, and is presented using arbitrary units (a.u.) with an offset. Plots were generated using Microsoft PowerPoint and Excel (Microsoft Corporation, Redmond, Washington, US).

To investigate the reversibility of oxidation and hemichrome formation, excess sodium dithionite was added to solutions of AHSP:(met)α^H-chain complexes, and spectra were recorded immediately following the addition. Sodium dithionite is a reducing agent which consumes O_2 in aqueous solutions and is commonly used to convert ferric Hb to ferrous Hb (*66*). As is shown in Figure 4-3, re-reduction with this reagent does not produce spectra suggestive

of a hemochrome, which would be indicated by the emergence of a weak peak at 529 and strong intense peak at 558 nm, but rather results in a single peak at 558 nm which is characteristic of pentacoordinated deoxy α^H chains (*496*, *529*). This finding indicates that the α^H chains are in the reduced and native deoxygenated form. This experiment was also investigated using a stopped-flow device, and re-reduction was found to occur with an observed rate constant of approximately 75 s^{-1} , reflecting the bimolecular rate of reduction of (met)α^H-chains with sodium dithionite (Figure 4-3, inset). Additionally, no hemochrome intermediates were observed in these rapid mixing reactions in which broad spectral ranges in the Soret region were measured throughout the transition using a rapid-scanning stopped-flow device (not shown).

Collectively, these data indicate that AHSP causes accelerated autooxidation and hemichrome formation in α^H chains but not hemochrome formation when the iron is reduced. These AHSP-induced changes appear to be fully reversible, suggesting that AHSP:(met)α^H-chain complexes can be readily reduced to the ferrous state and are not necessarily part of an irreversible protein degradative pathway. Although several alternative hypotheses exist regarding the purpose of the AHSP-induced hemichrome conformation, the possibility that it is a folding intermediate has not been the subject of any comprehensive investigation. The findings in Chapter 3 which indicate

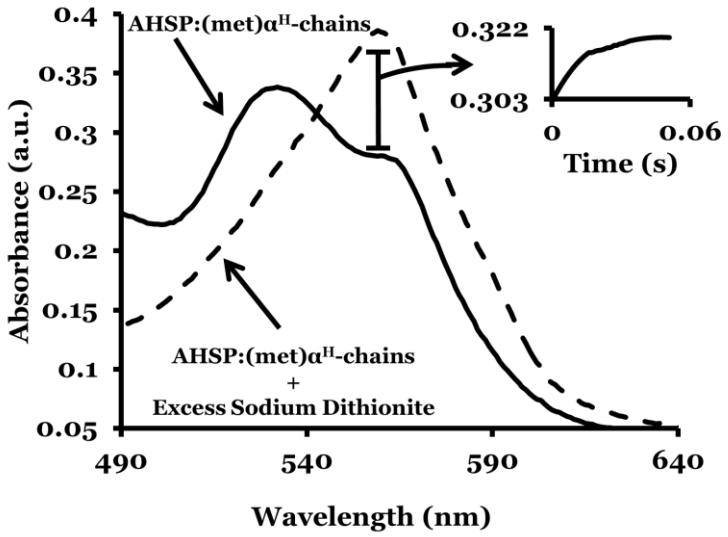

Figure 4-3. Reversibility of AHSP-induced α^H chain hemichromes

The experimental conditions used to collect these data are the same as those described in Figure 4-2. The Y-axis of the kinetic trace shown in the inset represents the absorbance increase following mixing, and is presented using arbitrary units (a.u.) with no offset. A Savitzky-Golay smoothing filter function (*535*) was applied to reduce signal noise in the inset using OriginPro 8.5.0 (OriginLab Corporation, Northhampton, Massachusetts, US). Unlike the inset in Figure 4-2, the post-mixing protein concentrations used in the inset for this figure were 2 μM. Plots were generated using Microsoft PowerPoint and Excel (Microsoft Corporation, Redmond, Washington, US).

a high affinity of AHSP for (met):α^H-chains, as well as the recent implication of hemichromes as HbA folding intermediates, raise the possibility of a novel AHSP mechanism. It may be that AHSP stabilizes ferric α^H chain folding intermediates until reduction can occur, after which the affinity of AHSP for α^H chains is lowered, facilitating its displacement by β^H chains and allowing HbA subunit assembly to proceed rapidly.

AHSP and Alpha Chain Hemin Loss and CO-Heme Binding

Another possible function of AHSP is that it favorably affects heme or hemin binding to or dissociation from α chains. Feng et al. (*445*, *471*) and Gell et al. (*508*) showed that AHSP binding to α^H chains (1) increases hemin solvent accessibility, (2) confers resistance to peroxide-induced hemin damage and loss, and (3) reduces the hemin-mediated catalysis of redox chemistry. These findings suggest that AHSP might affect the rate of heme binding and/or hemin loss from isolated α chains in solution, and these reactions were investigated using the methods of Hargrove et al. (*153-156*, *514*).

In the hemin loss experiments, solutions of α^H chains in complex with wild-type and mutant AHSP were reacted with excess potassium ferricyanide to oxidize the iron to the ferric state. This was done because the rate of reduced heme loss is too slow to measure, and the rate for hemin loss is readily obtained (*156*, *170*). Immediately following conversion to the met form, a myoglobin(Mb)–based hemin loss reagent was added to each solution. This hemin loss reagent consists of wild-type sperm whale apoMb (swMb^O) with the mutations His64Tyr and Val68Phe (*156*). These replacements enhance the stability of swMb^O and at the same time alter the spectral properties of the holo protein at 600 nm. Following the addition of excess H64Y/V68F swMb^O to the solutions, hemin is transferred from the (met)α^H-chains to the apoMb. The rate of increase in the absorbance signal at 600 nm is equal to the rate of hemin loss from the (met)α^H chains when the concentration of the apoMb is kept high.

As is depicted in Figure 4-4, AHSP increases the rate of hemin loss from α^H isolated chains. The observed rates of hemin loss from isolated (met)α^H

chains, AHSP:(met)α^H-chain complexes, AHSP^{P30A}:(met)α^H-chain complexes, and AHSP^{P30W}:(met)α^H-chain complexes are approximately 0.5 hr^{-1}, 0.9 hr^{-1}, 2 hr^{-1}, and 8.2 hr^{-1}, respectively, in 600 mM sucrose, 200 mM sodium acetate buffer, pH 5.5 at 10 ^{O}C. While an increase in hemin loss rates was the opposite of what was anticipated given that AHSP binding and hemichrome formation is thought to stabilize α^H chains (*443*, *445*, *471*), it is consistent with the finding of Feng et al. (*445*) that the F-helix holding the proximal histidine is disordered in AHSP:α^H-chain complexes. Also, as these data show, AHSP^{P30W} results in a dramatically increased rate of hemin loss. This finding supports the conclusion of Gell et al. (*508*) that Pro30 plays a prominent role in mediating heme-pocket structural alterations. In this case, these alterations result in an accelerated rate of hemin loss.

The rate of heme insertion into α^O globin was also investigated, again using methods reported by Hargrove et al. (*153*). In these experiments, solutions of CO-heme were mixed with α^O globin in a stopped-flow spectrophotometer at 5 ^{O}C to prevent thermal denaturation (*153*). Upon mixing, CO-heme insertion into the α^O globin distal pocket can be followed by monitoring absorbance increases at 419 nm (the CO-Soret peak) as a function of time (*153*). Data from representative experiments are show in Figure 4-5. In agreement with the report of Hargrove et al. (*153*), the resulting traces for these reactions are biphasic. Previous work has demonstrated that the fast phases correspond to CO-heme uptake by the distal pocket and the slow phases

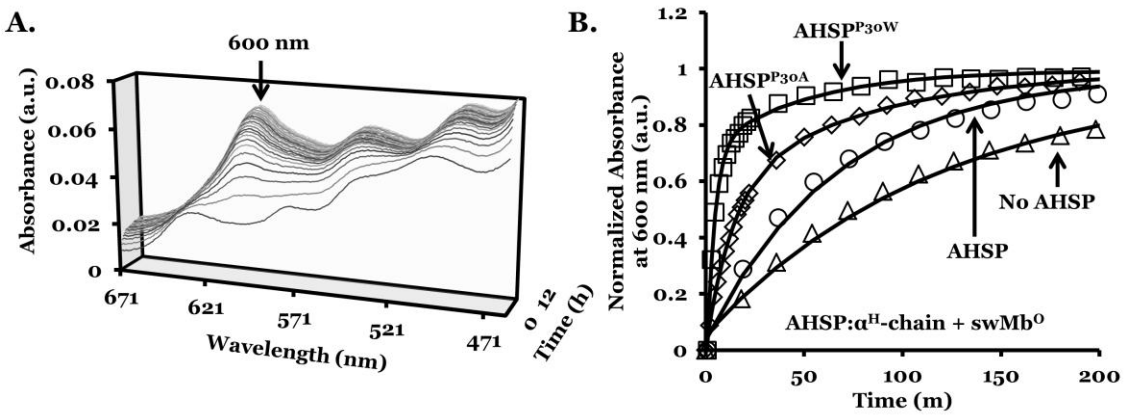

Figure 4-4. Effects of AHSP on α^H chain on hemin loss rates
Panel A, spectral changes during the course of a representative hemin loss reaction. Panel B, normalized time courses at 600 nm which indicate hemin loss rates. These experiments were conducted using buffer consisting of 600 mM sucrose, 200 mM sodium acetate buffer, pH 5.5 at 10 ^{O}C. Although it would have been preferable to study these reactions at 37 ^{O}C at pH 7.4, hemin loss causes immediate α^O globin precipitation and solution turbidity which interferes with monitoring the absorbance changes at 600 nm. Although lowering the temperature to 10 ^{O}C minimizes precipitation, these reactions are temperature dependent, and the pH was lowered to allow the hemin loss reactions to occur on measurable time scales. Each reaction included 6 μM α^H chains, 40 μM swMb^O, 30 μM potassium ferricyanide, and 6 μM of either AHSP, AHSP^{P30A}, or AHSP^{P30W}. Spectra were recorded every minute for approximately 12 hours. These reaction conditions were adapted from Hargrove et al. (*154-156*). In *Panel B*, data points are indicated by open squares, circles, triangles, and diamonds, with exponential fits depicted as lines. Plots were generated using Microsoft PowerPoint and Excel (Microsoft Corporation, Redmond, Washington, US).

correspond to CO-heme binding to non-specific sites on the protein (*153*). The rate of α^H chain formation during these reactions occurs with a second-order rate constant of approximately 4 x 10^7 M^{-1} s^{-1} in 50 mM Tris-HCl, 50 mM NaCl, pH 8.0 at 20 ^{O}C (*153*). This value agrees with the data presented here, and by comparing Figure 4-5A to Figure 4-5B, it is clear that AHSP does not detectably affect the rate of CO-heme binding to isolated α^O globin. This result, coupled with the hemin loss measurements, suggests that AHSP decreases the affinity of (met)α^H-chains for hemin by approximately 2-fold due to a 2-fold increase in the rate of hemin dissociation.

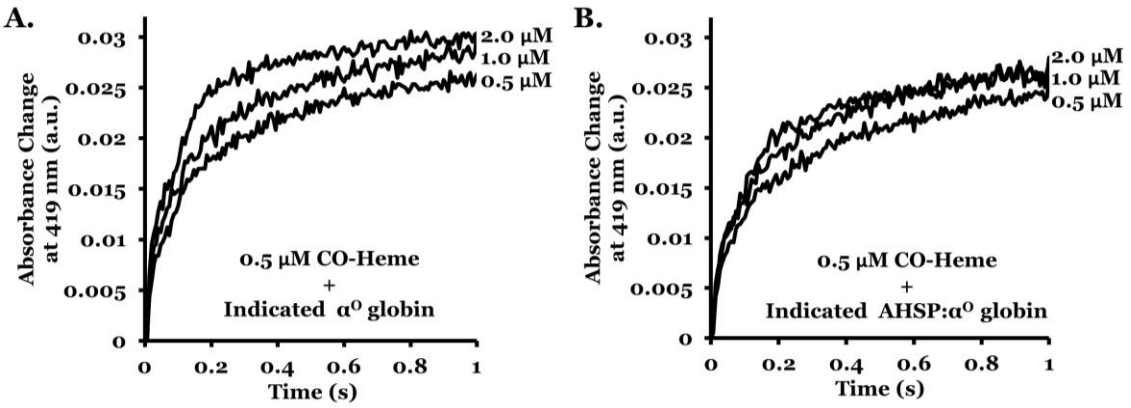

Figure 4-5. Effects of AHSP on αO globin CO-heme binding rates
Panel A, CO-heme uptake by α^O globin. *Panel B*, CO-heme uptake by AHSP:α^O-globin complexes. All reactions were performed using CO-saturated, 50 mM potassium phosphate buffer, pH 7.0 at 5 ^{O}C containing small amounts of sodium dithionite. The indicated concentrations are post-mixing values, and these traces were plotted with offsets. Plots were generated using Microsoft PowerPoint and Excel (Microsoft Corporation, Redmond, Washington, US).

AHSP and Alpha Chain O_2, CO Binding

The association and dissociation rate constants for O_2 binding to α^H chains in the presence and absence of AHSP were determined by laser flash photolysis using established methods (*512*, *536-538*). Complete sets of rate constants were measured for O_2 binding with the help of Mallory D. Salter (John S. Olson Laboratory, Rice University, Houston, Texas, US) and are shown in Table 4-1. These data show that wild-type AHSP binding causes a 33% decrease in the rate constant for O_2 association with α^H chains, implying that AHSP binding causes little change to the accessibility of the reduced heme group. However, the dissociation rate constant for O_2 release is increased by approximately 272% when α^H chains are bound to wild-type AHSP. This

increase suggests a weakening of the iron-ligand bond, possibly due to proximal strain caused by movement of the F-helix away from the heme plane (*445*, *471*).

	k'_{O_2} ($\mu M^{-1}s^{-1}$)	k_{O_2} (s^{-1})	k'_{CO} ($\mu M^{-1}s^{-1}$)	K_{A,O_2} (μM^{-1})	k_{autoox} (hr^{-1})
α^H-chain	45	36	5.5	1.2	0.06
AHSP:α^H-chain	30	98	1.2	0.30	0.98
AHSP^{P30A}:α^H-chain	31	39	2.3	0.80	0.30
AHSP^{P30W}:α^H-chain	28	24	4.0	1.2	0.23

Table 4-1. AHSP:α^H-chain ligand binding kinetic parameters
With the exception of the autooxidation studies, all measurements were made using 100 mM potassium phosphate buffer, pH 7.0 at 22 ^oC. The rate for α^H chain autooxidation in the absence of AHSP was taken from Zhou et al. (*473*). To prevent AHSP-induced autooxidation and hemichrome formation, all samples were kept on ice and were rapidly brought up to 22 ^oC before conducting the laser flash photolysis experiments. This table was generated using Microsoft PowerPoint (Microsoft Corporation, Redmond, Washington, US), and calculations were made using a Microsoft Excel spreadsheet that was created by George Blouin (Rice University, Houston, Texas, US).

These ideas are supported by the lowered bimolecular rate for CO binding to wild-type AHSP:α^H-chain complexes. O_2 binding to Hbs and Mbs is limited primarily by the rate of O_2 diffusion into the distal pocket, whereas CO binding is limited by the rate of bond formation from within the pocket (*512*). As a result, k'_{CO} is a more direct measure of the reactivity of the iron atom and restraints imposed by changes in the position of the proximal His(F8) and F-helix. The decrease in k'_{CO} and increase in k_{O_2} observed for binding to wild-type AHSP:α-chain complexes are consistent with 3-fold decreases in iron reactivity. These decreases appear to be caused by constraints imposed by AHSP Pro30,

because the values of k'_{CO} and k_{O_2} for α^H chains bound to $AHSP^{P30A}$ and $AHSP^{P30W}$ are more similar to those of free α^H chains.

Others have reported that higher O_2 dissociation rates correlate with increased autooxidation rates (*521*), and this trend is also observed for the AHSP:α^H-chain complexes shown in Figure 4-1 and Table 4-1 (*473*). The net effect of these alterations is that the affinity (K_A) of α^H chains for O_2 is diminished upon binding to wild-type AHSP and its resistance to autooxidation is decreased.

AHSP and Alpha Chain Secondary Structure

One hypothesis regarding AHSP function is that this protein binds α^O globins and α^H chains, and causes secondary structure changes within these subunits (*1*, *442*). Far ultra-violet circular dichroism (CD) spectropolarimetry is provides an estimate of the relative amounts of secondary structure that exists in a given protein sample (α-helices, β-sheets, random coils)(*539*). Because AHSP and α^H chains are almost exclusively α-helical in nature, light at wavelengths of 208 and 222 nm can be used in CD measurements to study the extent to which these proteins are fully folded (*539*).

In one experiment, CD spectra were recorded for samples of 10 μM AHSP, 10 μM α chains, and 10 μM AHSP:α-chain complexes. The resulting spectra were then plotted together, along with a theoretical trace that was generated by adding the individual spectra of AHSP and α chains together. By comparing this theoretical trace with the experimentally determined AHSP:α-chain complex spectrum, it is possible to probe whether AHSP and α chains

interact in a way that affects the sum of their secondary structure. Specifically, if AHSP binding causes α chains to fold, then stronger CD signals at 208 and 222 nm are predicted to be observed, giving the observed complex a greater CD signal intensity than the theoretical curve. According to the data set forth in Figure 4-6, it appears that AHSP does not increase the secondary structure of either α^O globins or α^H chains. These data agree with the work of Feng et al. (*445*, *471*) which show that AHSP binding results in several structural rearrangements, but that no new α-helices are formed upon complex formation. These findings can be contrasted with the recent work of Kumar et al. (*527*) which indicate using CD and NMR data that AHSP stabilizes α^O globin in a partially folded state.

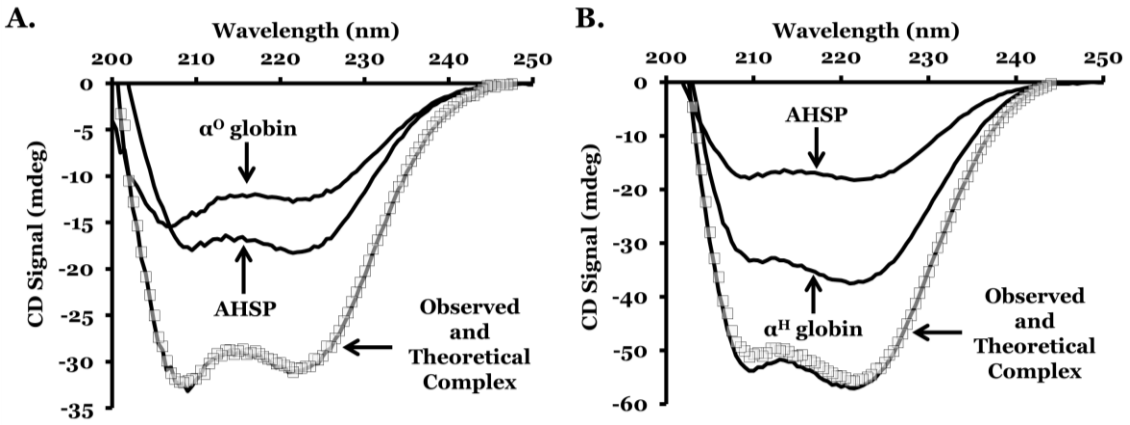

Figure 4-6. AHSP influence on α chain secondary structure
Panel A, CD spectra of AHSP, α^O globin, and AHSP:α^O-globin complexes. *Panel B*, CD spectra of AHSP, α^H globin, and AHSP:α-globin complexes. Experimentally recorded spectra (solid lines) were obtained in 50 mM potassium phosphate buffer, pH 7.0 at 5 ^{O}C. Theoretical spectra (shaded boxes) in each panel were computed by adding the individual AHSP and α chain spectra. AHSP, α chain, and AHSP:α-chain concentrations were fixed at 10 μM for these scans.

The main conclusions from these experiments are that (1) AHSP destabilizes $(O_2)\alpha^H$ chains with respect to hemin affinity, (2) AHSP does not appreciably alter the secondary structure of either α^H chains or α^O globins when

these proteins are co-incubated together, and (3) the high affinity of AHSP for (met)α^{H} chains and reversible AHSP-induced hemichrome formation indicate that AHSP may play a role in mediating α chain folding. This last conclusion is supported by the recent work of Culbertson et al. (*530*), who observed a (met)Mb hemichrome conformation during unfolding studies. Much like the data presented in this chapter, this intermediate exhibited a higher hemin loss rate than ferrous Mb, and could rapidly be converted to native and fully functional deoxy Mb with the addition of sodium dithionite (*530*).

Chapter 5: Hemoglobin Turriff (αK99E) as a Probe of AHSP Function

*Much of the information contained in this chapter was previously reported by Yu, Mollan et al. (*540*). The first section contains a review of that work, with subsequent sections presenting work that has been performed since that study was published.

Several members of the Mitchell J. Weiss Laboratory (University of Pennsylvania, Philadelphia, Pennsylvania, US), John S. Olson Laboratory (Rice University, Houston, Texas, US), and Andrew J. Gow Laboratory (Rutgers University, Piscataway, New Jersey, US) recently investigated the function of AHSP using a set of naturally occurring human α^H chain missense mutations, which were hypothesized to selectively affect binding to AHSP (*540*). One of these mutations occurs at position 99 of α chains, which is a lysine in wild-type subunits but is mutated to a glutamic acid (αK99E) in a hemoglobin variant called Hb Turriff (*540*, *541*). The importance of this variant as it relates to AHSP function was first discovered by Xiang Yu in the Mitchell J. Weiss Laboratory (*540*). Since that time, I have extended these studies at Rice University with the assistance of Jayashree Soman and Eileen Singleton.

Alpha Chain Mutants for Probing AHSP Function

In 2004, Feng et al. (*445*) reported detailed structural information regarding the AHSP:α^H-chain binding interface, including the identities of all the α^H chain residues which are thought to interact with AHSP during binding. Using this information, Yu et al. (*540*) conducted a series of literature-based searches for previously characterized α^H chain variants which contain mutations affecting these residues. Several naturally occurring α^H chain missense mutations were identified, and Yu et al. (*540*) hypothesized that these

mutations might result in altered or impaired interactions with AHSP which, in turn, might play a role in the phenotypes associated with these hemoglobinopathies. Yu et al. (*540*) undertook a series of binding studies designed to investigate this possibility.

AHSP and β^H chains have been shown to bind α^H subunits using a similar set of α^H subunit amino acids on the G and H helices (*445*, *471*). Competition between AHSP and β^H chains for the same surface implies that a missense mutation which affects AHSP:α^H-chain binding is also likely to affect interactions at the $\alpha^H_1\beta^H_1$ (or $\alpha^H_2\beta^H_2$) dimer interface, making it difficult to attribute missense mutation phenotypes to a single set of disrupted interactions. Additionally, it is possible for a missense mutation to adversely affect α^H chains through mechanisms that are unrelated to interactions with AHSP and β^H chains. For example, a particular mutation may destabilize α^H chains by causing abnormal or incomplete protein folding.

With these concerns in mind, Yu et al. (*540*) selected the following naturally occurring α^H chain missense mutations for analysis: R31S (Hb Prato), K99E (Hb Turriff), K99N (Hb Beziers), H103Y (Hb Lombard), H103R (Hb Contaldo), F117S (Hb Foggia), P119S (Groene-Hart), and A130D (Hb Yuda)(*487*, *540-551*). Structural work by Feng et al. (*445*) indicates that residues at positions 31, 103, 117, and 119 participate in interactions at the $\alpha^H_1\beta^H_1$ dimer interface, and that mutations corresponding to these positions will affect $\alpha^H_1\beta^H_1$ dimer formation (*540*). The same structural data indicate that residues at positions 99, 103, 117, and 119 participate in AHSP:α^H-chain interactions, and that that mutations corresponding to these positions will

affect AHSP:α^H-chain binding (*445*, *540*). Mutations affecting α^H chain position 130 were predicted to have little effect on either interface (*445*, *540*). These residue positions, their predicted contacts, and the names of the naturally occurring hemoglobinopathies (named after the city of discovery), are given in Figure 5-1.

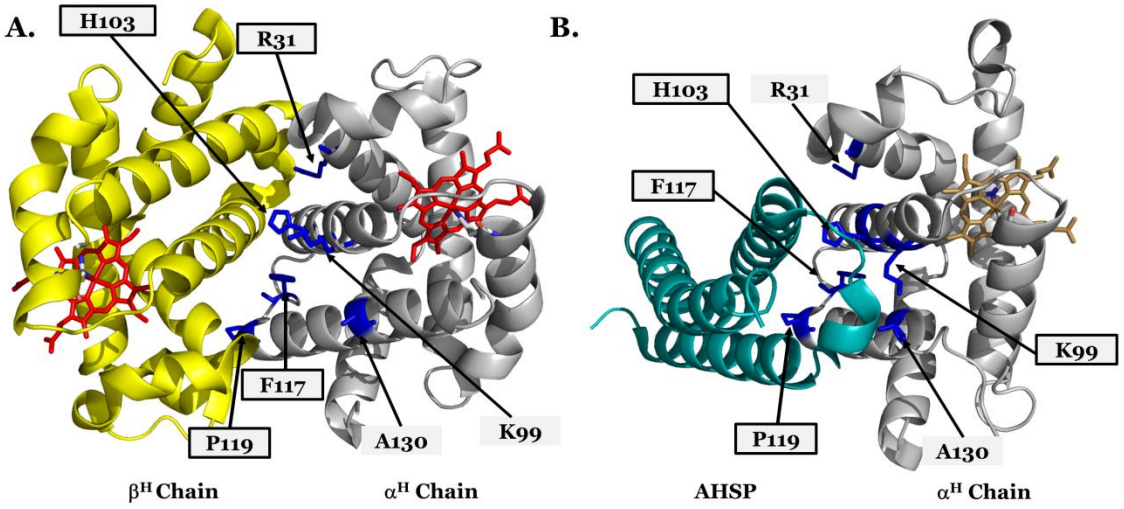

C.

	αWT	αR31S Prato	αK99E Turrif	αK99N Beziers	αH103Y Lombard	αH103R Contaldo	αF117S Foggia	αP119S Groene-Hart	αA130D Yuda
Predicted Contacts									
w/ AHSP	Yes	No	Yes	Yes	Yes	Yes	Yes	Yes	No
w/ β^H Chains	Yes	Yes	No	No	Yes	Yes	Yes	Yes	No

Figure 5-1. Clinically significant α^H chain residues
Panel A, $\alpha^H{}_1\beta^H{}_1$ dimer interface. *Panel B*, AHSP:α^H-chain interface. Panel C, predicted binding partner interactions for each interface. In Panels A and B, boxes around each label are used in to indicate predicted interactions based on available structural data (*445*, *471*). Colors and ribbon and stick forms are the same as those used in Figure 1-8, except residues of interest are shown in blue stick form with labels in Panels A and B. These panels depict wild-type proteins, except AHSP bears the P30A mutation and a C-terminal truncation of 11 residues. Drawings were produced using the PyMol Molecular Graphics System and PDB entries 1LFL and 1Z8U (DeLano Scientific, Palo Alto, California, US)(*113*, *471*). The table in Panel C was adapted from Yu et al. (*540*) and was generated using Microsoft PowerPoint (Microsoft Corporation, Redmond, Washington, US).

Three assays were used to investigate AHSP:α^H-chain binding: (1) AHSP co-expression with α^H chains in *E. coli* and measurement of relative α^H chain

levels by Western blotting, (2) α^H chain production using a eukaryote-based protein expression system, with binding to AHSP being investigated by GST pull-down methods using GST-AHSP as bait, and (3) α^H chain production using the same eukaryote-based system, with binding to AHSP being investigated by measuring resistance to trypsin digestion (*442*, *540*). Two assays were used to assess $\alpha^H{}_1\beta^H{}_1$ dimer formation: (1) electrophoretic mobility shift assays using isoelectric focusing and α^H chains that were expressed in the eukaryote-based protein production system, and (2) β^H chain co-expression with α^H chains in *E. coli*, with relative α^H chain expression yields being approximated by Western blot (*540*).

The *E. coli* expression assays described above were performed using protocols and vectors that were developed at Rice University (Houston, Texas, US). However, all the bench work was done by members of the Mitchell J. Weiss Laboratory (University of Pennsylvania, Philadelphia, Pennsylvania, US) (*540*). The underlying premise most of these experiments is that α^H chains will not be detectably produced unless they are bound to AHSP or β^H chains. This assumption has been verified by studies showing that in the absence of a binding partner, α^H chains are too unstable to remain in solution at 25 to 35 ^{O}C and are readily degraded in *E. coli* (*228*, *247*, *441*). The results of each of these assays are summarized in Table 5-1.

	WT	R31S Prato	K99E Turrif	K99N Beziers	H103Y Lombard	H103R Contaldo	F117S Foggia	P119S Groene-Hart	A130D Yuda
AHSP:α^H-Chain									
Co-expression in E. coli	++	++	+	+	+	-	+	-	++
GST Pulldown	++	+	-	-	-	-	-	-	++
Trypsin Digest	++	-	-	-	-	-	-	-	+
$\alpha^H{}_1\beta^H{}_1$									
Monomer Shift Assay	++	-	++	++	+	-	ND	++	++
Co-expression in E. coli	++	-	++	++	-	-	-	-	++
Summary of Effects									
AHSP Binding	++	++	+	+	+	-	+	-	++
β^H Chain Binding	++	-	++	++	+	-	-	+	++

Table 5-1. Summary of mutant α^H chain synthesis, binding evidence
In this table, ++ indicates normal α^H chain production and detection of partner binding, + indicates reduced interactions, – indicates no detectable production or partner binding, and ND indicates that the presence or absence of interactions were not determined. This table was adapted from Yu et al. (*540*) and was generated using Microsoft PowerPoint (Microsoft Corporation, Redmond, Washington, US).

In agreement with structural predictions, these data reveal that some of these mutations (H103Y, H103R, F117S, and P119S) impair both $\alpha^H{}_1\beta^H{}_1$ dimer and AHSP:α^H-chain complex formation, suggesting at least two plausible mechanisms which might explain the anemia, microcytosis, hypochromia, Heinz body formation, and other issues observed in individuals bearing these mutations (*540*). Also, as was initially predicted, one mutation (A130D) did not detectably disrupt binding at either interface. In contrast, mutations at α^H chain position 99 (K99E, K99N) selectively impaired AHSP:α^H-chain interactions while leaving $\alpha^H{}_1\beta^H{}_1$ dimer interface formation unaffected (*540*). This indicates that the clinical features associated with the K99 mutations are likely caused by impaired AHSP:α^H-chain interactions and not by disruption of the $\alpha^H{}_1\beta^H{}_1$ dimer interface (*540*).

Significance of Hb Turriff

The Hb Turriff (K99E) mutation is of particular interest, because previous studies using hemolysates from individuals bearing this mutation indicate that this mutation causes α^H chain instability leading to excess β^H chains (*540*, *541*, *552*). Consistent with this information, the work of Yu et al. (*540*) indicates that wild-type AHSP does not interact with K99E α^H chains, and that this disrupted interaction may lead directly to α^H chain instability and loss of expression in vivo. To test this idea directly, a series of revertant AHSP mutants were designed in our laboratory (*540*). We hypothesized that it should be possible to construct an AHSP mutant that would restore binding to and stabilization of K99E α^H chains (*540*). This restored binding is predicted to facilitate K99E α^H chain expression (*540*).

As is shown in Figure 5-2, the positively charged ε-amino group of K99 in α^H chains is in close proximity to the terminal atoms of the AHSP Q25 and D29 side chains. Mutating the α^H chain lysine to a glutamic acid (K99E) introduces a negative charge which is expected to cause unfavorable electrostatic interactions with the AHSP D29 side chain. To alter the charge on the complementary surface of AHSP and potentially restore binding to K99E α^H chains, AHSP Q25 and D29 were mutated to lysine and arginine residues (four single mutants were constructed: $AHSP^{Q25K}$, $AHSP^{Q25R}$, $AHSP^{D29K}$, $AHSP^{D29R}$). These mutant proteins were then assayed to determine whether they could bind to and stabilize Hb Turriff α^H chains.

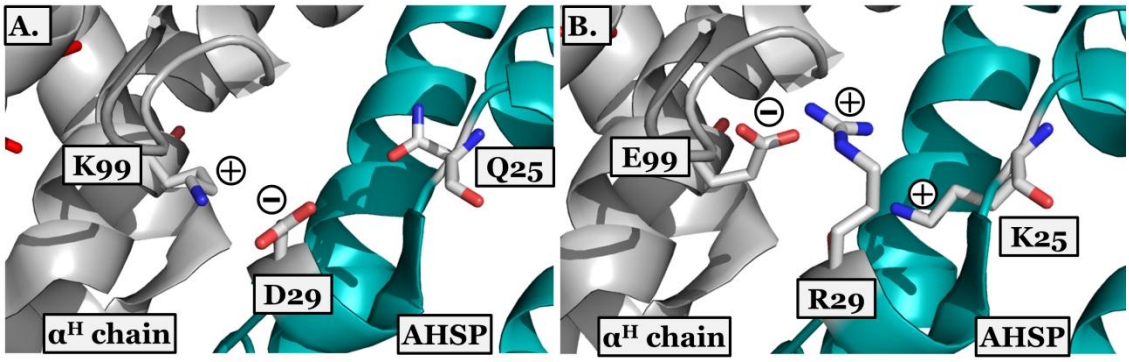

Figure 5-2. Wild-type, mutant AHSP:α^H-chain binding interfaces
Panel A, wild-type AHSP:α^H-chain interface. *Panel B*, theoretical model of mutant AHSP:α^H-chain interactions. The α^H chain K99 and AHSP Q25 and D29 side chains are depicted as CPK-colored sticks, and are predicted to stabilize the AHSP:α^H-chain interface in wild-type proteins. The α^H chain K99E mutation is predicted to disrupt these favorable electrostatic interactions. Favorable interactions between the negatively charged α^H chain E99 side chain and the positively charged AHSP revertants K25 and R29 are predicted to restore AHSP:α^H-chain heterodimerization. Colors and ribbon and stick forms are the same as those used in Figure 1-8. These panels depict wild-type proteins, except AHSP bears the P30A mutation and a C-terminal truncation of 11 residues. Drawings were produced using the PyMol Molecular Graphics System and PDB entry 1Z8U, and *Panel B* was generated using the mutagenesis wizard that is built-in to this software (DeLano Scientific, Palo Alto, California, US)(*471*).

Yu et al. (*540*) investigated binding between K99E α^H chains and the AHSP revertants using: (1) AHSP co-expression with α^H chains in *E. coli*, (2) α^H chain production using an in vitro wheat germ extract protein expression system with the addition of exogenous AHSP, and (3) co-expression of α^H chains and AHSP in murine erythroleukemia cells. These assays indicated that $AHSP^{D29R}$ and $AHSP^{Q25K}$ restored interactions with K99E α^H chains and increased K99E α^H chain expression levels (*540*). They also suggested that the AHSP mutants can stabilize K99E α^H chains, whereas wild-type AHSP does not appear to interact significantly with this mutant (*540*).

Binding of Hb Turriff α^H Chains to AHSP, β^H Chains

To verify the findings of Yu et al. (*540*), recombinant Hb Turriff was produced at Rice University using the methods described in Chapter 2. Individual subunits were isolated from these tetramers, and a series of binding studies were performed. The behavior of recombinant Hb Turriff during its expression and purification was not discernibly different from that of wild-type recombinant HbA. Because the recombinant Hb Turriff tetramers contain no wild-type α^H chains, this observation strengthens the previous conclusion that K99E α^H chains are able to interact relatively normally with wild-type β^H chains.

Two methods were used to confirm that the recombinant K99E α^H chains are capable of re-binding to wild-type β^H chains after separating and isolating the individual subunits. First, cellulose acetate electrophoresis was conducted on mutant and wild-type subunits. As shown in Figure 5-3 samples of native α^H chains (lane 1), native β^H chains (lane 2), and a mixture of these two samples (lane 3, slight excess of β^H chains) reveal that these proteins are capable of recombining to form HbA. Similarly, when recombinant K99E α^H chains (lane 4) are mixed with the same sample of native β^H chains, they recombine to form a band with a similar migration pattern to the one corresponding to HbA (lane 5, slight excess of β^H chains). The difference between the migration patterns of native α^H chains and K99E α^H chains is caused by differences in the isoelectric points of the proteins (*541*). As is apparent from comparisons between lanes 3 and 5, these differences also contribute to a slight difference in the migration pattern between the resulting

tetramer bands (*541*). Critically, these data show that K99E α^H chains are capable of recombining with native β^H chains to form Hb Turriff.

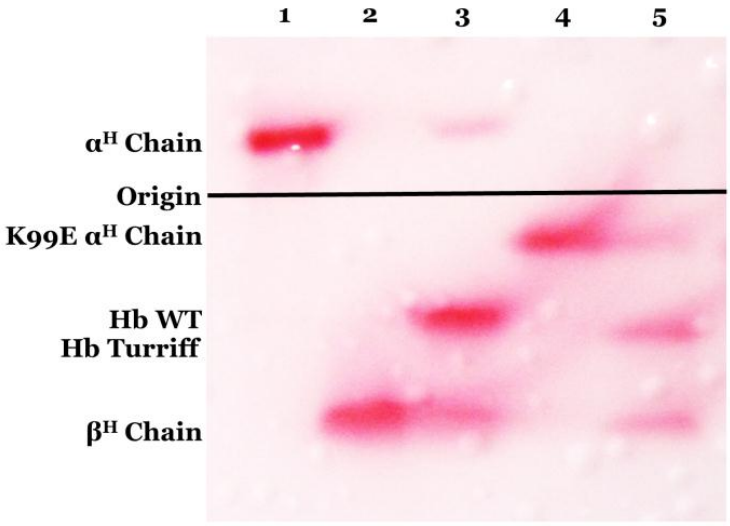

Figure 5-3 Electrophoresis of wild-type, mutant subunits
Materials, buffers, and apparatus for this cellulose acetate electrophoresis membrane were obtained from Helena Laboratories, Incorporated (Beaumont, Texas, US). Proteins were stained with Ponceau S stain. The following samples were run in accordance with manufacturer instructions: native α^H chains (lane 1), native β^H chains (lane 2), a mixture of native α^H chains and native β^H chains (lane 3), recombinant K99E α^H chains (lane 4), and a mixture of recombinant K99E α^H chains with native β^H chains (lane 5).

The second method of confirming that K99E α^H chains are capable of rebinding to wild-type β^H chains involves rapidly mixing the deoxygenated subunits and measuring absorbance changes associated with tetramer formation. Deoxy subunits exhibit unique absorbance spectra in the Soret spectral region depending on whether they are in the high affinity (R) or low affinity (T) quaternary state (*191*). Both monomers and dimers have R-state like conformations whereas associated deoxy tetramers exhibit T-state spectra (*191*). The molar extinction coefficients of isolated (deoxy)α^H chains and

(deoxy)β^H chains at 430 nm are 120 and 117 mM^{-1} cm^{-1}, respectively, and are significantly different from the molar extinction coefficient of deoxyHbA tetramers at this same wavelength, which is 145 mM^{-1} cm^{-1} (*494*). Differences also exist at 445 nm (*193*). Thus, when separated deoxy subunits are mixed together, spectral changes at these wavelengths can be followed as a function of time to observe tetramer formation (*193*). This method was used previously to study the kinetics of HbA formation from isolated α^H- and β^H-chains (*201*). As is shown in Figure 5-4, K99E and wild-type α^H chains combine with native β^H chains to form tetramers at roughly the same rate.

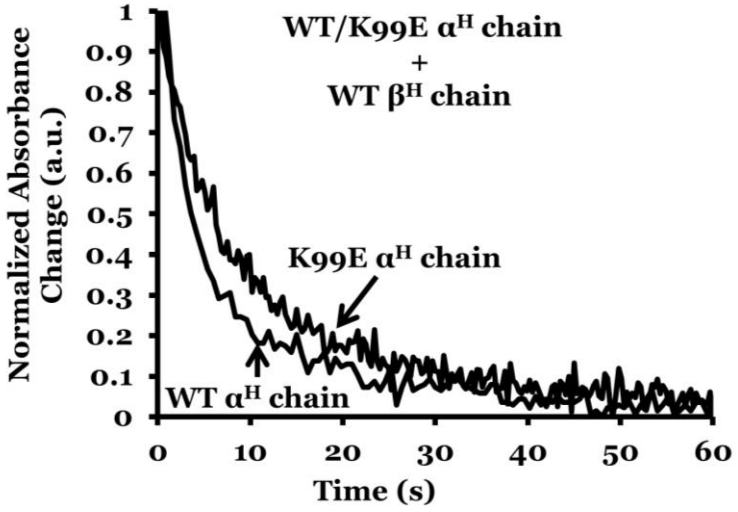

Figure 5-4. (K99E)α^H chain association with β^H chains
The buffer used for this experiment was 10 mM potassium phosphate buffer, pH 7.3 at 20 ^oC. For the reaction involving K99E α^H chains, the post-mixing concentration values were 5 μM for α^H and β^H chains, and reactions were followed at 430 and 445 nm. For the reaction involving wild-type (WT) α^H chains, the post-mixing concentrations were 3 μM for α^H and β^H chains, and reactions were followed at 445 nm only. Traces were normalized to total absorbance changes.

Next, two assays were used to investigate the presence or absence of binding between K99E α^H chains and wild-type human AHSP. Both approaches

are based on the experimental framework developed in Chapter 3. First, the fluorescence intensity of wild-type AHSP was measured as it was added into solutions of 15 μM K99E α^H chains, and little or no quenching of AHSP fluorescence was observed following each addition (Figure 5-5A). The pattern of fluorescence signal increases observed in this experiment resembles the trend observed for the titration of wild-type AHSP into β^H chains (Figure 3-1C), suggesting that there is no interaction between K99E α^H chains and wild-type AHSP. Second, samples of K99E α^H chains were mixed with wild-type AHSP using a stopped-flow fluorescence emission spectrophotometer (Figure 5-5B). Again, there is no fluorescence quenching of AHSP by K99E α^H chains, whereas a large and rapid decrease in intensity occurred when the same amount of wild-type α^H chains were mixed with wild-type AHSP.

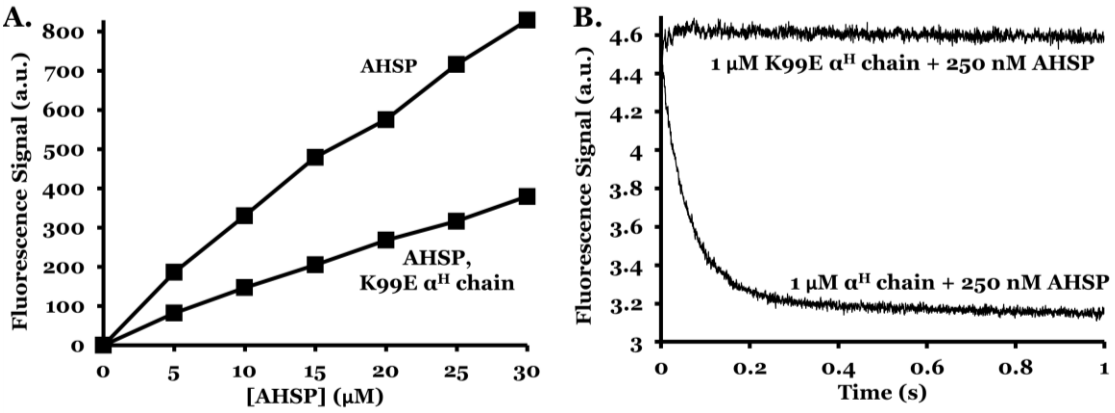

Figure 5-5. Intrinsic fluorescence emission of AHSP, (K99E)α^H chains
The buffer utilized for these experiments was 50 mM potassium phosphate, pH 7.0 at 21 ^{O}C, which had been saturated with CO prior to use. The experimental apparatus configurations were the same as those used in Figure 3-1. Plots were generated using Microsoft Excel and PowerPoint (Microsoft Corporation, Redmond, Washington, US).

Collectively, the data in Figures 5-3, 5-4, and 5-5 confirm the findings of Yu et al. (*540*) that K99E α^H chains are capable of interacting with β^H chains to

form tetrameric Hb Turriff, but that K99E α^H chains are incapable of binding to wild-type AHSP. The previous finding that K99E α^H chains are not detectably expressed in *E. coli* by themselves or with wild-type AHSP indicates that these chains are unstable by themselves. Thus, the clinical features associated with this hemoglobinopathy appear to be caused by impaired interactions with AHSP (*540*).

Interactions Between Hb Turriff α^H Chains and Wild-Type, Revertant AHSP

The data reported by Yu et al. (*540*) indicated that, although K99E α^H chains are capable of binding to both AHSP^{Q25K} and AHSP^{D29R}, the affinities for these interactions appear to be different. Using the methods described in Chapter 3, the following sets of binding and dissociation reactions were investigated: (1) AHSP^{Q25K} with K99E α^H chains, (2) AHSP^{Q25K} with wild-type α^H chains, (3) AHSP^{D29R} with K99E α^H chains, and (4) AHSP^{D29R} with wild-type α^H chain. These studies confirm the initial findings of Yu et al. (*540*), and extend this work by better defining the electrostatics at the AHSP:α^H-chain interface.

The bimolecular association experiments for reactions (1) and (3) are shown in Figure 5-6, along with plots of the observed rate constants versus α^H chain concentrations under pseudo-first order conditions. These data indicate that K99E α^H chains are capable of rapidly binding to both AHSP^{D29R} and AHSP^{Q25K} (Figure 5-6A). However, these binding events are associated with smaller fluorescence changes than those that are produced by wild-type

AHSP:α^H-chain binding under nearly identical conditions (Figure 5-6A). Also, small slow phases lasting longer than several hundred seconds were observed in these reactions at all concentrations assayed (not shown), indicating either cis/trans Pro30 isomerization or slow precipitation of the α^H chains. It is clear that the affinity of K99E α^H chains for AHSP^{Q25K} and AHSP^{D29R} is much less than that of wild-type α^H chains for wild-type AHSP.

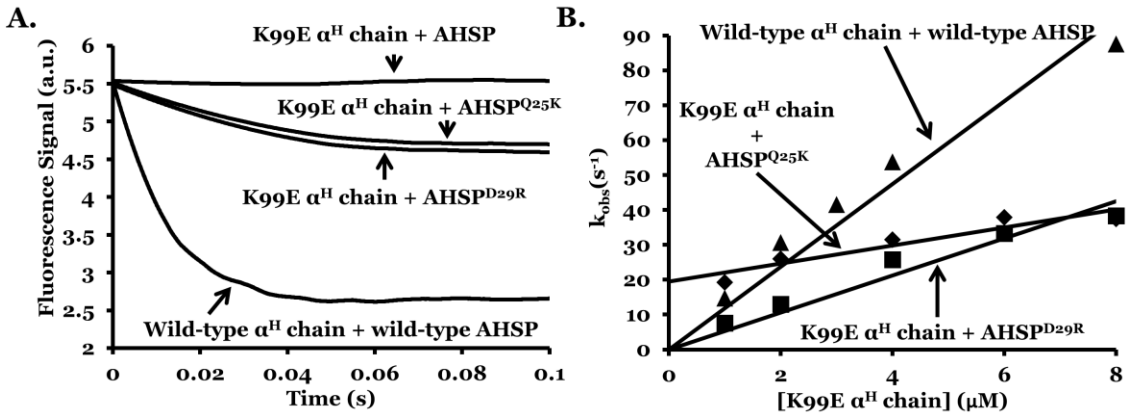

Figure 5-6. AHSP^{Q25K}, AHSP^{D29R} binding to Hb Turriff α^H chains
Panel A, (K99E)α^H chain association reactions with wild-type AHSP, AHSP^{Q25K}, and AHSP^{D29R}. *Panel B*, plots used to determine the bimolecular association rate constants for the proteins in *Panel A*. The instrumental configuration for these experiments was the same as was used in Figure 3-1, Panel D. Concentrations of AHSP were 250 nM post-mixing, and concentrations of α^H chains were 8 μM post-mixing in *Panel A* and were varied in *Panel B*. In both panels, the reactions of wild-type AHSP with wild-type α^H chains are included for comparison. In *Panel A*, an offset was used to normalize the data for comparison, and a Savitzky-Golay smoothing filter function (*535*) was applied to reduce signal noise using OriginPro 8.5.0 (OriginLab Corporation, Northhampton, Massachusetts, US). Plots generated using Microsoft Excel and PowerPoint (Microsoft Corporation, Redmond, Washington, US).

Because the AHSP revertants involve mutations to residues that are in close proximity Pro30, it is plausible that the slow phases observed during bimolecular association are related to structural alterations and/or altered cis-trans peptidyl-prolyl isomerization. Thus, apart from the predicted electrostatic changes that these mutations could induce, there may also be structural

rearrangements and changes in the cis/trans equilibrium. Consistent with this idea, it was found that wild-type α^H chains are capable of binding to both $AHSP^{Q25K}$ and $AHSP^{D29R}$ (Figures 5-7A and 5-7B), and very slow phases are still observed. Wild-type α^H chain binding reactions are associated with strong fluorescence changes that are similar to those seen with wild-type AHSP:α^H-chain binding. This finding suggests that the disrupted binding between wild-type AHSP and K99E α^H chains is not due exclusively to charge repulsion between D29 AHSP and E99 α^H chain side chains. If this were the case, wild-type α^H chains would be predicted to bind poorly to the revertant AHSP mutants, due in this case to repulsion between the positively charged (K99) α^H chain and AHSP R29 side chains. Thus, these data suggest that structural elements in the loop separating AHSP helices 1 and 2, as well as electrostatics, are important determinants of α^H chain binding.

The displacement reactions for wild-type and (K99E) α^H chain interactions with wild-type and mutant AHSP were also measured, and the resulting data are presented in Figure 5-8. The dissociation reactions involving $AHSP^{D29R}$:(K99E)α^H-chain and $AHSP^{Q25K}$:(K99E)α^H-chain complexes were found to be much more rapid than those for wild-type AHSP:α^H-chain complexes (Figures 5-8A and 5-8B). In the case of the $AHSP^{Q25K}$:(K99E)α^H-chain complex, no displacement reaction was observed at 250 nM concentrations and the fluorescence of the $AHSP^{Q25K}$:(K99E)α^H chain complex was similar to that of the AHSP mutant alone. Raising the post-mixing concentrations of the $AHSP^{Q25K}$:(K99E)α^H-chain mixture to 6 μM did result in

small and rapid fluorescence increases after mixing with (CO)β^H chains (Figure 5-8A, inset). Thus, some AHSP^{Q25K}:(K99E)α^H-chain complex did form

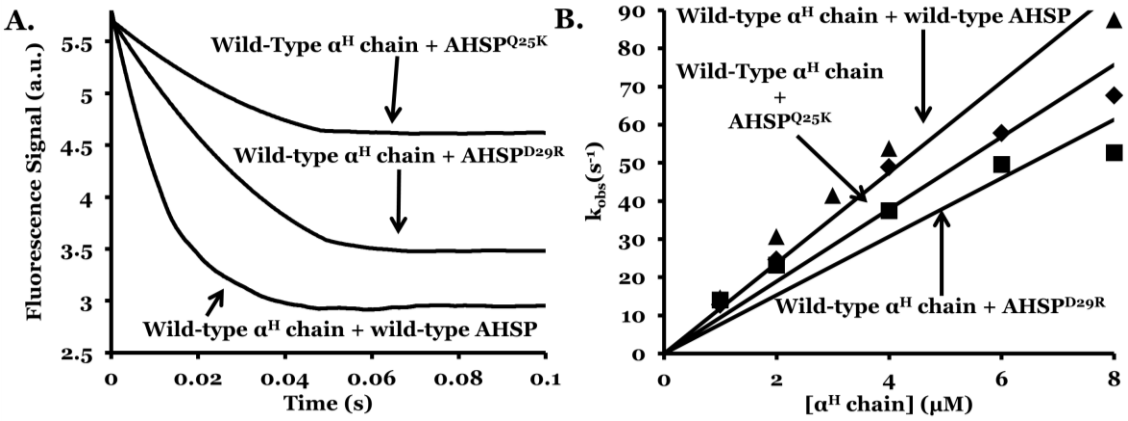

Figure 5-7. AHSP^{Q25K}, AHSP^{D29R} binding to wild-type α^H chains
Panel A, wild-type α^H chain association reactions with wild-type AHSP, AHSP^{Q25K}, and AHSP^{D29R}. *Panel B*, plots used to determine the bimolecular association rate constants for the proteins in *Panel A*. The instrumental configuration for these experiments was the same as was used in Figure 3-1, Panel D. Concentrations of AHSP were 250 nM post-mixing, and concentrations of α^H chains were either fixed at 8 μM post-mixing in *Panel A* or were varied as indicated in *Panel B*. In both panels, the reactions of wild-type AHSP with wild-type α^H chains are included for comparison. In *Panel A*, an offset was used to normalize the data for comparison, and a Savitzky-Golay smoothing filter function (*535*) was applied to reduce signal noise using OriginPro 8.5.0 (OriginLab Corporation, Northhampton, Massachusetts, US). Plots were generated using Microsoft Excel and PowerPoint (Microsoft Corporation, Redmond, Washington, US).

at this higher concentration, but clearly the K_D for complex formation is high. This conclusion is consistent with the bimolecular association data presented in Figure 5-6B. Using those data, the Y-intercept of the AHSP^{Q25K} trend line provides an estimate for the dissociation rate constant of 17 ± 2 s^{-1}, which is a much faster than the rate of dissociation of wild-type AHSP:α^H-chain complexes (~.19 s^{-1}, see Chapter 3). This value was used as the basis for generating the theoretical replacement reaction curve shown in Figure 5-8B (inset, dashed line).

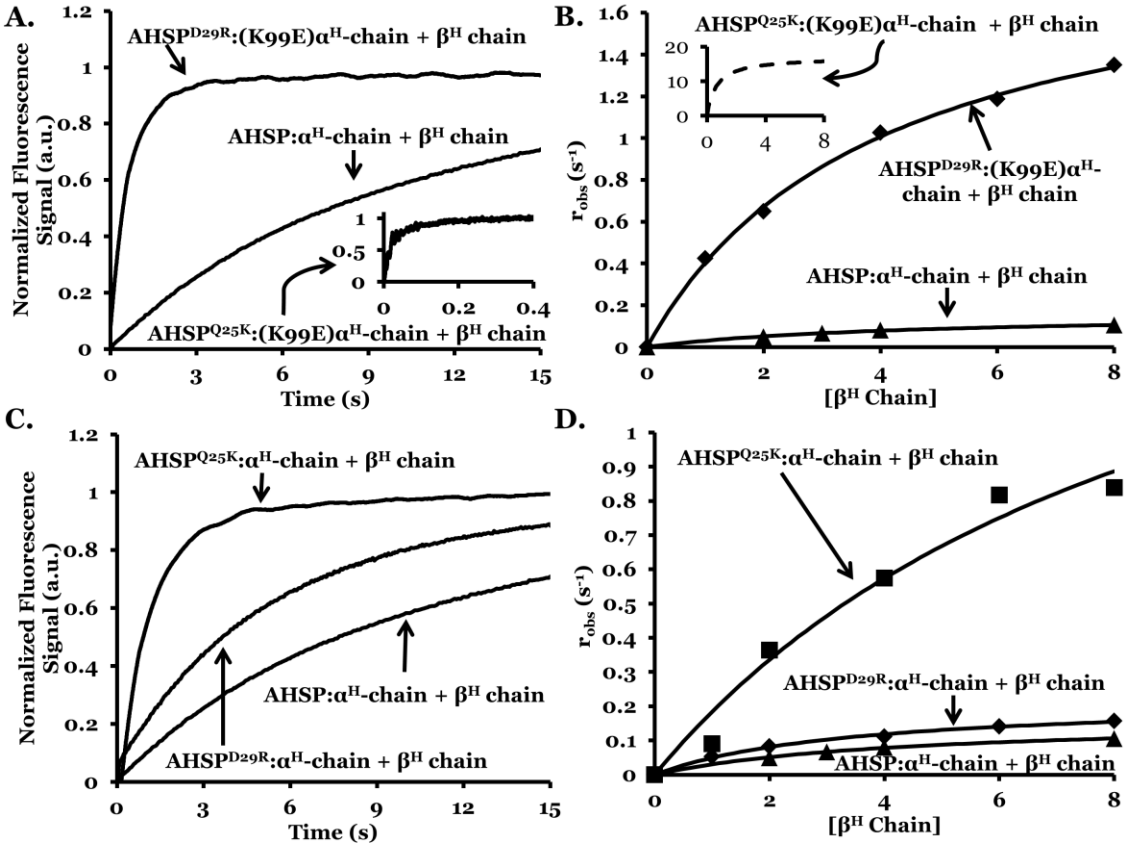

Figure 5-8. (K99E)α^H chain, AHSP revertant displacement reactions
Panel A, AHSP^{Q25K}, AHSP^{D29R} dissociation from (K99E)α^H chain complexes. *Panel B*, plot of the observed rates of AHSP^{D29R}:(K99E)α^H-chain dissociation at various concentrations of β^H chains, and an analogous theoretical curve for AHSP^{Q25k}:(K99E)α^H-chain dissociation (inset). Panel C, AHSP^{Q25K}, AHSP^{D29R} dissociation from wild-type α^H chain complexes. Panel D, plot of the observed rates of AHSP^{Q25K}:α^H-chain and AHSP^{D29R}:α^H-chain dissociation at various concentrations of β^H chains. The instrumental configuration for these experiments was the same as was used in Figure 3-1, Panel D. In Panels A and C, the concentrations of AHSP:α^H-chain complexes were 250 nM post-mixing and the concentrations of β^H chains were 8 μM post-mixing. In the inset of *Panel A*, AHSP:α^H-chain complexes were 6 μM post-mixing. In all panels, the reactions involving wild-type AHSP:α^H-chain dissociation are included for comparison. Plots were generated using Microsoft Excel and PowerPoint (Microsoft Corporation, Redmond, Washington, US).

The displacement reactions involving wild-type α^H chain dissociation from AHSP^{D29R} and AHSP^{Q25K} were also investigated, and the data are shown in Figures 5-8C and 5-8D. In both cases, dissociation was more rapid than what was observed for wild-type AHSP:α^H-chain complex dissociation, although

neither reaction was as rapid as the dissociation of AHSP^{D29R}:(K99E)α^{H}-chain and AHSP^{Q25K}:(K99E)α^{H}-chain complexes. The kinetic parameters calculated from these reactions are presented in Table 5-2.

	k_{AHSP} (s^{-1})	k'_{AHSP} ($\mu M^{-1}s^{-1}$)	$k'_{\alpha\beta}$ ($\mu M^{-1}s^{-1}$)	$K_{D, AHSP}$ (nM)
AHSP:α^{H}-chain	0.19 ± 0.02	8.5 ± 2.1	0.17 ± 0.07	22 ± 7.7
AHSP:(K99E)α^{H}-chain	nd	nd	nd	nd
AHSP^{Q25K}:(K99E)α^{H}-chain	17	2.5	nd	6,800
AHSP^{D29R}:(K99E)α^{H}-chain	1.6	4.7	0.17	340
AHSP^{Q25K}:α^{H}-chain	1.9	9.5	0.12	200
AHSP^{D29R}:α^{H}-chain	0.22	7.7	0.28	28

Table 5-2. Kinetic parameters for α^{H} chain, AHSP revertant interactions
The data used in these calculations were collected using the same instrumental configuration as described in Figure 3-1D. Rate parameters and dissociation equilibrium constants for these reactions were calculated using the same methods that were used in Chapter 3. However, AHSP^{Q25K}:α^{H}-chain dissociation could not be measured using these techniques due to its low affinity. In this case, the dissociation rate constant was estimated from the bimolecular association studies shown in Figure 5-6, and $k'_{\alpha\beta}$ was not determined (ND). Reactions involving these proteins were done twice, and the numbers provided in this table represent averages of the obtained values: AHSP^{Q25K}:(K99E)α^{H}-chain complexes and AHSP^{D29R}:(K99E)α^{H}-chain complexes. Reactions AHSP^{Q25K}:α^{H}-chain complexes and AHSP^{D29R}:α^{H}-chain complexes were only measured once. Calculations were done using Microsoft Excel and the table was constructed using Microsoft PowerPoint (Microsoft Corporation, Redmond, Washington, US).

Both the bimolecular association and the displacement studies of these proteins show that both AHSP^{Q25K} and AHSP^{D29R} can bind Turriff and wild-type α^{H} chains, with AHSP^{D29R} exhibiting tighter binding to both α^{H} chains. These data are in full agreement with the report of Yu et al. (*540*), which indicated

that AHSP^{D29R} was more effective at restoring binding to (K99E)α^{H} chains than AHSP^{Q25K}. These results also show that: (1) (K99E) α^{H} chains do not detectably bind to wild-type AHSP, and that these disrupted interactions can plausibly account for the clinical features associated with Hb Turriff, (2) electrostatics involving α^{H} chain K99 play a prominent role in binding to wild-type AHSP, and when these interactions are disrupted by the K99E mutation, they can be restored by compensatory AHSP mutations which similarly effect electrostatics, and (3) electrostatics are not the only factor involved with binding, because the loop separating AHSP helices 1 and 2 appears to mediate conformational changes which significantly affect binding.

Chapter 6: Co-Expression of AHSP with Recombinant HbA

This chapter describes the construction of a novel rHb expression system that is useful for assaying whether the co-expression of AHSP with HbA in *E. coli* results in increased HbA expression yields. This work was done with the assistance of Eileen Singleton, Jayashree Soman, and Neil Varnado of the John S. Olson Laboratory, and Mary Harrison of the George N. Bennett Laboratory at Rice University.

Expression System Construction

Optimizing rHb production from *E. coli*-based heterologous protein expression systems involves investigating a diverse set of variables relating to molecular biology, fermentation conditions, and downstream processing methods (*252*, *254-265*, *267-276*). Although significant work has already been done in this area (*211*, *225*, *226*, *282*, *283*), recent efforts have shown that the co-expression of hemin transport proteins with rHbs in *E. coli* helps to bolster expression yields (*39*, *213*, *216*, *436*, *437*, *553-555*). Available information regarding AHSP function suggests that it might be of similar utility.

AHSP has been co-expressed with α^{H} chains by several groups using several different expression systems (*440-442*, *445*, *471*, *540*). It has also been co-expressed with human-bovine hybrid rHb in *E. coli* (*556*). Additionally, AHSP has been expressed in a wheat germ transcription and translation system designed to study HbA subunit assembly (*442*). Although these studies have

consistently indicated that AHSP facilitates α^H chain expression, there remains very little published work addressing whether this protein can be used to increase production yields of tetrameric rHb.

Because GST has a molecular mass that is more than twice that of AHSP, overexpressing this protein along with AHSP is predicted to cause a significant strain on cellular resources. As an initial step towards optimizing the co-expression of AHSP with rHb, the *gst* gene was removed from the N-terminus of the *ahsp* gene in pre-existing expression vectors. To accomplish this, the *ahsp* gene was cloned into a vector, pBAD33, that was provided by George N. Bennett (Rice University, Houston, Texas, US)(*557*). This vector was chosen as an AHSP expression plasmid for the following reasons. First, AHSP expression can be induced with exogenous L-arabinose, which is an inexpensive alternative to IPTG (*557*). Second, AHSP expression levels can be fine-tuned by varying the amount of inducer added to the culture media (*557*). Third, high-yield heterologous protein expression using pBAD vectors has previously been well established (*557*). Fourth, pBAD33 has a selectable marker and an origin of replication which are compatible with those of other rHb expression vectors (*557*). The HbA expression vector rHb 0.0 was selected to be used in conjunction with pBAD33, since this plasmid has been used extensively in previous rHb expression studies (*211*, *225*, *226*, *248*, *250*). The features of each of these plasmids are depicted in Figure 6-1.

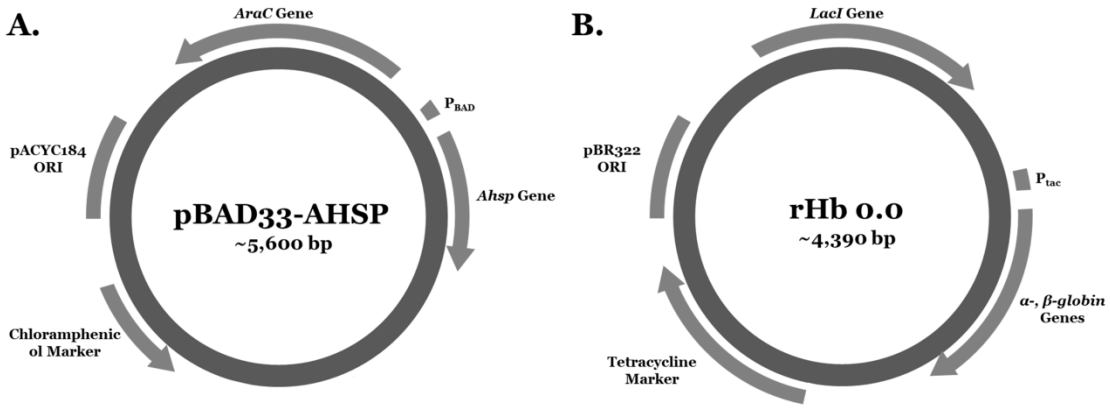

Figure 6-1. AHSP, rHb co-expression vectors
Panel A, AHSP expression vector. *Panel B*, HbA expression vector. HbA and AHSP production is induced using IPTG and L-arabinose, respectively. The selection of these disparate promoters allows for HbA expression to be studied in the presence and absence of AHSP expression. Although not depicted in *Panel B*, the *α and β globin* genes are transcribed into a single mRNA molecule which contains two ribosome binding sites. This allows each globin to be translated independently from the other. This figure was produced using Microsoft PowerPoint (Microsoft Corporation, Redmond, Washington, US)(*557*).

Following the construction of pBAD33-AHSP, Top10 cells were obtained from Invitrogen Corporation (Carlsbad, California, US) and co-transformed with pBAD33-AHSP and rHb 0.0. This strain of cells, which will be referred to as *E. coli* AH1, cannot metabolize arabinose due to an *AraD* disruption (*558*). This gene encodes L-ribulose-5-phosphate 4-epimerase, which is partly responsible for metabolizing arabinose once it is taken up by the cells. Its disruption in this strain prevents digestion of the AHSP inducer during the experiments described in the next section (*558*).

Co-Expression of AHSP with rHb

E. coli AH1 were used to assay the effects of the presence and absence of AHSP expression on HbA production using methods first developed by Antony

J. Mathews (Somatogen Incorporated, subsequently acquired by Baxter Healthcare Corporation)(*39*, *226*). Briefly, a 5 mL pre-culture of sterile LB media containing 10 μg/mL tetracycline and 25 μg/ml chloramphenicol was inoculated with a single colony of *E. coli* AH1 and grown overnight at 37 ^{O}C with 225 RPM shaking. The next morning, this entire culture was used to inoculate a 1 L Erlenmeyer flask containing 150 mL of sterile 2X TB media containing the same concentrations of antibiotics. The growth of this culture was monitored until the optical absorbance at 600 nm reached 0.8 to 1.0, at which time the temperature was dropped to 32 ^{O}C and 25 μM exogenous hemin was added. Then, 2.5 mL of this culture was added to each of ten, pre-sterilized glass test tubes. A titration of arabinose ranging from 0.0005% to 0.5% (m/v) was then added to the culture tubes, which were allowed to grow overnight before being harvested approximately 15 hours post-induction. During this phase of the experiments, IPTG was not added to the cultures to induce HbA production, because doing so was found to result in an appreciable amount of insoluble protein aggregates. Instead, leaky expression from the P_{tac} rHb promoter was used to produce rHb.

The cells harvested from each tube were resuspended in phosphate buffered saline (PBS) solution (140 mM NaCl, 3 mM KCl, 10 mM Na_2HPO_4, 2 mM KH_2PO_4, pH 7.4 at 20 ^{O}C) that had been bubbled with CO and chilled to 4 ^{O}C prior to use. Then, absorbance spectra were recorded after normalizing each sample for cell density as approximated by optical absorbance at 700 nm. In these spectra, peaks in the Soret regions begin to emerge as increasing amounts of hemoglobin are produced (*39*), and the first derivatives of these spectra

provide an estimate of relative hemoprotein expression levels. The peak-to-trough distances of these traces can be plotted against arabinose concentration to ascertain the effects of various levels of AHSP induction. Representative data from these experiments are presented in Figure 6-2.

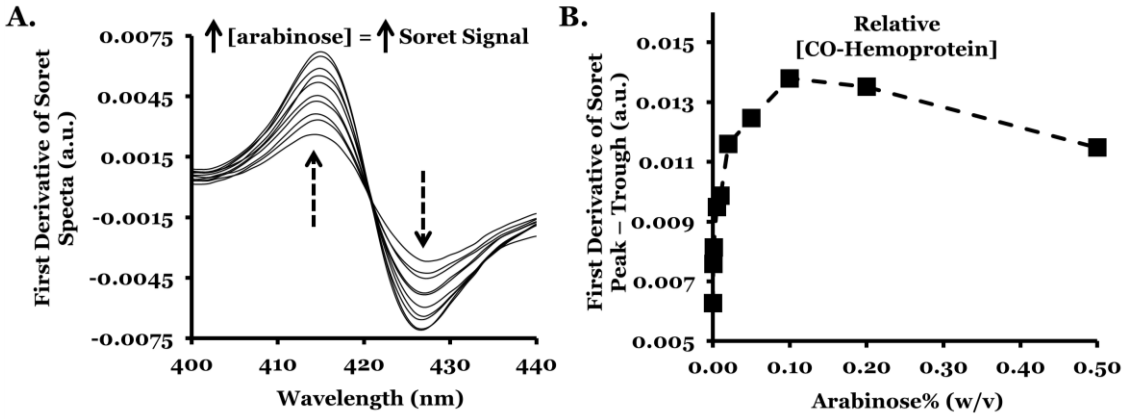

Figure 6-2. Co-expression of AHSP with rHb in E. coli
Panel A, first derivative spectra in the Soret region of *E. coli* AH1 under conditions of variable AHSP induction. *Panel B*, plot of arabinose concentration against relative hemoprotein production levels. In *Panel A*, a Savitzky-Golay smoothing filter function (*535*) was applied to reduce signal noise using the Cary WinUV Bio Pack software (Agilent Technologies, Incorporated, Santa Clara, California, US). Plots were generated using Microsoft Excel and PowerPoint (Microsoft Corporation, Redmond, Washington, US).

Although this method does not discern between α^H chain, AHSP:α^H-chain complex, β^H chain, and HbA production, it does report on total hemoprotein overexpression levels. As shown in Figure 6-2, AHSP appears to increase expression yields as long as its induction is weak. Under conditions of stronger AHSP induction, however, hemoprotein expression appears to diminish. Although the underlying mechanism giving rise to this trend is unclear, it is likely that high-level AHSP expression inhibits HbA production by binding to free α^H chains and competitively inhibiting their association with β^H chains. One effect might be that the resulting free β^H chains precipitate, causing

a decrease in Soret signal peak intensity. Although these assays are preliminary, they reveal that AHSP co-expression may be useful in rHBOC production efforts.

Chapter 7: Characterization of HbF Toms River

*Much of the prose, figures, and references that appear in this chapter were taken from Crowley, Mollan, et al. (*559*). The portions reproduced here are those which were written by the second author or have been paraphrased based on background case information provided by the co-authors of this study (personal communication).

The following information was discovered as a result of several studies of a novel hematological condition that was found in a newborn baby from Toms River, New Jersey, US. This work was done in collaboration with Moira A. Crowley (Case Western Reserve University), Osheisa Y. Abdulmalik (The Children's Hospital of Philadelphia), Andrew Butler (Rutgers University), Emily F. Goodwin (University of Alabama), Arindam Sarkar (Rice University), Catherine A. Stolle (The Children's Hospital of Philadelphia), Andrew J. Gow (Rutgers University), John S. Olson (Rice University), and Mitchell J. Weiss (Children's Hospital of Philadelphia).

Background, Case Information

Physicians from several institutions recently treated a full-term female neonate who was born with cyanosis ("a bluish or purplish discoloration (as of skin) due to deficient oxygenation of the blood" (*560*)). Physical examinations of this newborn revealed that the baby had normal APGAR scores ("an index used to evaluate the condition of a newborn infant…" (*560*)). Additionally, the chest X-ray, echocardiogram, and laboratory tests for various metabolic and infectious diseases did not reveal the presence of any known abnormalities or infections. There was also no evidence of elevated methemoglobin levels, which is a common cause of blue baby syndrome (*561-563*). Apart from the apparent

cyanosis, healthcare workers described the patient as “a happy blue baby” that was “clinically well.”

Several findings indicated that this patient’s unusual clinical presentation could be attributed to a hemoglobinopathy. First, the patient’s symptoms self-resolved within two months following her release from the hospital on day six of life, and the patient’s father apparently suffered from the same condition. Like his daughter, his symptoms disappeared within a few months post-birth. Second, clinical diagnostics and laboratory data from several blood tests indicated abnormalities relating to the patient’s hemoglobin (not shown). Third, the timing of the disappearance of the cyanosis coincided with a process called globin switching (*118*, *129*, *130*, *564*). During this process, fetal hemoglobin (HbF) production is dramatically decreased and its synthesis is replaced by adult hemoglobin (HbA) production in the two month period following birth (*131*). These observations prompted researchers to posit an etiology related to Fetal Hemoglobin (HbF).

Sequencing of the patient’s globin alleles revealed the presence of a heterozygous missense mutation in the Gamma G ($^{G}\gamma$) globin gene (*HBG2*, NCBI Accession NM_000184.2)(*114*). Specifically, a G to A substitution at nucleotide position 202 (c.202G>A) replaces valine with methionine at codon 68 or amino acid 67 in the post-translationally processed $^{G}\gamma$ chain product. This mutation will be referred to as the γ V67M mutation throughout this chapter. By convention, the name of this mutant HbF has been designated “Hemoglobin Toms River” (or HbF Toms River). BLAST searches for the γ V67M mutation were conducted to ensure that this mutation had not already been reported, and

these studies indicated that Hemoglobin Toms River was a novel fetal Hb variant.

Functional Studies of Hemoglobin Toms River

In order to understand the mechanism(s) underlying the clinical phenotype caused by Hemoglobin Toms River, it is important to know where the γ V67M (E11) mutation occurs within the structure of HbF. This is because mutations occurring at the $\alpha^{H_1}\gamma^{H_1}$ dimer interface, for example, suggest a different set of functional consequences than mutations in the distal pocket. As a preliminary step, a molecular model of HbF Toms River was generated and compared to wild-type protein.

Figure 7-1A shows an X-ray crystal structure of wild-type human (deoxy)HbF (*133*). The residue labeled 67^{Val} is mutated to a methionine in HbF Toms River. Figure 7-1B shows a structure which was modeled to depict this mutation. Position 67 (E11) is located in the distal pocket adjacent to bound ligands and the iron atom. Because methionine is significantly larger than valine (by approximately 32 atomic mass units (amu)), and because it has the potential to project further into the ligand binding pocket than valine, it is clear that the Toms River mutation is likely to affect O_2 binding and transport. Additionally, methionine side chains are known to participate in biochemically significant and potentially injurious redox chemistry (*565-567*). These observations suggested several functional assays.

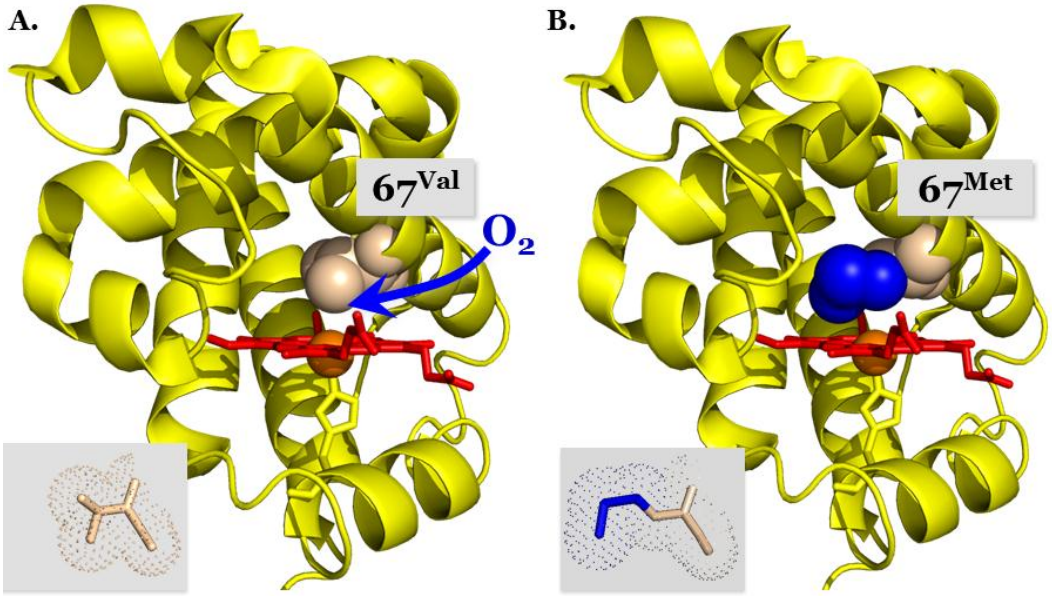

Figure 7-1. Wild-type HbF, HbF Toms River Structures
Panel A, native HbF γ subunit showing valine at position 67 (PDB 1FDH)(*133*). *Panel B*, predicted structure of HbF Toms River γ subunit showing the mutant methionine inserted into the wild-type structure at position 67. In both panels, γ subunits are depicted using yellow ribbons. The planar heme group and its associated histidine are shown using red and yellow stick models, respectively. The iron atom is shown as an orange sphere. Oxygen enters the heme pocket as indicated by the blue arrow and binds iron on the upper face of the heme ring opposite to the associated histidine. The residues at position 67 are shown using spheres, with blue indicating the additional methionine atoms that hinder oxygen access to the iron atom in the center of the heme ring. The insets show the native valine and mutant methionine in stick and spherical dot format to indicate the size difference between the amino acids. Both panels were constructed using the PyMOL Molecular Graphics System, with the HbF Toms River mutation being modeled using the mutagenesis wizard that is built-in to this software (DeLano Scientific, Palo Alto, California, US).

Preliminary experiments were conducted in the Mitchell J. Weiss Laboratory (University of Philadelphia, Philadelphia, Pennsylvania, US) using hemolysates that were obtained from whole blood samples from the patient. These experiments were significantly informed by literature-based research which revealed that the V67M mutation was known to occur in rare instances in β^H chains of adult human HbA (HbA Bristol-Alesha)(*568-571*). Because studies of HbA Bristol-Alesha have shown that the methionine at position 67 is spontaneously and post-translationally oxidized to an aspartate residue, the

presence of Asp67 in the γ chains of HbF Toms River was investigated. Mass spectrometry data provided evidence for the existence of this conversion event. These data are discussed further by Crowley, Mollan, et al. (*559*), but they were not obtained at Rice University and will not be reviewed here.

Because the patient ceased producing HbF Toms River, it became necessary to produce this protein using recombinant technology in order to continue studies of its functional properties. The methods described in Chapter 2 were used to produce and purify both wild-type HbF and HbF Toms River. Using the resulting proteins, autooxidation studies were performed for wild-type and mutant HbF using previously established methods (*339*, *473*, *572*, *573*). Data from these experiments are presented in Figure 7-2, and they suggest that the Toms River mutation does increase the apparent rate of HbF autooxidation by approximately two- to three-fold at 37 ^{O}C in air equilibrated buffer, but this process is still very slow and unlikely to account for the patient's phenotype.

Laser flash photolysis techniques were then used to investigate the effect of the Toms River mutation on the rate of O_2 binding. The association (k'_{O2}) and dissociation (k_{O2}) rate constants for the last step of O_2 binding to the individual globin subunits in both proteins were measured using previously established methods (*112*, *512*, *538*). The V67M mutant was found to bind O_2 and CO ~25 times more slowly than wild-type subunits (Table 7-1). In contrast, this mutation was found to have little effect on the rate of O_2 release (k_{O2}) from saturated oxygenated HbF. Consequently, the mutated γ subunits in the high-

affinity state (R) of HbF has a ~30-fold increased P_{50} (~12 μM or ~7 mm Hg) compared to that of wild-type R-state γ subunits.

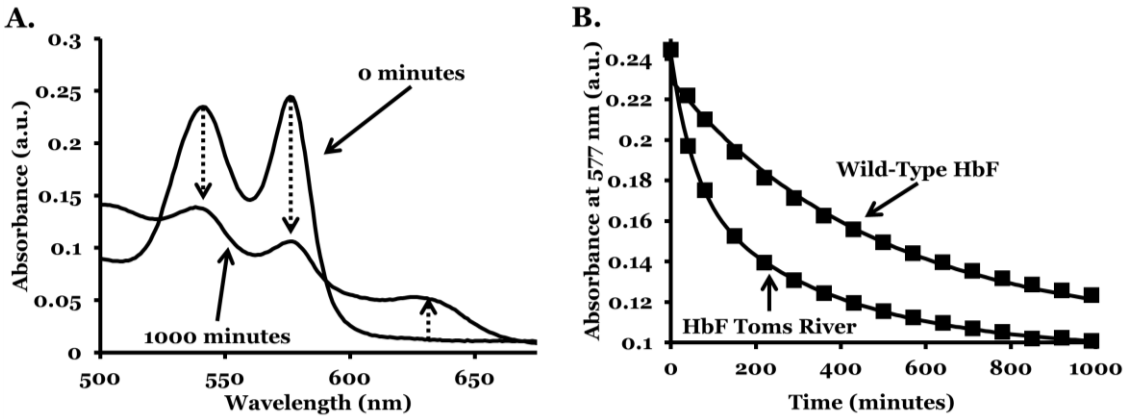

Figure 7-2. Autooxidation of wild-type, mutant HbF
Panel A, spectra at the start of the autooxidation reaction and 1000 minutes into the reaction for wild-type HbF. *Panel B*, time course of the reaction as followed at 577 nm. Reactions used air equilibrated 100 mM potassium phosphate buffer, pH 7.4 at 37 ^{O}C. Autooxidation was followed at 577 nm, with absorbance signals at this wavelength plotted against time for wild-type HbF and HbF Toms River. *Panel B* data points are shown with exponential fits overlaid for clarity. Plots were generated using Microsoft Excel and PowerPoint (Microsoft Corporation, Redmond, Washington, US).

	k'_{O2} $\mu M^{-1}s^{-1}$	k_{O2} s^{-1}	P_{50} (k_{O2}/k'_{O2}) (μM)	k'_{CO} $\mu M^{-1}s^{-1}$
Fetal Hb ($\alpha_2\gamma_2$)				
α(wt)	40	12	0.30	4.0
γ(wt)	88	37	0.42	7.0
γ(V67M)	3.6	43	12.0	0.22
HbA ($\alpha_2\beta_2$)				
α(wt)*	29±11	14±8	0.48±0.11	4.0±1.1
β(wt)*	60±12	31±13	0.53±0.15	7.0±2.0

Table 7-1. Kinetic parameters for ligand binding to wild-type, mutant HbF
Reactions were studied using 100 mM potassium phosphate buffer, pH 7.0 at 20 ^{O}C. Parameters marked with an asterisk were taken from Birukou et al. (*500*) and are included as a general reference. The data for wild-type HbF roughly agree with the values reported by Noble et al. (*574*). This figure was produced using Microsoft PowerPoint (Microsoft Corporation, Redmond, Washington, US).

These findings partially explain the cyanosis observed in the patient. The effects of this mutation on the ligand binding rates clearly alters the O_2 affinity

of HbF Toms River, likely resulting in impaired O_2 transport. Also, the post-translational conversion of methionine to aspartic acid is predicted to destabilize the Hb tetramer. The phenotypes associated with Hb Bristol-Alesha (mainly hemolytic) and Hb Toms River (mainly cyanotic) may be related to these two proteins having different rates of methionine to aspartate conversion. Also, Hb Bristol-Alesha affects one of two β globin alleles, whereas Hb Toms River is present in one of four γ globin genes. In future work, the John S. Olson Laboratory (Rice University, Houston, Texas, US) and Abdu I. Alayash Laboratory (Center for Biologics Evaluation and Research, Food and Drug Administration, NIH campus, Bethesda, Maryland, US) intend to compare the properties of recombinant HbA and HbF tetramers containing E11 valine to methionine substitutions in order to resolve questions of this type.

Chapter 8: Summary of Findings

Prior to this work, the association and dissociation rate constants for AHSP:α^H-chain interactions had not been reported. The kinetic parameters determined from these experiments show that AHSP binds to α^H chains more rapidly than β^H chains bind to α^H chains, but that β^H chains have a higher affinity. This explains previous reports of others that AHSP is competitively displaced from AHSP:α^H-chain complexes by β^H chains. It is also consistent with a molecular chaperone function of AHSP. This idea is supported by the finding that AHSP has a relatively high affinity for (met)α^H chains, which are unstable when free in solution, and that co-incubation of AHSP with α^H chains causes them to adopt a reversible hemichrome conformation that has recently been implicated as a globin folding intermediate. All these data are consistent with the Hb Turriff studies which show that AHSP helps to stabilze α^H chains during in vivo HbA biosynthesis.

Although wild-type AHSP does not appear to dramatically affect heme affinity and α^H chain secondary structure (though slight differences do exist in the case of hemin loss), it is clear from the studies involving AHSP Pro30 mutants and (K99E)α^H chains that the loop separating AHSP helices 1 and 2 is critical to AHSP function, both because of electrostatic interactions and structural conformational issues. This is evident in the studies of the impact of AHSP and the Pro30 mutants on ligand binding kinetics as well. Also, these findings confirm and extend the NMR work of others, which originally established the existence of cis and trans AHSP conformations, with work here

demonstrating the impact of this isomerization event on the rates of AHSP binding.

The finding that AHSP helps with HbA production in *E. coli* is consistent with what others have found regarding the co-expression of AHSP with α^H chains alone. Although the HbA expression yields gained by co-expressing AHSP with both α^H and β^H chains are modest, it is clear that this is an effective strategy that is worth pursuing in future studies.

Lastly, using several of the methods that were used to study AHSP function, the HbF Toms River mutation was studied, and several plausible mechanisms have been uncovered that may explain the clinical features of this hemoglobinopathy.

References Cited

1. Mollan, T. L., Yu, X., Weiss, M. J., and Olson, J. S. (2010) The role of alpha-hemoglobin stabilizing protein in redox chemistry, denaturation, and hemoglobin assembly, *Antioxid Redox Signal 12*, 219-31.
2. Whitaker, B., Henry, R., Green, J., King, M., Leibeg, L., Mathew, S., Schlumpf, K., and Schreiber, G. (2010, April 30) *The 2007 National Blood Collection and Utilization Survey*.
3. Cinat, M. E., Wallace, W. C., Nastanski, F., West, J., Sloan, S., Ocariz, J., and Wilson, S. E. (1999) Improved survival following massive transfusion in patients who have undergone trauma, *Arch Surg 134*, 964-8; discussion 968-70.
4. Vincent, J. L., Sakr, Y., De Backer, D., and Van der Linden, P. (2007) Efficacy of allogeneic red blood cell transfusions, *Best Pract Res Clin Anaesthesiol 21*, 209-19.
5. Pape, A., Stein, P., Horn, O., and Habler, O. (2009) Clinical evidence of blood transfusion effectiveness, *Blood Transfus 7*, 250-8.
6. Pape, A., and Habler, O. (2007) Alternatives to allogeneic blood transfusions, *Best Pract Res Clin Anaesthesiol 21*, 221-39.
7. Busch, M. P., Kleinman, S. H., and Nemo, G. J. (2003) Current and emerging infectious risks of blood transfusions, *J Am Med Assoc 289*, 959-62.
8. Eder, A. F., and Chambers, L. A. (2007) Noninfectious complications of blood transfusion, *Arch Pathol Lab Med 131*, 708-18.
9. Klein, H. (2000) Will Blood Transfusion Ever Be Safe Enough?, *J Am Med Assoc 284*, 238-40.
10. Klein, H. (2010) How safe is blood, really?, *Advances in Transfusion Safety 38*, 1-104.
11. Luban, N. L. (2005) Transfusion safety: Where are we today?, *Ann N Y Acad Sci 1054*, 325-41.

12. Zou, S., Musavi, F., Notari, E. P. t, and Fang, C. T. (2008) Changing age distribution of the blood donor population in the United States, *Transfusion 48*, 251-7.
13. Sullivan, M. T., Cotten, R., Read, E. J., and Wallace, E. L. (2007) Blood collection and transfusion in the United States in 2001, *Transfusion 47*, 385-94.
14. Schreiber, G. B., Sanchez, A. M., Glynn, S. A., and Wright, D. J. (2003) Increasing blood availability by changing donation patterns, *Transfusion 43*, 591-7.
15. Greinacher, A., Fendrich, K., and Hoffmann, W. (2010) Demographic Changes: The Impact for Safe Blood Supply, *Transfus Med Hemother 37*, 141-148.
16. Greinacher, A., Fendrich, K., Alpen, U., and Hoffmann, W. (2007) Impact of demographic changes on the blood supply: Mecklenburg-West Pomerania as a model region for Europe, *Transfusion 47*, 395-401.
17. Winslow, R. M. (2006) Blood Substitutes. Academic Press, Oxford, UK.
18. Brooks, J. P. (2005) Reengineering transfusion and cellular therapy processes hospitalwide: ensuring the safe utilization of blood products, *Transfusion 45*, 159S-71S.
19. Goodnough, L. T., Shander, A., and Brecher, M. E. (2003) Transfusion medicine: looking to the future, *Lancet 361*, 161-9.
20. Kolins, J., and Herron, R. (2003) On bowling alone and donor recruitment: lessons to be learned, *Transfusion 43*, 1634-8.
21. Cyranoski, D. (2004) Tainted transfusion leaves Japan scrambling for safer blood tests, *Nat Med 10*, 217.
22. Otsubo, H., and Yamaguchi, K. (2008) Current risks in blood transfusion in Japan, *Jpn J Infect Dis 61*, 427-33.
23. Solheim, B. G. (2008) Pathogen reduction of blood components, *Transfus Apher Sci 39*, 75-82.
24. Hess, J., and Thomas, M. (2003) Blood use in war and disaster: lessons from the past century, *Transfusion 43*, 1622-1633.

25. Hess, J. R. (2005) Blood use in war and disaster: The U.S. experience, *Scand J Trauma Resusc Emerg Med 13*, 74-81.
26. Mujeeb, S. A., and Jaffery, S. H. (2007) Emergency blood transfusion services after the 2005 earthquake in Pakistan, *Emerg Med J 24*, 22-4.
27. Abolghasemi, H., Radfar, M. H., Tabatabaee, M., Hosseini-Divkolayee, N. S., and Burkle, F. M. (2008) Revisiting blood transfusion preparedness: experience from the Bam earthquake response, *Prehosp Disaster Med 23*, 391-4.
28. Chamberland, M. E., Alter, H. J., Busch, M. P., Nemo, G., and Ricketts, M. (2001) Emerging infectious disease issues in blood safety, *Emerg Infect Dis 7*, 552-3.
29. Chamberland, M. E. (2002) Emerging infectious agents: do they pose a risk to the safety of transfused blood and blood products?, *Clin Infect Dis 34*, 797-805.
30. Dodd, R. Y., and Leiby, D. A. (2004) Emerging infectious threats to the blood supply, *Annu Rev Med 55*, 191-207.
31. Dong, J., Olano, J. P., McBride, J. W., and Walker, D. H. (2008) Emerging pathogens: challenges and successes of molecular diagnostics, *J Mol Diagn 10*, 185-97.
32. Amin, M., Fergusson, D., Aziz, A., Wilson, K., Coyle, D., and Hebert, P. (2003) The cost of allogeneic red blood cells--a systematic review, *Transfus Med 13*, 275-85.
33. Basha, J., Dewitt, R., Cable, D., and Jones, G. (2006) Transfusions And Their Costs: Managing Patients Needs And Hospitals Economics, *Internet J Emerg Intensive Care Med 9*.
34. Shander, A., Hofmann, A., Gombotz, H., Theusinger, O. M., and Spahn, D. R. (2007) Estimating the cost of blood: past, present, and future directions, *Best Pract Res Clin Anaesthesiol 21*, 271-89.
35. Kumar, R. (1995) Recombinant hemoglobins as blood substitutes: a biotechnology perspective, *Proc Soc Exp Biol Med 208*, 150-8.
36. Sanders, K. E., Ackers, G., and Sligar, S. (1996) Engineering and design of blood substitutes, *Curr Opin Struct Biol 6*, 534-40.

37. Fronticelli, C., and Koehler, R. C. (2009) Design of recombinant hemoglobins for use in transfusion fluids, *Crit Care Clin 25*, 357-71, Table of Contents.
38. Olson, J. S., Eich, R. F., Smith, L. P., Warren, J. J., and Knowles, B. C. (1997) Protein engineering strategies for designing more stable hemoglobin-based blood substitutes, *Artif Cells Blood Substit Immobil Biotechnol 25*, 227-41.
39. Graves, P. E., Henderson, D. P., Horstman, M. J., Solomon, B. J., and Olson, J. S. (2008) Enhancing stability and expression of recombinant human hemoglobin in E. coli: Progress in the development of a recombinant HBOC source, *Biochim Biophys Acta 1784*, 1471-9.
40. Alayash, A. I. (1999) Hemoglobin-based blood substitutes: oxygen carriers, pressor agents, or oxidants?, *Nat Biotechnol 17*, 545-9.
41. Alayash, A. I. (2001) Oxidative mechanisms of hemoglobin-based blood substitutes, *Artif Cells Blood Substit Immobil Biotechnol 29*, 415-25.
42. Alayash, A. I. (2004) Oxygen therapeutics: can we tame haemoglobin?, *Nat Rev Drug Discov 3*, 152-9.
43. Baron, J. F. (1999) Blood substitutes. Haemoglobin therapeutics in clinical practice, *Crit Care 3*, R99-102.
44. Buehler, P. W., and Alayash, A. I. (2008) All hemoglobin-based oxygen carriers are not created equally, *Biochim Biophys Acta 1784*, 1378-81.
45. Chang, T. M. (2003) Future generations of red blood cell substitutes, *J Intern Med 253*, 527-35.
46. Ferguson, E., Prowse, C., Townsend, E., Spence, A., Hilten, J. A., and Lowe, K. (2008) Acceptability of blood and blood substitutes, *J Intern Med 263*, 244-55.
47. Goorha, B. Y., Deb, M., Chatterjee, T., Dhot, P., and Prasad, B. R. (2003) Artificial Blood, *Med J Armed Forces India 59*, 45-50.
48. Silverman, T. A., and Weiskopf, R. B. (2009) Hemoglobin-based oxygen carriers: current status and future directions, *Transfusion 49*, 2495-515.
49. Stowell, C. P. (2005) What happened to blood substitutes?, *Transfus Clin Biol 12*, 374-9.

50. Moore, E. (2003) Blood Substitutes: The Future is Now *196*, 1-17.
51. Moore, E. (2005) Emerging Role of Hemoglobin Solutions in Trauma Care, *Transfus Altern Tranfus Med 6*, 69-77.
52. Henkel-Honke, T., and Oleck, M. (2007) Artificial oxygen carriers: a current review, *Aana J 75*, 205-11.
53. Intaglietta, M. (2008) Editorial: Blood Substitutes Better Than Blood, *Transfus Altern Tranfus Med 9*, 199-203.
54. Jones, J. A. (1995) Red blood cell substitutes: current status, *Br J Anaesth 74*, 697-703.
55. Kim, H. W., and Greenburg, A. G. (2004) Artificial oxygen carriers as red blood cell substitutes: a selected review and current status, *Artif Organs 28*, 813-28.
56. Kresie, L. (2001) Artificial blood: an update on current red cell and platelet substitutes, *Proc (Bayl Univ Med Cent) 14*, 158-61.
57. Shirley, P. (2008) Fluids as oxygen carriers and the potential role in trauma resuscitation, *Trauma 10*, 139-47.
58. Chen, J. Y., Scerbo, M., and Kramer, G. (2009) A review of blood substitutes: examining the history, clinical trial results, and ethics of hemoglobin-based oxygen carriers, *Clinics (Sao Paulo) 64*, 803-13.
59. Mozzarelli, A., Ronda, L., Faggiano, S., Bettati, S., and Bruno, S. Haemoglobin-based oxygen carriers: research and reality towards an alternative to blood transfusions, *Blood Transfus 8 Suppl 3*, s59-68.
60. Kluger, R. (2010) Red cell substitutes from hemoglobin-Do we start all over again?, *Curr Opin Chem Biol*.
61. Lowe, K. (2006) Blood substitutes: from chemistry to clinic, *J Mat Chem 16*, 4189-96.
62. Ness, P. M., and Cushing, M. M. (2007) Oxygen therapeutics: pursuit of an alternative to the donor red blood cell, *Arch Pathol Lab Med 131*, 734-41.
63. Tappenden, J. (2007) Artificial blood substitutes, *J R Army Med Corps 153*, 3-9.

64. Napolitano, L. M. (2009) Hemoglobin-based oxygen carriers: first, second or third generation? Human or bovine? Where are we now?, *Crit Care Clin 25*, 279-301, Table of Contents.
65. Estep, T., Bucci, E., Farmer, M., Greenburg, G., Harrington, J., Kim, H. W., Klein, H., Mitchell, P., Nemo, G., Olsen, K., Palmer, A., Valeri, C. R., and Winslow, R. (2008) Basic science focus on blood substitutes: a summary of the NHLBI Division of Blood Diseases and Resources Working Group Workshop, March 1, 2006, *Transfusion 48*, 776-82.
66. Bunn, H. F., and Forget, B. G. (1986) Hemoglobin, molecular, genetic and clinical aspects. Saunders, Philadelphia.
67. Rodak, B. F., Fritsma, G. A., and Doig, K. (2007) Hematology : clinical principles and applications. Saunders Elsevier, St. Louis, MO.
68. Speiss, B., Spence, R., and Shander, A. (2006) Perioperative Transfusion Medicine. Lippincott Williams and Wilkins, Philadelphia, PA.
69. Freitas, T. A., Hou, S., Dioum, E. M., Saito, J. A., Newhouse, J., Gonzalez, G., Gilles-Gonzalez, M. A., and Alam, M. (2004) Ancestral hemoglobins in Archaea, *Proc Natl Acad Sci U S A 101*, 6675-80.
70. Freitas, T. A., Saito, J. A., Hou, S., and Alam, M. (2005) Globin-coupled sensors, protoglobins, and the last universal common ancestor, *J Inorg Biochem 99*, 23-33.
71. Frey, A. D., Farres, J., Bollinger, C. J., and Kallio, P. T. (2002) Bacterial hemoglobins and flavohemoglobins for alleviation of nitrosative stress in Escherichia coli, *Appl Environ Microbiol 68*, 4835-40.
72. Hardison, R. C. (1996) A brief history of hemoglobins: plant, animal, protist, and bacteria, *Proc Natl Acad Sci U S A 93*, 5675-9.
73. Hardison, R. (1998) Hemoglobins from bacteria to man: evolution of different patterns of gene expression, *J Exp Biol 201*, 1099-117.
74. Lecomte, J. T., Vuletich, D. A., and Lesk, A. M. (2005) Structural divergence and distant relationships in proteins: evolution of the globins, *Curr Opin Struct Biol 15*, 290-301.

75. Fago, A., Hundahl, C., Malte, H., and Weber, R. E. (2004) Functional properties of neuroglobin and cytoglobin. Insights into the ancestral physiological roles of globins, *IUBMB Life 56*, 689-96.
76. Hundahl, C., Fago, A., Dewilde, S., Moens, L., Hankeln, T., Burmester, T., and Weber, R. E. (2006) Oxygen binding properties of non-mammalian nerve globins, *Febs J 273*, 1323-9.
77. Wittenberg, J. B., Bolognesi, M., Wittenberg, B. A., and Guertin, M. (2002) Truncated hemoglobins: a new family of hemoglobins widely distributed in bacteria, unicellular eukaryotes, and plants, *J Biol Chem 277*, 871-4.
78. Kundu, S., Trent, J. T., and Hargrove, M. S. (2003) Plants, humans and hemoglobins, *Trends Plant Sci 8*, 387-93.
79. Weber, R. E., and Vinogradov, S. N. (2001) Nonvertebrate hemoglobins: functions and molecular adaptations, *Physiol Rev 81*, 569-628.
80. Bolognesi, M., Bordo, D., Rizzi, M., Tarricone, C., and Ascenzi, P. (1997) Nonvertebrate hemoglobins: structural bases for reactivity, *Prog Biophys Mol Biol 68*, 29-68.
81. Poole, R. K., and Hughes, M. N. (2000) New functions for the ancient globin family: bacterial responses to nitric oxide and nitrosative stress, *Mol Microbiol 36*, 775-83.
82. Goldberg, D. E. (1999) Oxygen-Avid Hemoglobin of Ascaris, *Chem Rev 99*, 3371-3378.
83. Hsia, C. C. (1998) Respiratory function of hemoglobin, *N Engl J Med 338*, 239-47.
84. Riggs, A. (1965) Functional properties of hemoglobins, *Physiol Rev 45*, 619-73.
85. Bunn, H. F. (1981) Evolution of mammalian hemoglobin function, *Blood 58*, 189-97.
86. Poyart, C., Wajcman, H., and Kister, J. (1992) Molecular adaptation of hemoglobin function in mammals, *Respir Physiol 90*, 3-17.
87. Gardner, P. R. (2005) Nitric oxide dioxygenase function and mechanism of flavohemoglobin, hemoglobin, myoglobin and their associated reductases, *J Inorg Biochem 99*, 247-66.

88. Jensen, F. B. (2004) Red blood cell pH, the Bohr effect, and other oxygenation-linked phenomena in blood O2 and CO2 transport, *Acta Physiol Scand 182*, 215-27.
89. Rifkind, J. M., Nagababu, E., Ramasamy, S., and Ravi, L. B. (2003) Hemoglobin redox reactions and oxidative stress, *Redox Rep 8*, 234-7.
90. Rifkind, J. M., Ramasamy, S., Manoharan, P. T., Nagababu, E., and Mohanty, J. G. (2004) Redox reactions of hemoglobin, *Antioxid Redox Signal 6*, 657-66.
91. Riggs, A. F. (1988) The Bohr effect, *Annu Rev Physiol 50*, 181-204.
92. Jensen, F. B. (2009) The dual roles of red blood cells in tissue oxygen delivery: oxygen carriers and regulators of local blood flow, *J Exp Biol 212*, 3387-93.
93. Buerk, D. G. (2007) Nitric oxide regulation of microvascular oxygen, *Antioxid Redox Signal 9*, 829-43.
94. Kim-Shapiro, D. B. (2004) Hemoglobin-nitric oxide cooperativity: is NO the third respiratory ligand?, *Free Radic Biol Med 36*, 402-12.
95. Kim-Shapiro, D. B., Schechter, A. N., and Gladwin, M. T. (2006) Unraveling the reactions of nitric oxide, nitrite, and hemoglobin in physiology and therapeutics, *Arterioscler Thromb Vasc Biol 26*, 697-705.
96. Godecke, A. (2006) On the impact of NO-globin interactions in the cardiovascular system, *Cardiovasc Res 69*, 309-17.
97. Allen, B. W., and Piantadosi, C. A. (2006) How do red blood cells cause hypoxic vasodilation? The SNO-hemoglobin paradigm, *Am J Physiol Heart Circ Physiol 291*, H1507-12.
98. Giustarini, D., Milzani, A., Colombo, R., Dalle-Donne, I., and Rossi, R. (2004) Nitric oxide, S-nitrosothiols and hemoglobin: is methodology the key?, *Trends Pharmacol Sci 25*, 311-6.
99. Bonaventura, C., Fago, A., Henkens, R., and Crumbliss, A. L. (2004) Critical redox and allosteric aspects of nitric oxide interactions with hemoglobin, *Antioxid Redox Signal 6*, 979-91.

100. Hobbs, A. J., Gladwin, M. T., Patel, R. P., Williams, D. L., and Butler, A. R. (2002) Haemoglobin: NO transporter, NO inactivator or NOne of the above?, *Trends Pharmacol Sci 23*, 406-11.

101. Henry, Y., and Guissani, A. (1999) Interactions of nitric oxide with hemoproteins: roles of nitric oxide in mitochondria, *Cell Mol Life Sci 55*, 1003-14.

102. Azarov, I., Huang, K. T., Basu, S., Gladwin, M. T., Hogg, N., and Kim-Shapiro, D. B. (2005) Nitric oxide scavenging by red blood cells as a function of hematocrit and oxygenation, *J Biol Chem 280*, 39024-32.

103. Light-Wahl, K., Schwartz, B., and Richard D. Smith, R. (1994) Observation of the Noncovalent Quaternary Associations of Proteins by Electrospray Ionization Mass Spectrometry, *J Am Chem Soc 116*, 5271-5278.

104. Perutz, M. F., Rossman, M. G., Cullis, A. F., Muirhead, H., Will, G., and North, A. C. T. (1960) Structure of Hæmoglobin: A Three-Dimensional Fourier Synthesis at 5.5-Å. Resolution, Obtained by X-Ray Analysis, *Nature 185*, 416-421.

105. Perutz, M. F., Muirhead, H., Cox, J. M., and Goaman, L. C. (1968) Three-dimensional Fourier synthesis of horse oxyhaemoglobin at 2.8 A resolution: the atomic model, *Nature 219*, 131-9.

106. Kendrew, J. C., Bodo, G., Dintzis, H. M., Parrish, R. G., Wyckoff, H., and Phillips, D. C. (1958) A three-dimensional model of the myoglobin molecule obtained by x-ray analysis, *Nature 181*, 662-6.

107. Dickerson, R. E., and Geis, I. (1983) Hemoglobin: Structure, Function, Evolution, and Pathology (Hagopian, P., Ed.). The Benjamin/Cummings Publishing Company, Inc., Menlo Park, CA.

108. Sharma, V. S., Traylor, T. G., Gardiner, R., and Mizukami, H. (1987) Reaction of nitric oxide with heme proteins and model compounds of hemoglobin, *Biochemistry 26*, 3837-43.

109. Smith, D. W., and Williams, R. J. P. (1970) Structure and Bonding: The spectra of ferric haems and haemoproteins. Springer, Berlin / Heidelberg.

110. Springer, B. A., Sligar, S. G., Olson, J. S., and Phillips, G. N. (1994) Mechanisms of Ligand Recognition in Myoglobin, *Chem Rev 94*, 699-714.

111. Gibson, Q. H., and Edelstein, S. J. (1987) Oxygen binding and subunit interaction of hemoglobin in relation to the two-state model, *J Biol Chem 262*, 516-9.

112. Olson, J. S., Rohlfs, R. J., and Gibson, Q. H. (1987) Ligand recombination to the alpha and beta subunits of human hemoglobin, *J Biol Chem 262*, 12930-8.

113. Biswal, B. K., and Vijayan, M. (2002) Structures of human oxy- and deoxyhaemoglobin at different levels of humidity: variability in the T state, *Acta Crystallogr D Biol Crystallogr 58*, 1155-61.

114. Pruitt, K., Tatusova, T., and Maglott, D. (2002) The NCBI handbook [Internet]: Chapter 18, The Reference Sequence (RefSeq) Project. (McEntyre, J., and Ostell, J., Eds.). National Library of Medicine (US), National Center for Biotechnology Information (Bethesda, MD) (available: http://www.ncbi.nlm.nih.gov/books/n/handbook/ch18/, accessed November 25, 2010).

115. Maniatis, T., Fritsch, E. F., Lauer, J., and Lawn, R. M. (1980) The molecular genetics of human hemoglobins, *Annu Rev Genet 14*, 145-78.

116. Adamczyk, M., and Gebler, J. C. (1997) Electrospray mass spectrometry of alpha and beta chains of selected hemoglobins and their TNBA and TNB conjugates, *Bioconjug Chem 8*, 400-6.

117. Stamatoyannopoulos, G. (2005) Control of globin gene expression during development and erythroid differentiation, *Experimental hematology 33*, 259-71.

118. Orkin, S. H. (1990) Globin gene regulation and switching: circa 1990, *Cell 63*, 665-72.

119. Orkin, S. H. (1995) Transcription factors and hematopoietic development, *J Biol Chem 270*, 4955-8.

120. Orkin, S. H. (1995) Regulation of globin gene expression in erythroid cells, *Eur J Biochem 231*, 271-81.

121. Orkin, S. H., and Zon, L. I. (2008) Hematopoiesis: an evolving paradigm for stem cell biology, *Cell 132*, 631-44.

122. Ottersbach, K., Smith, A., Wood, A., and Gottgens, B. (2009) Ontogeny of haematopoiesis: recent advances and open questions, *Br J Haematol 148*, 343-55.
123. Zhu, J., and Emerson, S. G. (2002) Hematopoietic cytokines, transcription factors and lineage commitment, *Oncogene 21*, 3295-313.
124. Dzierzak, E., and Speck, N. A. (2008) Of lineage and legacy: the development of mammalian hematopoietic stem cells, *Nat Immunol 9*, 129-36.
125. Mikkola, H. K., and Orkin, S. H. (2006) The journey of developing hematopoietic stem cells, *Development 133*, 3733-44.
126. Molineux, G., Foote, M. A., and Elliott, S. G. (2006) Erythropoietins and Erythropoiesis: Molecular, Cellular, Preclinical, and Clinical Biology. Birkhäuser Verlag, Basel, Switzerland.
127. Kim, S. I., and Bresnick, E. H. (2007) Transcriptional control of erythropoiesis: emerging mechanisms and principles, *Oncogene 26*, 6777-94.
128. Huisman, T. H. J., Carver, M. F. H., Baysal, E., Efremov, G. D., Wajcman, H., and Patrinos, G. (2010, November 5) The Globin Gene Server: A Database of Human Hemoglobin Variants and Thalassemias.
129. Bank, A. (2006) Regulation of human fetal hemoglobin: new players, new complexities, *Blood 107*, 435-43.
130. Sankaran, V. G., Xu, J., and Orkin, S. H. (2010) Advances in the understanding of haemoglobin switching, *Br J Haematol 149*, 181-94.
131. Karlsson, S., and Nienhuis, A. W. (1985) Developmental regulation of human globin genes, *Annu Rev Biochem 54*, 1071-108.
132. Kingsley, P. D., Malik, J., Emerson, R. L., Bushnell, T. P., McGrath, K. E., Bloedorn, L. A., Bulger, M., and Palis, J. (2006) “Maturational” globin switching in primary primitive erythroid cells, *Blood 107*, 1665-72.
133. Frier, J. A., and Perutz, M. F. (1977) Structure of human foetal deoxyhaemoglobin, *J Mol Biol 112*, 97-112.
134. Bertles, J. F. (1974) Human fetal hemoglobin: significance in disease, *Ann N Y Acad Sci 241*, 638-52.

135. Schechter, A. N. (2008) Hemoglobin research and the origins of molecular medicine, *Blood 112*, 3927-38.
136. Steinberg, M. H. (2001) Disorders of hemoglobin : genetics, pathophysiology, and clinical management. Cambridge University Press, Cambridge; New York.
137. Dintzis, H. M. (1961) Assembly of the peptide chains of hemoglobin, *Proc Natl Acad Sci U S A 47*, 247-61.
138. Hunt, T., Hunter, T., and Munro, A. (1969) Control of haemoglobin synthesis: rate of translation of the messenger RNA for the alpha and beta chains, *J Mol Biol 43*, 123-33.
139. Knopf, P. M., and Lamfrom, H. (1965) Changes in the Ribosome Distribution During Incubation of Rabbit Reticulocytes in Vitro, *Biochim Biophys Acta 95*, 398-407.
140. Lingrel, J. B., and Borsook, H. (1963) A Comparison of Amino Acid Incorporation into the Hemoglobin and Ribosomes of Marrow Erythroid Cells and Circulating Reticulocytes of Severely Anemic Rabbits, *Biochemistry 2*, 309-14.
141. Lodish, H. F., and Jacobsen, M. (1972) Regulation of hemoglobin synthesis. Equal rates of translation and termination of - and -globin chains, *J Biol Chem 247*, 3622-9.
142. Eaton, W. A., Munoz, V., Thompson, P. A., Chan, C. K., and Hofrichter, J. (1997) Submillisecond kinetics of protein folding, *Curr Opin Struct Biol 7*, 10-4.
143. Fersht, A. (1998) Structure and Mechanism in Protein Science: A Guide to Enzyme Catalysis and Protein Folding. W. H. Freeman Company, New York, NY.
144. Gilmanshin, R., Williams, S., Callender, R. H., Woodruff, W. H., and Dyer, R. B. (1997) Fast events in protein folding: relaxation dynamics of secondary and tertiary structure in native apomyoglobin, *Proc Natl Acad Sci U S A 94*, 3709-13.

145. Williams, S., Causgrove, T. P., Gilmanshin, R., Fang, K. S., Callender, R. H., Woodruff, W. H., and Dyer, R. B. (1996) Fast events in protein folding: helix melting and formation in a small peptide, *Biochemistry 35*, 691-7.

146. Komar, A. A., Kommer, A., Krasheninnikov, I. A., and Spirin, A. S. (1993) Cotranslational heme binding to nascent globin chains, *FEBS Lett 326*, 261-3.

147. Komar, A. A., Kommer, A., Krasheninnikov, I. A., and Spirin, A. S. (1997) Cotranslational folding of globin, *J Biol Chem 272*, 10646-51.

148. Baglioni, C., and Campana, T. (1967) Alpha-chain and globin: intermediates in the synthesis of rabbit hemoglobin, *Eur J Biochem 2*, 480-92.

149. Benz, E. J., and Forget, B. G. (1974) The biosynthesis of hemoglobin, *Semin Hematol 11*, 463-523.

150. Felicetti, L., Colombo, B., and Baglioni, C. (1966) Assembly of Hemoglobin, *Biochim Biophys Acta 129*, 380.

151. Winterhalter, K. H., Heywood, J. D., Huehns, E. R., and Finch, C. A. (1969) The free globin in human erythrocytes. I, *Br J Haematol 16*, 523-35.

152. Kawamura-Konishi, Y., and Suzuki, H. (1985) Binding reaction of hemin to globin, *J Biochem 98*, 1181-90.

153. Hargrove, M. S., Barrick, D., and Olson, J. S. (1996) The association rate constant for heme binding to globin is independent of protein structure, *Biochemistry 35*, 11293-9.

154. Hargrove, M. S., Wilkinson, A. J., and Olson, J. S. (1996) Structural factors governing hemin dissociation from metmyoglobin, *Biochemistry 35*, 11300-9.

155. Hargrove, M. S., Whitaker, T., Olson, J. S., Vali, R. J., and Mathews, A. J. (1997) Quaternary structure regulates hemin dissociation from human hemoglobin, *J Biol Chem 272*, 17385-9.

156. Hargrove, M. S., Singleton, E. W., Quillin, M. L., Ortiz, L. A., Phillips, G. N., Olson, J. S., and Mathews, A. J. (1994) His64(E7)-->Tyr apomyoglobin as a reagent for measuring rates of hemin dissociation, *J Biol Chem 269*, 4207-14.

157. Gattoni, M., Boffi, A., Sarti, P., and Chiancone, E. (1996) Stability of the heme-globin linkage in alphabeta dimers and isolated chains of human hemoglobin. A study of the heme transfer reaction from the immobilized proteins to albumin, *J Biol Chem 271*, 10130-6.

158. Benesch, R. E., and Kwong, S. (1995) Coupled reactions in hemoglobin. Heme-globin and dimer-dimer association, *J Biol Chem 270*, 13785-6.

159. Benesch, R. E., and Kwong, S. (1990) The stability of the heme-globin linkage in some normal, mutant, and chemically modified hemoglobins, *J Biol Chem 265*, 14881-5.

160. Park, R. Y., and McDonald, M. J. (1989) Kinetics of heme binding to semi-alpha-hemoglobin, *Biochem Biophys Res Commun 162*, 522-7.

161. Vasudevan, G., and McDonald, M. J. (1997) Spectral demonstration of semihemoglobin formation during CN-hemin incorporation into human apohemoglobins, *J Biol Chem 272*, 517-24.

162. Vasudevan, G., and McDonald, M. J. (2000) Wavelength-dependent spectral changes accompany CN-hemin binding to human apohemoglobin, *J Protein Chem 19*, 583-90.

163. Vasudevan, G., and McDonald, M. J. (2002) Ordered heme binding ensures the assembly of fully functional hemoglobin: a hypothesis, *Curr Protein Pept Sci 3*, 461-6.

164. Rose, M. Y., and Olson, J. S. (1983) The kinetic mechanism of heme binding to human apohemoglobin, *J Biol Chem 258*, 4298-303.

165. Chiu, F., Vasudevan, G., Morris, A., and McDonald, M. J. (1998) Fluorescence studies of human semi-beta-hemoglobin assembly, *Biochem Biophys Res Commun 242*, 365-8.

166. Chiu, F., Vasudevan, G., Morris, A., and McDonald, M. J. (2000) Soret spectroscopic and molecular graphic analysis of human semi-beta-hemoglobin formation, *J Protein Chem 19*, 157-62.

167. Gibson, Q. H., and Antonini, E. (1963) Rates of Reaction of Native Human Globin with Some Hemes, *J Biol Chem 238*, 1384-88.

168. Brown, S. B., Dean, T. C., and Jones, P. (1970) Aggregation of ferrihaems. Dimerization and protolytic equilibria of protoferrihaem and deuteroferrihaem in aqueous solution, *Biochem J 117*, 733-9.
169. Gibson, Q. H., and Antonini, E. (1960) Kinetic Studies on the Reaction Between Native Globin and Haem Derivatives, *Biochem J 77*, 328-41.
170. Bunn, H. F., and Jandl, J. H. (1966) Exchange of heme among hemoglobin molecules, *Proc Natl Acad Sci U S A 56*, 974-8.
171. Waks, M., Yip, Y. K., and Beychok, S. (1973) Influence of prosthetic groups on protein folding and subunit assembly. Recombination of separated human alpha-and beta-globin chains with heme and alloplex interactions of globin chains with heme-containing subunits, *J Biol Chem 248*, 6462-70.
172. Yip, Y. K., Waks, M., and Beychok, S. (1972) Influence of prosthetic groups on protein folding and subunit assembly. I. Conformational differences between separated human alpha- and beta- globins, *J Biol Chem 247*, 7237-44.
173. Yip, Y. K., Waks, M., and Beychok, S. (1977) Reconstitution of native human hemoglobin from separated globin chains and alloplex intermediates, *Proc Natl Acad Sci U S A 74*, 64-8.
174. Lau, P., and Asakura, T. (1976) Spin label studies on conformational changes of aphohemoglobin due to heme binding, *J Biol Chem 251*, 6838-43.
175. Javaherian, K., and Beychok, S. (1968) Subunit interactions in the conformational change of horse apohemoglobin on binding of hemin, *J Mol Biol 37*, 1-11.
176. Winterhalter, K. H. (1966) Sequence of linkage between the prosthetic groups and the polypeptide chains of haemoglobin, *Nature 211*, 932-4.
177. Winterhalter, K. H., and Glatthaar, B. (1971) Intermediates of hemoglobin and their relation to biosynthesis, *Ser Haematol 4*, 84-96.
178. Winterhalter, K. H., Ioppolo, C., and Antonini, E. (1971) Distribution of heme in systems containing heme-free and heme-bound hemoglobin chains, *Biochemistry 10*, 3790-5.

179. Adachi, K., Zhao, Y., and Surrey, S. (2002) Assembly of human hemoglobin (Hb) beta- and gamma-globin chains expressed in a cell-free system with alpha-globin chains to form Hb A and Hb F, *J Biol Chem 277*, 13415-20.

180. Adachi, K., Zhao, Y., and Surrey, S. (2003) Effects of heme addition on formation of stable human globin chains and hemoglobin subunit assembly in a cell-free system, *Arch Biochem Biophys 413*, 99-106.

181. Winterhalter, K. H., and Deranleau, D. A. (1967) The structure of a hemoglobin carrying only two hemes, *Biochemistry 6*, 3136-43.

182. Oton, J., Bucci, E., Steiner, R. F., Fronticelli, C., Franchi, D., Montemarano, J., and Martinez, A. (1981) Molecular dynamics of hemoglobin subunits as seen by fluorescence spectroscopy, *J Biol Chem 256*, 7248-56.

183. Oton, J., Franchi, D., Steiner, R. F., Martinez, C. F., and Bucci, E. (1984) Fluorescence studies of internal rotation in apohemoglobin alpha-chains, *Arch Biochem Biophys 228*, 519-24.

184. Valdes, R., and Ackers, G. K. (1977) Thermodynamic studies on subunit assembly in human hemoglobin. Self-association of oxygenated chains (alphaSH and betaSH): determination of stoichiometries and equilibrium constants as a function of temperature, *J Biol Chem 252*, 74-81.

185. Valdes, R., and Ackers, G. K. (1978) Self-association of hemoglobin betaSH chains is linked to oxygenation, *Proc Natl Acad Sci U S A 75*, 311-4.

186. Rachmilewitz, E. A., Peisach, J., and Blumberg, W. E. (1971) Studies on the stability of oxyhemoglobin A and its constituent chains and their derivatives, *J Biol Chem 246*, 3356-66.

187. Bissell, D. M., Hammaker, L., and Schmid, R. (1972) Hemoglobin and erythrocyte catabolism in rat liver: the separate roles of parenchymal and sinusoidal cells, *Blood 40*, 812-22.

188. Borgstahl, G. E., Rogers, P. H., and Arnone, A. (1994) The 1.8 A structure of carbonmonoxy-beta 4 hemoglobin. Analysis of a homotetramer with the R quaternary structure of liganded alpha 2 beta 2 hemoglobin, *J Mol Biol 236*, 817-30.

189. Andersen, M. E., Moffat, J. K., and Gibson, Q. H. (1971) The kinetics of ligand binding and of the association-dissociation reactions of human hemoglobin. Properties of deoxyhemoglobin dimers, *J Biol Chem 246*, 2796-807.

190. Antonini, E., Bucci, E., Fronticelli, C., Chiancone, E., Wyman, J., and Rossi-Fanelli, A. (1966) The properties and interactions of the isolated alpha- and beta-chains of human haemoglobin. V. The reaction of alpha- and beta-chains, *J Mol Biol 17*, 29-46.

191. Antonini, E., and Chiancone, E. (1977) Assembly of multisubunit respiratory proteins, *Ann Rev Biophys Bioeng 6*, 239-71.

192. Ascoli, F., Fanelli, M. R., and Antonini, E. (1981) Preparation and properties of apohemoglobin and reconstituted hemoglobins, *Meth Enzymol 76*, 72-87.

193. Brunori, M., Antonini, E., Wyman, J., and Anderson, S. R. (1968) Spectral differences between haemoglobin and isolated haemoglobin chains in the deoxygenated state, *J Mol Biol 34*, 199-377.

194. Bucci, E., Fronticelli, C., Chiancone, E., Wyman, J., Antonini, E., and Rossi-Fanelli, A. (1965) Properties and interactions of the isolated alpha and beta chains of human haemoglobin. I. Sedimentation and Electrophoretic Behaviour, *J Mol Biol 12*, 183-92.

195. Geraci, G., Parkhurst, L. J., and Gibson, Q. H. (1969) Preparation and properties of alpha- and beta-chains from human hemoglobin, *J Biol Chem 244*, 4664-7.

196. Ip, S. H., and Ackers, G. K. (1977) Thermodynamic studies on subunit assembly in human hemoglobin. Temperature dependence of the dimer-tetramer association constants for oxygenated and unliganded hemoglobins, *J Biol Chem 252*, 82-7.

197. Ip, S. H., Johnson, M. L., and Ackers, G. K. (1976) Kinetics of deoxyhemoglobin subunit dissociation determined by haptoglobin binding: estimation of the equilibrium constant from forward and reverse rates, *Biochemistry 15*, 654-60.

198. Kawamura, Y., and Nakamura, S. (1983) Assembly of oxyhemoglobin from isolated alpha and beta chains, *J Biochem 93*, 1159-66.

199. Kawamura-Konishi, Y., Chiba, K., Kihara, H., and Suzuki, H. (1992) Kinetics of the reconstitution of hemoglobin from semihemoglobins alpha and beta with heme, *Eur Biophys J 21*, 85-92.

200. McDonald, M. J., Turci, S. M., Mrabet, N. T., Himelstein, B. P., and Bunn, H. F. (1987) The kinetics of assembly of normal and variant human oxyhemoglobins, *J Biol Chem 262*, 5951-6.

201. McGovern, P., Reisberg, P., and Olson, J. S. (1976) Aggregation of deoxyhemoglobin subunits, *J Biol Chem 251*, 7871-9.

202. Mrabet, N. T., Shaeffer, J. R., McDonald, M. J., and Bunn, H. F. (1986) Dissociation of dimers of human hemoglobins A and F into monomers, *J Biol Chem 261*, 1111-5.

203. Mrabet, N. T., McDonald, M. J., Turci, S., Sarkar, R., Szabo, A., and Bunn, H. F. (1986) Electrostatic attraction governs the dimer assembly of human hemoglobin, *J Biol Chem 261*, 5222-8.

204. Nagel, R. L., and Gibson, Q. H. (1971) The binding of hemoglobin to haptoglobin and its relation to subunit dissociation of hemoglobin, *J Biol Chem 246*, 69-73.

205. Shaeffer, J. R., McDonald, M. J., Turci, S. M., Dinda, D. M., and Bunn, H. F. (1984) Dimer-monomer dissociation of human hemoglobin A, *J Biol Chem 259*, 14544-7.

206. Friedman, F. K., and Beychok, S. (1979) Probes of subunit assembly and reconstitution pathways in multisubunit proteins, *Annu Rev Biochem 48*, 217-50.

207. Kendrew, J. C., Watson, H. C., Strandberg, B. E., Dickerson, R. E., Phillips, D. C., and Shore, V. C. (1961) The amino-acid sequence x-ray methods, and its correlation with chemical data, *Nature 190*, 666-70.

208. Coghlan, D., Jones, G., Denton, K. A., Wilson, M. T., Chan, B., Harris, R., Woodrow, J. R., and Ogden, J. E. (1992) Structural and functional characterisation of recombinant human haemoglobin A expressed in Saccharomyces cerevisiae, *Eur J Biochem 207*, 931-6.

209. Ogden, J. E., Coghlan, D., Jones, G., Denton, K. A., Harris, R., Chan, B., Woodrow, J., and Wilson, M. T. (1992) Expression and assembly of functional human hemoglobin in S. cerevisiae, *Biomater Artif Cells Immobilization Biotechnol 20*, 473-5.

210. Adachi, K., Konitzer, P., Lai, C. H., Kim, J., and Surrey, S. (1992) Oxygen binding and other physical properties of human hemoglobin made in yeast, *Protein Eng 5*, 807-10.

211. Hoffman, S. J., Looker, D. L., Roehrich, J. M., Cozart, P. E., Durfee, S. L., Tedesco, J. L., and Stetler, G. L. (1990) Expression of fully functional tetrameric human hemoglobin in Escherichia coli, *Proc Natl Acad Sci U S A 87*, 8521-5.

212. Ogden, J. E., Harris, R., and Wilson, M. T. (1994) Production of recombinant human hemoglobin A in Saccharomyces cerevisiae, *Meth Enzymol 231*, 374-90.

213. Shen, T. J., Ho, N. T., Simplaceanu, V., Zou, M., Green, B. N., Tam, M. F., and Ho, C. (1993) Production of unmodified human adult hemoglobin in Escherichia coli, *Proc Natl Acad Sci U S A 90*, 8108-12.

214. Wagenbach, M., O'Rourke, K., Vitez, L., Wieczorek, A., Hoffman, S., Durfee, S., Tedesco, J., and Stetler, G. (1991) Synthesis of wild type and mutant human hemoglobins in Saccharomyces cerevisiae, *Biotechnology (N Y) 9*, 57-61.

215. Sharma, A., Martin, M. J., Okabe, J. F., Truglio, R. A., Dhanjal, N. K., Logan, J. S., and Kumar, R. (1994) An isologous porcine promoter permits high level expression of human hemoglobin in transgenic swine, *Biotechnology (NY) 12*, 55-9.

216. Shen, T. J., Ho, N. T., Zou, M., Sun, D. P., Cottam, P. F., Simplaceanu, V., Tam, M. F., Bell, D. A., and Ho, C. (1997) Production of human normal adult and fetal hemoglobins in Escherichia coli, *Protein Eng 10*, 1085-97.

217. Apostol, I., Levine, J., Lippincott, J., Leach, J., Hess, E., Glascock, C. B., Weickert, M. J., and Blackmore, R. (1997) Incorporation of norvaline at leucine positions in recombinant human hemoglobin expressed in Escherichia coli, *J Biol Chem 272*, 28980-8.

218. Apostol, I., Aitken, J., Levine, J., Lippincott, J., Davidson, J. S., and Abbott-Brown, D. (1995) Recombinant protein sequences can trigger methylation of N-terminal amino acids in Escherichia coli, *Protein Sci 4*, 2616-8.

219. Behringer, R. R., Ryan, T. M., Reilly, M. P., Asakura, T., Palmiter, R. D., Brinster, R. L., and Townes, T. M. (1989) Synthesis of functional human hemoglobin in transgenic mice, *Science 245*, 971-3.

220. Chada, K., Magram, J., Raphael, K., Radice, G., Lacy, E., and Costantini, F. (1985) Specific expression of a foreign beta-globin gene in erythroid cells of transgenic mice, *Nature 314*, 377-80.

221. Dieryck, W., Pagnier, J., Poyart, C., Marden, M. C., Gruber, V., Bournat, P., Baudino, S., and Merot, B. (1997) Human haemoglobin from transgenic tobacco, *Nature 386*, 29-30.

222. Groebe, D. R., Busch, M. R., Tsao, T. Y., Luh, F. Y., Tam, M. F., Chung, A. E., Gaskell, M., Liebhaber, S. A., and Ho, C. (1992) High-level production of human alpha- and beta-globins in insect cells, *Protein Expr Purif 3*, 134-41.

223. Lippincott, J., Hess, E., and Apostol, I. (1997) Mapping of recombinant hemoglobin using immobilized trypsin cartridges, *Anal Biochem 252*, 314-25.

224. Logan, J. S., and Martin, M. J. (1994) Transgenic swine as a recombinant production system for human hemoglobin, *Meth Enzymol 231*, 435-45.

225. Looker, D., Abbott-Brown, D., Cozart, P., Durfee, S., Hoffman, S., Mathews, A. J., Miller-Roehrich, J., Shoemaker, S., Trimble, S., and Fermi, G., et al. (1992) A human recombinant haemoglobin designed for use as a blood substitute, *Nature 356*, 258-60.

226. Looker, D., Mathews, A. J., Neway, J. O., and Stetler, G. L. (1994) Expression of recombinant human hemoglobin in Escherichia coli, *Meth Enzymol 231*, 364-74.

227. Manjula, B. N., Kumar, R., Sun, D. P., Ho, N. T., Ho, C., Rao, J. M., Malavalli, A., and Acharya, A. S. (1998) Correct assembly of human normal adult hemoglobin when expressed in transgenic swine: chemical,

conformational and functional equivalence with the human-derived protein, *Protein Eng 11*, 583-8.

228. Nagai, K., and Thogersen, H. C. (1987) Synthesis and sequence-specific proteolysis of hybrid proteins produced in Escherichia coli, *Meth Enzymol 153*, 461-81.
229. Nagai, K., Luisi, B., Shih, D., Miyazaki, G., Imai, K., Poyart, C., De Young, A., Kwiatkowsky, L., Noble, R. W., and Lin, S. H., et al. (1987) Distal residues in the oxygen binding site of haemoglobin studied by protein engineering, *Nature 329*, 858-60.
230. O'Donnell, J. K., Martin, M. J., Logan, J. S., and Kumar, R. (1993) Production of human hemoglobin in transgenic swine: an approach to a blood substitute, *Cancer Detect Prev 17*, 307-12.
231. Olson, J. S., Mathews, A. J., Rohlfs, R. J., Springer, B. A., Egeberg, K. D., Sligar, S. G., Tame, J., Renaud, J. P., and Nagai, K. (1988) The role of the distal histidine in myoglobin and haemoglobin, *Nature 336*, 265-6.
232. Ryan, T. M., Townes, T. M., Reilly, M. P., Asakura, T., Palmiter, R. D., Brinster, R. L., and Behringer, R. R. (1990) Human sickle hemoglobin in transgenic mice, *Science 247*, 566-8.
233. Shoemaker, S. A., Gerber, M. J., Evans, G. L., Archer-Paik, L. E., and Scoggin, C. H. (1994) Initial clinical experience with a rationally designed, genetically engineered recombinant human hemoglobin, *Artif Cells Blood Substit Immobil Biotechnol 22*, 457-65.
234. Springer, B. A., and Sligar, S. G. (1987) High-level expression of sperm whale myoglobin in Escherichia coli, *Proc Natl Acad Sci U S A 84*, 8961-5.
235. Swanson, M. E., Martin, M. J., O'Donnell, J. K., Hoover, K., Lago, W., Huntress, V., Parsons, C. T., Pinkert, C. A., Pilder, S., and Logan, J. S. (1992) Production of functional human hemoglobin in transgenic swine, *Biotechnology (NY) 10*, 557-9.
236. Townes, T. M., Lingrel, J. B., Chen, H. Y., Brinster, R. L., and Palmiter, R. D. (1985) Erythroid-specific expression of human beta-globin genes in transgenic mice, *Eur Mol Biol J 4*, 1715-23.

237. Townes, T. M., Chen, H. Y., Lingrel, J. B., Palmiter, R. D., and Brinster, R. L. (1985) Expression of human beta-globin genes in transgenic mice: effects of a flanking metallothionein-human growth hormone fusion gene, *Mol Cell Biol 5*, 1977-83.

238. Trimble, S. P., Marquardt, D., and Anderson, D. C. (1997) Use of designed peptide linkers and recombinant hemoglobin mutants for drug delivery: in vitro release of an angiotensin II analog and kinetic modeling of delivery, *Bioconjug Chem 8*, 416-23.

239. Apostol, I. (1999) Assessing the relative stabilities of engineered hemoglobins using electrospray mass spectrometry, *Anal Biochem 272*, 8-18.

240. Apostol, I., Brooks, P. D., and Mathews, A. J. (2001) Application of high-precision isotope ratio monitoring mass spectrometry to identify the biosynthetic origins of proteins, *Protein Sci 10*, 1466-9.

241. Doherty, D. H., Doyle, M. P., Curry, S. R., Vali, R. J., Fattor, T. J., Olson, J. S., and Lemon, D. D. (1998) Rate of reaction with nitric oxide determines the hypertensive effect of cell-free hemoglobin, *Nat Biotechnol 16*, 672-6.

242. Hartman, J. C., Argoudelis, G., Doherty, D., Lemon, D., and Gorczynski, R. (1998) Reduced nitric oxide reactivity of a new recombinant human hemoglobin attenuates gastric dysmotility, *Eur J Pharmacol 363*, 175-8.

243. Lippincott, J., Fattor, T. J., Lemon, D. D., and Apostol, I. (2000) Application of native-state electrospray mass spectrometry to identify zinc-binding sites on engineered hemoglobin, *Anal Biochem 284*, 247-55.

244. Raat, N. J., Liu, J. F., Doyle, M. P., Burhop, K. E., Klein, J., and Ince, C. (2005) Effects of recombinant-hemoglobin solutions rHb2.0 and rHb1.1 on blood pressure, intestinal blood flow, and gut oxygenation in a rat model of hemorrhagic shock, *J Lab Clin Med 145*, 21-32.

245. Rao, M. J., Schneider, K., Chait, B. T., Chao, T. L., Keller, H., Anderson, S., Manjula, B. N., Kumar, R., and Acharya, A. S. (1994) Recombinant hemoglobin A produced in transgenic swine: structural equivalence with human hemoglobin A, *Artif Cells Blood Substit Immobil Biotechnol 22*, 695-700.

246. Rao, M. J., Manjula, B. N., Kumar, R., and Acharya, A. S. (1996) Chimeric hemoglobins--hybrids of human and swine hemoglobin: assembly and stability of interspecies hybrids, *Protein Sci 5*, 956-65.

247. Weickert, M. J., and Curry, S. R. (1997) Turnover of recombinant human hemoglobin in Escherichia coli occurs rapidly for insoluble and slowly for soluble globin, *Arch Biochem Biophys 348*, 337-46.

248. Weickert, M. J., Doherty, D. H., Best, E. A., and Olins, P. O. (1996) Optimization of heterologous protein production in Escherichia coli, *Curr Opin Biotechnol 7*, 494-9.

249. Weickert, M. J., Pagratis, M., Curry, S. R., and Blackmore, R. (1997) Stabilization of apoglobin by low temperature increases yield of soluble recombinant hemoglobin in Escherichia coli, *Appl Environ Microbiol 63*, 4313-20.

250. Weickert, M. J., Pagratis, M., Glascock, C. B., and Blackmore, R. (1999) A mutation that improves soluble recombinant hemoglobin accumulation in Escherichia coli in heme excess, *Appl Environ Microbiol 65*, 640-7.

251. Weickert, M. J., and Apostol, I. (1998) High-fidelity translation of recombinant human hemoglobin in Escherichia coli, *Appl Environ Microbiol 64*, 1589-93.

252. Andersen, D. C., and Krummen, L. (2002) Recombinant protein expression for therapeutic applications, *Curr Opin Biotechnol 13*, 117-23.

253. Baneyx, F. (1999) Recombinant protein expression in Escherichia coli, *Curr Opin Biotechnol 10*, 411-21.

254. Barnard, A., Wolfe, A., and Busby, S. (2004) Regulation at complex bacterial promoters: how bacteria use different promoter organizations to produce different regulatory outcomes, *Curr Opin Microbiol 7*, 102-8.

255. Chu, L., and Robinson, D. K. (2001) Industrial choices for protein production by large-scale cell culture, *Curr Opin Biotechnol 12*, 180-7.

256. Cornelis, P. (2000) Expressing genes in different Escherichia coli compartments, *Curr Opin Biotechnol 11*, 450-4.

257. Dyson, M. R., Shadbolt, S. P., Vincent, K. J., Perera, R. L., and McCafferty, J. (2004) Production of soluble mammalian proteins in Escherichia coli:

identification of protein features that correlate with successful expression, *BMC Biotechnol 4*, 32.

258. Georgiou, G., and Valax, P. (1996) Expression of correctly folded proteins in Escherichia coli, *Curr Opin Biotechnol 7*, 190-7.

259. Hannig, G., and Makrides, S. C. (1998) Strategies for optimizing heterologous protein expression in Escherichia coli, *Trends Biotechnol 16*, 54-60.

260. Hockney, R. C. (1994) Recent developments in heterologous protein production in Escherichia coli, *Trends Biotechnol 12*, 456-63.

261. Jana, S., and Deb, J. K. (2005) Strategies for efficient production of heterologous proteins in Escherichia coli, *Appl Microbiol Biotechnol 67*, 289-98.

262. Lee, S. Y. (1996) High cell-density culture of Escherichia coli, *Trends Biotechnol 14*, 98-105.

263. Makrides, S. C. (1996) Strategies for achieving high-level expression of genes in Escherichia coli, *Microbiol Rev 60*, 512-38.

264. Mergulhao, F., Monteiro, G., Cabral, J., and Taipa, M. (2003) Design of Bacterial Vector Systems for the Production of Recombinant Proteins in Escherichia coli, *J Microbiol Biotechnol 14*, 1-14.

265. Miroux, B., and Walker, J. E. (1996) Over-production of proteins in Escherichia coli: mutant hosts that allow synthesis of some membrane proteins and globular proteins at high levels, *J Mol Biol 260*, 289-98.

266. Olson, P., Zhang, Y., Olsen, D., Owens, A., Cohen, P., Nguyen, K., Ye, J. J., Bass, S., and Mascarenhas, D. (1998) High-level expression of eukaryotic polypeptides from bacterial chromosomes, *Protein Expr Purif 14*, 160-6.

267. Peredelchuk, M. Y., and Bennett, G. N. (1997) A method for construction of E. coli strains with multiple DNA insertions in the chromosome, *Gene 187*, 231-8.

268. Schmidt, F. R. (2004) Recombinant expression systems in the pharmaceutical industry, *Appl Microbiol Biotechnol 65*, 363-72.

269. Shiloach, J., and Fass, R. (2005) Growing E. coli to high cell density--a historical perspective on method development, *Biotechnol Adv 23*, 345-57.

270. Sorensen, H. P., and Mortensen, K. K. (2005) Advanced genetic strategies for recombinant protein expression in Escherichia coli, *J Biotechnol 115*, 113-28.

271. Summers, D. (1998) Timing, self-control and a sense of direction are the secrets of multicopy plasmid stability, *Mol Microbiol 29*, 1137-45.

272. Swartz, J. R. (2001) Advances in Escherichia coli production of therapeutic proteins, *Curr Opin Biotechnol 12*, 195-201.

273. Tan, S. (2001) A modular polycistronic expression system for overexpressing protein complexes in Escherichia coli, *Protein Expr Purif 21*, 224-34.

274. Terpe, K. (2006) Overview of bacterial expression systems for heterologous protein production: from molecular and biochemical fundamentals to commercial systems, *Appl Microbiol Biotechnol 72*, 211-22.

275. Vasina, J. A., and Baneyx, F. (1997) Expression of aggregation-prone recombinant proteins at low temperatures: a comparative study of the Escherichia coli cspA and tac promoter systems, *Protein Expr Purif 9*, 211-8.

276. Zhang, Y., Olsen, D. R., Nguyen, K. B., Olson, P. S., Rhodes, E. T., and Mascarenhas, D. (1998) Expression of eukaryotic proteins in soluble form in Escherichia coli, *Protein Expr Purif 12*, 159-65.

277. Fronticelli, C., O'Donnell, J. K., and Brinigar, W. S. (1991) Recombinant human hemoglobin: expression and refolding of beta-globin from Escherichia coli, *J Protein Chem 10*, 495-501.

278. Guarente, L., Lauer, G., Roberts, T. M., and Ptashne, M. (1980) Improved methods for maximizing expression of a cloned gene: a bacterium that synthesizes rabbit beta-globin, *Cell 20*, 543-53.

279. Nagai, K., and Thogersen, H. C. (1984) Generation of beta-globin by sequence-specific proteolysis of a hybrid protein produced in Escherichia coli, *Nature 309*, 810-2.

280. Nagai, K., Perutz, M. F., and Poyart, C. (1985) Oxygen binding properties of human mutant hemoglobins synthesized in Escherichia coli, *Proc Natl Acad Sci U S A 82*, 7252-5.

281. Adachi, K., Yamaguchi, T., Yang, Y., Konitzer, P. T., Pang, J., Reddy, K. S., Ivanova, M., Ferrone, F., and Surrey, S. (2000) Expression of functional soluble human alpha-globin chains of hemoglobin in bacteria, *Protein Expr Purif 20*, 37-44.

282. Sanna, M. T., Razynska, A., Karavitis, M., Koley, A. P., Friedman, F. K., Russu, I. M., Brinigar, W. S., and Fronticelli, C. (1997) Assembly of human hemoglobin. Studies with Escherichia coli-expressed alpha-globin, *J Biol Chem 272*, 3478-86.

283. Tame, J., Shih, D. T., Pagnier, J., Fermi, G., and Nagai, K. (1991) Functional role of the distal valine (E11) residue of alpha subunits in human haemoglobin, *J Mol Biol 218*, 761-7.

284. Hernan, R. A., and Sligar, S. G. (1995) Tetrameric hemoglobin expressed in Escherichia coli. Evidence of heterogeneous subunit assembly, *J Biol Chem 270*, 26257-64.

285. Hernan, R. A., Hui, H. L., Andracki, M. E., Noble, R. W., Sligar, S. G., Walder, J. A., and Walder, R. Y. (1992) Human hemoglobin expression in Escherichia coli: importance of optimal codon usage, *Biochemistry 31*, 8619-28.

286. Jessen, T. H., Komiyama, N. H., Tame, J., Pagnier, J., Shih, D., Luisi, B., Fermi, G., and Nagai, K. (1994) Production of human hemoglobin in Escherichia coli using cleavable fusion protein expression vector, *Meth Enzymol 231*, 347-64.

287. Yamaguchi, T., Pang, J., Reddy, K. S., Witkowska, H. E., Surrey, S., and Adachi, K. (1996) Expression of soluble human beta-globin chains in bacteria and assembly in vitro with alpha-globin chains, *J Biol Chem 271*, 26677-83.

288. Bobofchak, K. M., Mito, T., Texel, S. J., Bellelli, A., Nemoto, M., Traystman, R. J., Koehler, R. C., Brinigar, W. S., and Fronticelli, C. (2003) A recombinant polymeric hemoglobin with conformational, functional, and physiological characteristics of an in vivo O2 transporter, *Am J Physiol Heart Circ Physiol 285*, H549-61.

289. Faggiano, S., Bruno, S., Ronda, L., Pizzonia, P., Pioselli, B., and Mozzarelli, A. (2010) Modulation of expression and polymerization of Hemoglobin Polytaur, a potential blood substitute, *Arch Biochem Biophys epub ahead of print edition*.

290. Fronticelli, C., Arosio, D., Bobofchak, K. M., and Vasquez, G. B. (2001) Molecular engineering of a polymer of tetrameric hemoglobins, *Proteins 44*, 212-22.

291. Harnois, T., Rousselot, M., Rogniaux, H., and Zal, F. (2009) High-level production of recombinant Arenicola marina globin chains in Escherichia coli: a new generation of blood substitute, *Artif Cells Blood Substit Immobil Biotechnol 37*, 106-16.

292. Harrington, J. P., Kobayashi, S., Dorman, S. C., Zito, S. L., and Hirsch, R. E. (2007) Acellular invertebrate hemoglobins as model therapeutic oxygen carriers: unique redox potentials, *Artif Cells Blood Substit Immobil Biotechnol 35*, 53-67.

293. Hirsch, R. E., Jelicks, L. A., Wittenberg, B. A., Kaul, D. K., Shear, H. L., and Harrington, J. P. (1997) A first evaluation of the natural high molecular weight polymeric Lumbricus terrestris hemoglobin as an oxygen carrier, *Artif Cells Blood Substit Immobil Biotechnol 25*, 429-44.

294. Leon, R. G., Munier-Lehmann, H., Barzu, O., Baudin-Creuza, V., Pietri, R., Lopez-Garriga, J., and Cadilla, C. L. (2004) High-level production of recombinant sulfide-reactive hemoglobin I from Lucina pectinata in Escherichia coli. High yields of fully functional holoprotein synthesis in the BLi5 E. coli strain, *Protein Expr Purif 38*, 184-95.

295. Rousselot, M., Delpy, E., Drieu La Rochelle, C., Lagente, V., Pirow, R., Rees, J. F., Hagege, A., Le Guen, D., Hourdez, S., and Zal, F. (2006) Arenicola marina extracellular hemoglobin: a new promising blood substitute, *Biotechnol J 1*, 333-45.

296. Amberson, W. R., Jennings, J. J., and Rhode, C. M. (1949) Clinical experience with hemoglobin-saline solutions, *J Appl Physiol 1*, 469-89.

297. Blackburn, C. R., Hensley, W. J., Grant, D. K., and Wright, F. B. (1954) Studies on intravascular hemolysis in man: the pathogenesis of the initial stages of acute renal failure, *J Clin Invest 33*, 825-34.

298. Brandt, J. L., Frank, N. R., and Lichtman, H. C. (1951) The effects of hemoglobin solutions on renal functions in man, *Blood 6*, 1152-8.

299. Bunn, H. F., and Jandl, J. H. (1968) The renal handling of hemoglobin, *Trans Assoc Am Physicians 81*, 147-52.

300. Feola, M., Simoni, J., Tran, R., and Canizaro, P. C. (1990) Nephrotoxicity of hemoglobin solutions, *Biomater Artif Cells Artif Organs 18*, 233-49.

301. Gilligan, D. R., Altschule, M. D., and Katersky, E. M. (1941) Studies of Hemoglobinemia and Hemoglobinuria Produced in Man by Intravenous Injection of Hemoglobin Solutions, *J Clin Invest 20*, 177-87.

302. Goldberg, M. (1962) Studies of the acute renal effects of hemolyzed red blood cells in dogs including estimations of renal blood flow with krypton, *J Clin Invest 41*, 2112-22.

303. Jaenike, J. R. (1966) The renal lesion associated with hemoglobinemia. I. Its production and functional evolution in the rat, *J Exp Med 123*, 523-35.

304. Jaenike, J. R. (1967) The renal lesion associated with hemoglobinemia: a study of the pathogenesis of the excretory defect in the rat, *J Clin Invest 46*, 378-87.

305. Jaenike, J. R., and Schneeberger, E. E. (1966) The renal lesion associated with hemoglobinemia. II. Its structural characteristics in the rat, *J Exp Med 123*, 537-45.

306. Lieberthal, W., Wolf, E. F., Merrill, E. W., Levinsky, N. G., and Valeri, C. R. (1987) Hemodynamic effects of different preparations of stroma free hemolysates in the isolated perfused rat kidney, *Life Sci 41*, 2525-33.

307. Miller, J. H., and Mc, D. R. (1951) The effect of hemoglobin on renal function in the human, *J Clin Invest 30*, 1033-40.

308. Paller, M. S. (1988) Hemoglobin- and myoglobin-induced acute renal failure in rats: role of iron in nephrotoxicity, *Am J Physiol 255*, F539-44.

309. Rabiner, S. F., Helbert, J. R., Lopas, H., and Friedman, L. H. (1967) Evaluation of a stroma-free hemoglobin solution for use as a plasma expander, *J Exp Med 126*, 1127-42.

310. Rosoff, C. B., and Walter, C. W. (1952) The controlled laboratory production of hemoglobinuric nephrosis, *Ann Surg 135*, 324-31.

311. Savitsky, J. P., Doczi, J., Black, J., and Arnold, J. D. (1978) A clinical safety trial of stroma-free hemoglobin, *Clin Pharmacol Ther 23*, 73-80.

312. Sellards, A. W., and Minot, G. R. (1916) Injection of Hemoglobin in Man and its Relation to Blood Destruction, with especial reference to the Anemias, *J Med Res 34*, 469-94.

313. Zager, R. A., and Gamelin, L. M. (1989) Pathogenetic mechanisms in experimental hemoglobinuric acute renal failure, *Am J Physiol 256*, F446-55.

314. Ascenzi, P., Bocedi, A., Visca, P., Altruda, F., Tolosano, E., Beringhelli, T., and Fasano, M. (2005) Hemoglobin and heme scavenging, *IUBMB Life 57*, 749-59.

315. Bunn, H. F., Esham, W. T., and Bull, R. W. (1969) The renal handling of hemoglobin. I. Glomerular filtration, *J Exp Med 129*, 909-23.

316. Chiancone, E., Alfsen, A., Ioppolo, C., Vecchini, P., Agro, A. F., Wyman, J., and Antonini, E. (1968) Studies on the reaction of haptoglobin with haemoglobin and haemoglobin chains. I. Stoichiometry and affinity, *J Mol Biol 34*, 347-56.

317. Garby, L., and Noyes, W. D. (1959) Studies on hemoglobin metabolism. I. The kinetic properties of the plasma hemoglobin pool in normal man, *J Clin Invest 38*, 1479-83.

318. Garby, L., and Noyes, W. D. (1959) Studies on hemoglobin metabolism. II. Pathways of hemoglobin iron metabolism in normal man, *J Clin Invest 38*, 1484-6.

319. Greer, J., Foerster, J., Rodgers, G., Paraskevas, F., Glader, B., Arber, D., and Means, R. (2009) Wintrobe's Clinical Hematology (Pine, J., Ed.). Lippincott Williams & Wilkins, Philadelphia, PA.

320. Higa, Y., Oshiro, S., Kino, K., Tsunoo, H., and Nakajima, H. (1981) Catabolism of globin-haptoglobin in liver cells after intravenous administration of hemoglobin-haptoglobin to rats, *J Biol Chem 256*, 12322-8.

321. Keipert, P. E., Gomez, C. L., Gonzales, A., Macdonald, V. W., and Winslow, R. M. (1992) The role of the kidneys in the excretion of chemically modified hemoglobins, *Biomater Artif Cells Immobilization Biotechnol 20*, 737-45.

322. Kino, K., Tsunoo, H., Higa, Y., Takami, M., and Nakajima, H. (1982) Kinetic aspects of hemoglobin.haptoglobin-receptor interaction in rat liver plasma membranes, isolated liver cells, and liver cells in primary culture, *J Biol Chem 257*, 4828-33.

323. Kino, K., Tsunoo, H., Higa, Y., Takami, M., Hamaguchi, H., and Nakajima, H. (1980) Hemoglobin-haptoglobin receptor in rat liver plasma membrane, *J Biol Chem 255*, 9616-20.

324. Knutson, M., and Wessling-Resnick, M. (2003) Iron metabolism in the reticuloendothelial system, *Crit Rev Biochem Mol Biol 38*, 61-88.

325. Kristiansen, M., Graversen, J. H., Jacobsen, C., Sonne, O., Hoffman, H. J., Law, S. K., and Moestrup, S. K. (2001) Identification of the haemoglobin scavenger receptor, *Nature 409*, 198-201.

326. Lathem, W. (1959) The renal excretion of hemoglobin: regulatory mechanisms and the differential excretion of free and protein-bound hemoglobin, *J Clin Invest 38*, 652-8.

327. Matheson, B., Razynska, A., Kwansa, H., and Bucci, E. (2000) Appearance of dissociable and cross-linked hemoglobins in the renal hilar lymph, *J Lab Clin Med 135*, 459-64.

328. Okuda, M., Tokunaga, R., and Taketani, S. (1992) Expression of haptoglobin receptors in human hepatoma cells, *Biochim Biophys Acta 1136*, 143-9.

329. Oshiro, S., Yajima, Y., Kawamura, K., Kubota, M., Yokofujita, J., Nishibe, Y., Takahama, M., and Nakajima, H. (1992) Catabolism of hemoglobin-haptoglobin complex in microsome subfractions, *Chem Pharm Bull (Tokyo) 40*, 1847-51.

330. Szabo, G., Magyar, S., and Kocsar, L. (1965) Passage of haemoglobin into urine and lymph, *Acta Med Acad Sci Hung 21*, 349-59.

331. Urbaitis, B. K., Razynska, A., Corteza, Q., Fronticelli, C., and Bucci, E. (1991) Intravascular retention and renal handling of purified natural and intramolecularly cross-linked hemoglobins, *J Lab Clin Med 117*, 115-21.

332. Boland, E. J., Nair, P. K., Lemon, D. D., Olson, J. S., and Hellums, J. D. (1987) An in vitro capillary system for studies on microcirculatory O2 transport, *J Appl Physiol 62*, 791-7.

333. Clark, A., Federspiel, W. J., Clark, P. A., and Cokelet, G. R. (1985) Oxygen delivery from red cells, *Biophys J 47*, 171-81.

334. Coin, J. T., and Olson, J. S. (1979) The rate of oxygen uptake by human red blood cells, *J Biol Chem 254*, 1178-90.

335. Gould, S. A., Sehgal, L. R., Rosen, A. L., Sehgal, H. L., Levine, H. D., Rice, C. L., and Moss, G. S. (1982) Hemoglobin solution: is a normal [Hb] or P50 more important?, *J Surg Res 33*, 189-93.

336. Kavdia, M., Pittman, R. N., and Popel, A. S. (2002) Theoretical analysis of effects of blood substitute affinity and cooperativity on organ oxygen transport, *J Appl Physiol 93*, 2122-8.

337. Lemon, D. D., Nair, P. K., Boland, E. J., Olson, J. S., and Hellums, J. D. (1987) Physiological factors affecting O2 transport by hemoglobin in an in vitro capillary system, *J Appl Physiol 62*, 798-806.

338. Lemon, D. D., Boland, E. J., Nair, P. K., Olson, J. S., and Hellums, J. D. (1988) Effects of physiological factors on oxygen transport in an in vitro capillary system, *Adv Exp Med Biol 222*, 37-44.

339. Marden, M. C., Griffon, N., and Poyart, C. (1995) Oxygen delivery and autoxidation of hemoglobin, *Transfus Clin Biol 2*, 473-80.

340. McCarthy, M. R., Vandegriff, K. D., and Winslow, R. M. (2001) The role of facilitated diffusion in oxygen transport by cell-free hemoglobins: implications for the design of hemoglobin-based oxygen carriers, *Biophys Chem 92*, 103-17.

341. Messmer, K., Jesch, F., Peters, W., and Schoenberg, M. (1977) Oxygen affinity of stroma free hemoglobin and its effect on tissue oxygenation, *Bibl Anat* 375-9.

342. Nair, P. K., Huang, N. S., Hellums, J. D., and Olson, J. S. (1990) A simple model for prediction of oxygen transport rates by flowing blood in large capillaries, *Microvasc Res 39*, 203-11.

343. Nair, P. K., Hellums, J. D., and Olson, J. S. (1989) Prediction of oxygen transport rates in blood flowing in large capillaries, *Microvasc Res 38*, 269-85.

344. Page, T., and Hellums, J. (2006) Oxygen Transport Properties of Hemoglobin-Based Oxygen Carriers: Studies using Artificial Capillaries and Mathematical Simulation, in *Blood Substitutes* (Winslow, N., Ed.), pp 72-83. Academic Press (Elsevier), San Diego, CA.

345. Page, T. C., Light, W. R., McKay, C. B., and Hellums, J. D. (1998) Oxygen transport by erythrocyte/hemoglobin solution mixtures in an in vitro capillary as a model of hemoglobin-based oxygen carrier performance, *Microvasc Res 55*, 54-64.

346. Rosen, A. L., Sehgal, L. R., Gould, S. A., Sehgal, H. L., and Moss, G. S. (1986) Methodology to assess the oxygen concentration of red cells and stroma-free hemoglobin solutions, *Crit Care Med 14*, 147-50.

347. Scholander, P. F. (1960) Oxygen transport through hemoglobin solutions, *Science 131*, 585-90.

348. Standl, T., Horn, P., Wilhelm, S., Greim, C., Freitag, M., Freitag, U., Sputtek, A., Jacobs, E., and Schulte am Esch, J. (1996) Bovine haemoglobin is more potent than autologous red blood cells in restoring muscular tissue oxygenation after profound isovolaemic haemodilution in dogs, *Can J Anaesth 43*, 714-23.

349. Tsai, A. G., Vandegriff, K. D., Intaglietta, M., and Winslow, R. M. (2003) Targeted O2 delivery by low-P50 hemoglobin: a new basis for O2 therapeutics, *Am J Physiol Heart Circ Physiol 285*, H1411-9.

350. Tsai, A., Cabrales, P., and Intaglietta, M. (2006) Mechanisms of Oxygen Transport in the Microcirculation: Effects of Cell-Free Oxygen Carriers, in

Blood Substitutes (Winslow, N., Ed.), pp 84-92. Academic Press (Elsevier), San Diego, CA.

351. Vadapalli, A., Goldman, D., and Popel, A. S. (2002) Calculations of oxygen transport by red blood cells and hemoglobin solutions in capillaries, *Artif Cells Blood Substit Immobil Biotechnol 30*, 157-88.
352. Vandegriff, K. D., and Olson, J. S. (1984) Morphological and physiological factors affecting oxygen uptake and release by red blood cells, *J Biol Chem 259*, 12619-27.
353. Vandegriff, K. D., and Olson, J. S. (1984) A quantitative description in three dimensions of oxygen uptake by human red blood cells, *Biophys J 45*, 825-35.
354. Weingarden, M., Mizukami, H., and Rice, S. A. (1982) Factors defining the rate of oxygen uptake by the red blood cell, *Bull Math Biol 44*, 135-47.
355. Winslow, R. M., Samaja, M., Winslow, N. J., Rossi-Bernardi, L., and Shrager, R. I. (1983) Simulation of continuous blood O2 equilibrium curve over physiological pH, DPG, and Pco2 range, *J Appl Physiol 54*, 524-9.
356. Alayash, A. I., and Cashon, R. E. (1995) Hemoglobin and free radicals: implications for the development of a safe blood substitute, *Mol Med Today 1*, 122-7.
357. Amend, J., Ou, C., Ryan-MacFarlane, C., Anderson, P. J., Amend, N., and Biro, G. P. (1996) Systemic responses to SFHS-infusion in hemorrhaged dogs, *Artif Cells Blood Substit Immobil Biotechnol 24*, 19-34.
358. Balla, G., Vercellotti, G. M., Muller-Eberhard, U., Eaton, J., and Jacob, H. S. (1991) Exposure of endothelial cells to free heme potentiates damage mediated by granulocytes and toxic oxygen species, *Lab Invest 64*, 648-55.
359. Balla, J., Jacob, H. S., Balla, G., Nath, K., Eaton, J. W., and Vercellotti, G. M. (1993) Endothelial-cell heme uptake from heme proteins: induction of sensitization and desensitization to oxidant damage, *Proc Natl Acad Sci U S A 90*, 9285-9.
360. Biro, G. P., Taichman, G. C., Lada, B., Keon, W. J., Rosen, A. L., and Sehgal, L. R. (1988) Coronary vascular actions of stroma-free hemoglobin preparations, *Artif Organs 12*, 40-50.

361. Biro, G. P., Anderson, P. J., Curtis, S. E., and Cain, S. M. (1991) Stroma-free hemoglobin: its presence in plasma does not improve oxygen supply to the resting hindlimb vascular bed of hemodiluted dogs, *Can J Physiol Pharmacol 69*, 1656-62.

362. Biro, G. P., Ou, C., Ryan-MacFarlane, C., and Anderson, P. J. (1995) Oxyradical generation after resuscitation of hemorrhagic shock with blood or stroma-free hemoglobin solution, *Artif Cells Blood Substit Immobil Biotechnol 23*, 631-45.

363. Burhop, K. E., Farrell, L., Nigro, C., Tan, D., and Estep, T. (1992) Effects of intravenous infusions of diaspirin cross-linked hemoglobin (DCLHb) on sheep, *Biomater Artif Cells Immobilization Biotechnol 20*, 581-5.

364. Everse, J., and Hsia, N. (1997) The toxicities of native and modified hemoglobins, *Free Radic Biol Med 22*, 1075-99.

365. Faivre-Fiorina, B., Caron, A., Fassot, C., Fries, I., Menu, P., Labrude, P., and Vigneron, C. (1999) Presence of hemoglobin inside aortic endothelial cells after cell-free hemoglobin administration in guinea pigs, *Am J Physiol 276*, H766-70.

366. Feola, M., Simoni, J., Tran, R., and Canizaro, P. C. (1988) Mechanisms of toxicity of hemoglobin solutions, *Biomater Artif Cells Artif Organs 16*, 217-26.

367. Feola, M., Simoni, J., Dobke, M., and Canizaro, P. C. (1988) Complement activation and the toxicity of stroma-free hemoglobin solutions in primates, *Circ Shock 25*, 275-90.

368. Feola, M., Simoni, J., Fishman, D., Tran, R., and Canizaro, P. C. (1989) Biocompatibility of hemoglobin solutions. I. Reactions of vascular endothelial cells to pure and impure hemoglobins, *Artif Organs 13*, 209-15.

369. Giulivi, C., and Cadenas, E. (1998) Heme protein radicals: formation, fate, and biological consequences, *Free Radic Biol Med 24*, 269-79.

370. Goldman, D. W., Breyer, R. J., Yeh, D., Brockner-Ryan, B. A., and Alayash, A. I. (1998) Acellular hemoglobin-mediated oxidative stress toward endothelium: a role for ferryl iron, *Am J Physiol 275*, H1046-53.

371. Gulati, A., Sharma, A. C., and Burhop, K. E. (1994) Effect of stroma-free hemoglobin and diaspirin cross-linked hemoglobin on the regional circulation and systemic hemodynamics, *Life Sci 55*, 827-37.

372. Gulati, A., Singh, G., Rebello, S., and Sharma, A. C. (1995) Effect of diaspirin crosslinked and stroma-reduced hemoglobin on mean arterial pressure and endothelin-1 concentration in rats, *Life Sci 56*, 1433-42.

373. Harrington, J. P., Gonzalez, Y., and Hirsch, R. E. (2000) Redox concerns in the use of acellular hemoglobin-based therapeutic oxygen carriers: the role of plasma components, *Artif Cells Blood Substit Immobil Biotechnol 28*, 477-92.

374. Hess, J. R. (1995) Review of modified hemoglobin research at Letterman: attempts to delineate the toxicity of cell-free tetrameric hemoglobin, *Artif Cells Blood Substit Immobil Biotechnol 23*, 277-89.

375. Hess, J. R., MacDonald, V. W., and Brinkley, W. W. (1993) Systemic and pulmonary hypertension after resuscitation with cell-free hemoglobin, *J Appl Physiol 74*, 1769-78.

376. Hsia, N., and Everse, J. (1996) The cytotoxic activities of human hemoglobin and diaspirin crosslinked hemoglobin, *Artif Cells Blood Substit Immobil Biotechnol 24*, 533-51.

377. Kaca, W., Roth, R. I., and Levin, J. (1994) Hemoglobin, a newly recognized lipopolysaccharide (LPS)-binding protein that enhances LPS biological activity, *J Biol Chem 269*, 25078-84.

378. Kim, M. S., Kim, H. W., Sweeney, J. D., and Greenburg, A. G. (1997) Decreased whole blood factor IX activity following hemodilution with hemoglobin A-zero in-vitro, *Artif Cells Blood Substit Immobil Biotechnol 25*, 289-95.

379. Koch, T., Duncker, H. P., Heller, A., Schaible, R., Ackern, K. van, and Neuhof, H. (1994) Effects of stroma-free hemoglobin solutions on pulmonary vascular resistance and mediator release in the isolated perfused rabbit lung, *Shock 1*, 146-52.

380. Macdonald, R. L., and Weir, B. K. (1991) A review of hemoglobin and the pathogenesis of cerebral vasospasm, *Stroke 22*, 971-82.

381. MacDonald, V. W., and Winslow, R. M. (1992) Oxygen delivery and myocardial function in rabbit hearts perfused with cell-free hemoglobin, *J Appl Physiol 72*, 476-83.

382. Macdonald, V. W., Winslow, R. M., Marini, M. A., and Klinker, M. T. (1990) Coronary vasoconstrictor activity of purified and modified human hemoglobin, *Biomater Artif Cells Artif Organs 18*, 263-82.

383. Martin, W., Villani, G. M., Jothianandan, D., and Furchgott, R. F. (1985) Selective blockade of endothelium-dependent and glyceryl trinitrate-induced relaxation by hemoglobin and by methylene blue in the rabbit aorta, *J Pharmacol Exp Ther 232*, 708-16.

384. Matz, P. G., Fujimura, M., and Chan, P. H. (2000) Subarachnoid hemolysate produces DNA fragmentation in a pattern similar to apoptosis in mouse brain, *Brain Res 858*, 312-9.

385. McFaul, S. J., Bowman, P. D., and Villa, V. M. (2000) Hemoglobin stimulates the release of proinflammatory cytokines from leukocytes in whole blood, *J Lab Clin Med 135*, 263-9.

386. Motterlini, R., and Macdonald, V. W. (1993) Cell-free hemoglobin potentiates acetylcholine-induced coronary vasoconstriction in rabbit hearts, *J Appl Physiol 75*, 2224-33.

387. Motterlini, R., Foresti, R., Vandegriff, K., Intaglietta, M., and Winslow, R. M. (1995) Oxidative-stress response in vascular endothelial cells exposed to acellular hemoglobin solutions, *Am J Physiol 269*, H648-55.

388. Muldoon, S. M., Ledvina, M. A., Hart, J. L., and Macdonald, V. W. (1996) Hemoglobin-induced contraction of pig pulmonary veins, *J Lab Clin Med 128*, 579-84.

389. Rabiner, S. F., and Friedman, L. H. (1968) The role of intravascular haemolysis and the reticulo-endothelial system in the production of a hypercoagulable state, *Br J Haematol 14*, 105-18.

390. Regan, R. F., and Panter, S. S. (1993) Neurotoxicity of hemoglobin in cortical cell culture, *Neurosci Lett 153*, 219-22.

391. Regan, R. F., and Panter, S. S. (1996) Hemoglobin potentiates excitotoxic injury in cortical cell culture, *J Neurotrauma 13*, 223-31.

392. Rohlfs, R. J., Bruner, E., Chiu, A., Gonzales, A., Gonzales, M. L., Magde, D., Magde, M. D., Vandegriff, K. D., and Winslow, R. M. (1998) Arterial blood pressure responses to cell-free hemoglobin solutions and the reaction with nitric oxide, *J Biol Chem 273*, 12128-34.

393. Roth, R. I. (1994) Hemoglobin enhances the production of tissue factor by endothelial cells in response to bacterial endotoxin, *Blood 83*, 2860-5.

394. Sadrzadeh, S. M., Anderson, D. K., Panter, S. S., Hallaway, P. E., and Eaton, J. W. (1987) Hemoglobin potentiates central nervous system damage, *J Clin Invest 79*, 662-4.

395. Schuschereba, S. T., Friedman, H. I., DeVenuto, F., and Beatrice, E. S. (1983) Morphologic effects on the retina of massive exchange transfusion with stroma-free hemoglobin solution, *Lab Invest 48*, 339-52.

396. Simoni, J., Feola, M., Tran, R., Buckner, M., and Canizaro, P. C. (1990) Biocompatibility of hemoglobin solutions. II. The inflammatory reaction of human monocytes and mouse peritoneal macrophages, *Artif Organs 14*, 98-109.

397. Smith, D. J., and Winslow, R. M. (1992) Effects of extraerythrocytic hemoglobin and its components on mononuclear cell procoagulant activity, *J Lab Clin Med 119*, 176-82.

398. Thompson, A., McGarry, A. E., Valeri, C. R., and Lieberthal, W. (1994) Stroma-free hemoglobin increases blood pressure and GFR in the hypotensive rat: role of nitric oxide, *J Appl Physiol 77*, 2348-54.

399. Velky, T. S., Lee, E. S., Maffuid, P. W., Robinson, G. T., Yang, J. C., and Greenburg, A. G. (1987) Peritoneal accumulation of infused stroma-free hemoglobin. Potential toxicity of an oxygen-carrying substitute, *Arch Surg 122*, 355-7.

400. Vercellotti, G. M., Balla, G., Balla, J., Nath, K., Eaton, J. W., and Jacob, H. S. (1994) Heme and the vasculature: an oxidative hazard that induces antioxidant defenses in the endothelium, *Artif Cells Blood Substit Immobil Biotechnol 22*, 207-13.

401. Vogel, W. M., Dennis, R. C., Cassidy, G., Apstein, C. S., and Valeri, C. R. (1986) Coronary constrictor effect of stroma-free hemoglobin solutions, *Am J Physiol 251*, H413-20.

402. Wang, X., Mori, T., Sumii, T., and Lo, E. H. (2002) Hemoglobin-induced cytotoxicity in rat cerebral cortical neurons: caspase activation and oxidative stress, *Stroke 33*, 1882-8.

403. White, C. T., Murray, A. J., Greene, J. R., Smith, D. J., Medina, F., Makovec, G. T., Martin, E. J., and Bolin, R. B. (1986) Toxicity of human hemoglobin solution infused into rabbits, *J Lab Clin Med 108*, 121-31.

404. White, C. T., Murray, A. J., Smith, D. J., Greene, J. R., and Bolin, R. B. (1986) Synergistic toxicity of endotoxin and hemoglobin, *J Lab Clin Med 108*, 132-7.

405. Yeh, L. H., and Alayash, A. I. (2003) Redox side reactions of haemoglobin and cell signalling mechanisms, *J Intern Med 253*, 518-26.

406. Yeh, L. H., and Alayash, A. I. (2004) Effects of cell-free hemoglobin on hypoxia-inducible factor (HIF-1alpha) and heme oxygenase (HO-1) expressions in endothelial cells subjected to hypoxia, *Antioxid Redox Signal 6*, 944-53.

407. Brown, M. M., and Marshall, J. (1985) Regulation of cerebral blood flow in response to changes in blood viscosity, *Lancet 1*, 604-9.

408. Cabrales, P., Tsai, A. G., and Intaglietta, M. (2005) Alginate plasma expander maintains perfusion and plasma viscosity during extreme hemodilution, *Am J Physiol Heart Circ Physiol 288*, H1708-16.

409. Cabrales, P., Martini, J., Intaglietta, M., and Tsai, A. G. (2006) Blood viscosity maintains microvascular conditions during normovolemic anemia independent of blood oxygen-carrying capacity, *Am J Physiol Heart Circ Physiol 291*, H581-90.

410. Cameron, I. L., and Fullerton, G. D. (1990) A model to explain the osmotic pressure behavior of hemoglobin and serum albumin, *Biochem Cell Biol 68*, 894-8.

411. Cameron, I. L., Ord, V. A., and Fullerton, G. D. (1988) Water of hydration in the intra- and extra-cellular environment of human erythrocytes, *Biochem Cell Biol 66*, 1186-99.

412. Chen, R. Y., Carlin, R. D., Simchon, S., Jan, K. M., and Chien, S. (1989) Effects of dextran-induced hyperviscosity on regional blood flow and hemodynamics in dogs, *Am J Physiol 256*, H898-905.

413. Cole, D. J., Drummond, J. C., Patel, P. M., and Marcantonio, S. (1994) Effects of viscosity and oxygen content on cerebral blood flow in ischemic and normal rat brain, *J Neurol Sci 124*, 15-20.

414. Wit, C. de, Schafer, C., Bismarck, P. von, Bolz, S. S., and Pohl, U. (1997) Elevation of plasma viscosity induces sustained NO-mediated dilation in the hamster cremaster microcirculation in vivo, *Pflugers Arch 434*, 354-61.

415. Devereux, R. B., Drayer, J. I., Chien, S., Pickering, T. G., Letcher, R. L., DeYoung, J. L., Sealey, J. E., and Laragh, J. H. (1984) Whole blood viscosity as a determinant of cardiac hypertrophy in systemic hypertension, *Am J Cardiol 54*, 592-5.

416. Devereux, R. B., Case, D. B., Alderman, M. H., Pickering, T. G., Chien, S., and Laragh, J. H. (2000) Possible role of increased blood viscosity in the hemodynamics of systemic hypertension, *Am J Cardiol 85*, 1265-8.

417. Koller, A., Sun, D., and Kaley, G. (1993) Role of shear stress and endothelial prostaglandins in flow- and viscosity-induced dilation of arterioles in vitro, *Circ Res 72*, 1276-84.

418. Kuchan, M. J., and Frangos, J. A. (1993) Shear stress regulates endothelin-1 release via protein kinase C and cGMP in cultured endothelial cells, *Am J Physiol 264*, H150-6.

419. Martini, J., Carpentier, B., Negrete, A. C., Frangos, J. A., and Intaglietta, M. (2005) Paradoxical hypotension following increased hematocrit and blood viscosity, *Am J Physiol Heart Circ Physiol 289*, H2136-43.

420. Massik, J., Tang, Y. L., Hudak, M. L., Koehler, R. C., Traystman, R. J., and Jones, M. D. (1987) Effect of hematocrit on cerebral blood flow with induced polycythemia, *J Appl Physiol 62*, 1090-6.

421. Melkumyants, A. M., Balashov, S. A., and Khayutin, V. M. (1989) Endothelium dependent control of arterial diameter by blood viscosity, *Cardiovasc Res 23*, 741-7.

422. Muizelaar, J. P., Wei, E. P., Kontos, H. A., and Becker, D. P. (1986) Cerebral blood flow is regulated by changes in blood pressure and in blood viscosity alike, *Stroke 17*, 44-8.

423. Rebel, A., Lenz, C., Krieter, H., Waschke, K. F., Van Ackern, K., and Kuschinsky, W. (2001) Oxygen delivery at high blood viscosity and decreased arterial oxygen content to brains of conscious rats, *Am J Physiol Heart Circ Physiol 280*, H2591-7.

424. Rochon, G., Caron, A., Toussaint-Hacquard, M., Alayash, A. I., Gentils, M., Labrude, P., Stoltz, J. F., and Menu, P. (2004) Hemodilution with stroma-free [correction of stoma-free] hemoglobin at physiologically maintained viscosity delays the onset of vasoconstriction, *Hypertension 43*, 1110-5.

425. Rosenkrantz, T. S., Stonestreet, B. S., Hansen, N. B., Nowicki, P., and Oh, W. (1984) Cerebral blood flow in the newborn lamb with polycythemia and hyperviscosity, *J Pediatr 104*, 276-80.

426. Ross, P. D., and Minton, A. P. (1977) Analysis of non-ideal behavior in concentrated hemoglobin solutions, *J Mol Biol 112*, 437-52.

427. Starling, E. H. (1896) On the Absorption of Fluids from the Connective Tissue Spaces, *J Physiol 19*, 312-26.

428. Tomiyama, Y., Brian, J. E., and Todd, M. M. (2000) Plasma viscosity and cerebral blood flow, *Am J Physiol Heart Circ Physiol 279*, H1949-54.

429. Tsai, A. G., Friesenecker, B., McCarthy, M., Sakai, H., and Intaglietta, M. (1998) Plasma viscosity regulates capillary perfusion during extreme hemodilution in hamster skinfold model, *Am J Physiol 275*, H2170-80.

430. Tsai, A. G., Acero, C., Nance, P. R., Cabrales, P., Frangos, J. A., Buerk, D. G., and Intaglietta, M. (2005) Elevated plasma viscosity in extreme hemodilution increases perivascular nitric oxide concentration and microvascular perfusion, *Am J Physiol Heart Circ Physiol 288*, H1730-9.

431. Vandegriff, K. D., McCarthy, M., Rohlfs, R. J., and Winslow, R. M. (1997) Colloid osmotic properties of modified hemoglobins: chemically cross-

linked versus polyethylene glycol surface-conjugated, *Biophys Chem 69*, 23-30.

432. Waschke, K. F., Krieter, H., Hagen, G., Albrecht, D. M., Van Ackern, K., and Kuschinsky, W. (1994) Lack of dependence of cerebral blood flow on blood viscosity after blood exchange with a Newtonian O2 carrier, *J Cereb Blood Flow Metab 14*, 871-6.
433. Webb, A. R., Barclay, S. A., and Bennett, E. D. (1989) In vitro colloid osmotic pressure of commonly used plasma expanders and substitutes: a study of the diffusibility of colloid molecules, *Intensive Care Med 15*, 116-20.
434. Como, J. J., Dutton, R. P., Scalea, T. M., Edelman, B. B., and Hess, J. R. (2004) Blood transfusion rates in the care of acute trauma, *Transfusion 44*, 809-13.
435. Wudel, J. H., Morris, J. A., Yates, K., Wilson, A., and Bass, S. M. (1991) Massive transfusion: outcome in blunt trauma patients, *J Trauma 31*, 1-7.
436. Henderson, D. P., and Payne, S. M. (1993) Cloning and characterization of the Vibrio cholerae genes encoding the utilization of iron from haemin and haemoglobin, *Mol Microbiol 7*, 461-9.
437. Henderson, D. P., and Payne, S. M. (1994) Characterization of the Vibrio cholerae outer membrane heme transport protein HutA: sequence of the gene, regulation of expression, and homology to the family of TonB-dependent proteins, *J Bacteriol 176*, 3269-77.
438. Henderson, D. P., Wyckoff, E. E., Rashidi, C. E., Verlei, H., and Oldham, A. L. (2001) Characterization of the Plesiomonas shigelloides genes encoding the heme iron utilization system, *J Bacteriol 183*, 2715-23.
439. Panetta, G., Arcovito, A., Morea, V., Bellelli, A., and Miele, A. E. (2008) Hb(alphaalpha,betabeta): a novel fusion construct for a dimeric, four-domain hemoglobin, *Biochim Biophys Acta 1784*, 1462-70.
440. Vasseur, C., Domingues-Hamdi, E., Brillet, T., Marden, M. C., and Baudin-Creuza, V. (2009) The alpha-hemoglobin stabilizing protein and expression of unstable alpha-Hb variants, *Clin Biochem*.

441. Vasseur-Godbillon, C., Hamdane, D., Marden, M. C., and Baudin-Creuza, V. (2006) High-yield expression in Escherichia coli of soluble human alpha-hemoglobin complexed with its molecular chaperone, *Protein Eng Des Sel 19*, 91-7.

442. Yu, X., Kong, Y., Dore, L. C., Abdulmalik, O., Katein, A. M., Zhou, S., Choi, J. K., Gell, D., Mackay, J. P., Gow, A. J., and Weiss, M. J. (2007) An erythroid chaperone that facilitates folding of alpha-globin subunits for hemoglobin synthesis, *J Clin Invest 117*, 1856-65.

443. Kihm, A. J., Kong, Y., Hong, W., Russell, J. E., Rouda, S., Adachi, K., Simon, M. C., Blobel, G. A., and Weiss, M. J. (2002) An abundant erythroid protein that stabilizes free alpha-haemoglobin, *Nature 417*, 758-63.

444. Gell, D., Kong, Y., Eaton, S. A., Weiss, M. J., and Mackay, J. P. (2002) Biophysical characterization of the alpha-globin binding protein alpha-hemoglobin stabilizing protein, *J Biol Chem 277*, 40602-9.

445. Feng, L., Gell, D. A., Zhou, S., Gu, L., Kong, Y., Li, J., Hu, M., Yan, N., Lee, C., Rich, A. M., Armstrong, R. S., Lay, P. A., Gow, A. J., Weiss, M. J., Mackay, J. P., and Shi, Y. (2004) Molecular mechanism of AHSP-mediated stabilization of alpha-hemoglobin, *Cell 119*, 629-40.

446. Hendrick, J. P., and Hartl, F. U. (1993) Molecular chaperone functions of heat-shock proteins, *Annu Rev Biochem 62*, 349-84.

447. Ellis, J. (1987) Proteins as molecular chaperones, *Nature 328*, 378-9.

448. Ellis, R. J. (1990) The molecular chaperone concept, *Semin Cell Biol 1*, 1-9.

449. Ellis, R. J. (1993) The general concept of molecular chaperones, *Philos Trans R Soc Lond B Biol Sci 339*, 257-61.

450. Ellis, R. J., and Hemmingsen, S. M. (1989) Molecular chaperones: proteins essential for the biogenesis of some macromolecular structures, *Trends Biochem Sci 14*, 339-42.

451. Hartl, F. U., and Martin, J. (1995) Molecular chaperones in cellular protein folding, *Curr Opin Struct Biol 5*, 92-102.

452. Hartl, F. U. (1996) Molecular chaperones in cellular protein folding, *Nature 381*, 571-9.

453. Chang, H. C., Tang, Y. C., Hayer-Hartl, M., and Hartl, F. U. (2007) SnapShot: molecular chaperones, Part I, *Cell 128*, 212e1.

454. Tang, Y. C., Chang, H. C., Hayer-Hartl, M., and Hartl, F. U. (2007) SnapShot: molecular chaperones, Part II, *Cell 128*, 412.

455. Aguzzi, A., Heikenwalder, M., and Miele, G. (2004) Progress and problems in the biology, diagnostics, and therapeutics of prion diseases, *J Clin Invest 114*, 153-60.

456. Miele, G., Manson, J., and Clinton, M. (2001) A novel erythroid-specific marker of transmissible spongiform encephalopathies, *Nat Med 7*, 361-4.

457. Watts, J. C., Balachandran, A., and Westaway, D. (2006) The expanding universe of prion diseases, *PLoS Pathog 2*, e26.

458. Harris, D. A. (1999) Cellular biology of prion diseases, *Clin Microbiol Rev 12*, 429-44.

459. Ferreira, R., Ohneda, K., Yamamoto, M., and Philipsen, S. (2005) GATA1 function, a paradigm for transcription factors in hematopoiesis, *Mol Cell Biol 25*, 1215-27.

460. Orkin, S. H. (1992) GATA-binding transcription factors in hematopoietic cells, *Blood 80*, 575-81.

461. Patient, R. K., and McGhee, J. D. (2002) The GATA family (vertebrates and invertebrates), *Curr Opin Genet Dev 12*, 416-22.

462. Chiba, T., Nagata, Y., Kishi, A., Sakamaki, K., Miyajima, A., Yamamoto, M., Engel, J. D., and Todokoro, K. (1993) Induction of erythroid-specific gene expression in lymphoid cells, *Proc Natl Acad Sci U S A 90*, 11593-7.

463. Fujiwara, Y., Browne, C. P., Cunniff, K., Goff, S. C., and Orkin, S. H. (1996) Arrested development of embryonic red cell precursors in mouse embryos lacking transcription factor GATA-1, *Proc Natl Acad Sci U S A 93*, 12355-8.

464. Pevny, L., Simon, M. C., Robertson, E., Klein, W. H., Tsai, S. F., D'Agati, V., Orkin, S. H., and Costantini, F. (1991) Erythroid differentiation in chimaeric mice blocked by a targeted mutation in the gene for transcription factor GATA-1, *Nature 349*, 257-60.

465. Gregory, T., Yu, C., Ma, A., Orkin, S. H., Blobel, G. A., and Weiss, M. J. (1999) GATA-1 and erythropoietin cooperate to promote erythroid cell survival by regulating bcl-xL expression, *Blood 94*, 87-96.

466. Shirihai, O. S., Gregory, T., Yu, C., Orkin, S. H., and Weiss, M. J. (2000) ABC-me: a novel mitochondrial transporter induced by GATA-1 during erythroid differentiation, *Eur Mol Biol Org J 19*, 2492-502.

467. Weiss, M. J., Yu, C., and Orkin, S. H. (1997) Erythroid-cell-specific properties of transcription factor GATA-1 revealed by phenotypic rescue of a gene-targeted cell line, *Mol Cell Biol 17*, 1642-51.

468. Santos, C. O. dos, Duarte, A. S., Saad, S. T., and Costa, F. F. (2004) Expression of alpha-hemoglobin stabilizing protein gene during human erythropoiesis, *Exp Hematol 32*, 157-62.

469. Kong, Y., Zhou, S., Kihm, A. J., Katein, A. M., Yu, X., Gell, D. A., Mackay, J. P., Adachi, K., Foster-Brown, L., Louden, C. S., Gow, A. J., and Weiss, M. J. (2004) Loss of alpha-hemoglobin-stabilizing protein impairs erythropoiesis and exacerbates beta-thalassemia, *J Clin Invest 114*, 1457-66.

470. Santiveri, C. M., Perez-Canadillas, J. M., Vadivelu, M. K., Allen, M. D., Rutherford, T. J., Watkins, N. A., and Bycroft, M. (2004) NMR structure of the alpha-hemoglobin stabilizing protein: insights into conformational heterogeneity and binding, *J Biol Chem 279*, 34963-70.

471. Feng, L., Zhou, S., Gu, L., Gell, D. A., Mackay, J. P., Weiss, M. J., Gow, A. J., and Shi, Y. (2005) Structure of oxidized alpha-haemoglobin bound to AHSP reveals a protective mechanism for haem, *Nature 435*, 697-701.

472. Paoli, M., Liddington, R., Tame, J., Wilkinson, A., and Dodson, G. (1996) Crystal structure of T state haemoglobin with oxygen bound at all four haems, *J Mol Biol 256*, 775-92.

473. Zhou, S., Olson, J. S., Fabian, M., Weiss, M. J., and Gow, A. J. (2006) Biochemical fates of alpha hemoglobin bound to alpha hemoglobin-stabilizing protein AHSP, *J Biol Chem 281*, 32611-8.

474. Chernoff, A. (1964) Hgb A4. A normal component of human hemoglobin composed only of alpha chains., *J Clin Invest 43*, 1266.

475. Gill, F. M., and Schwartz, E. (1973) Free alpha-globin pool in human bone marrow, *J Clin Invest 52*, 3057-63.

476. Kohne, E., and Kleihauer, E. (1973) Free alpha chains in adult and cord blood haemolysates. I. Quantitative data and identification, *Res Exp Med (Berl) 161*, 243-50.

477. Modell, C. B., Latter, A., Steadman, J. H., and Huehns, E. R. (1969) Haemoglobin synthesis in beta-thalassaemia, *Br J Haematol 17*, 485-501.

478. Tavill, A. S., Grayzel, A. I., London, I. M., Williams, M. K., and Vanderhoff, G. A. (1968) The role of heme in the synthesis and assembly of hemoglobin, *J Biol Chem 243*, 4987-99.

479. Shaeffer, J. R. (1967) Evidence for soluble alpha-chains as intermediates in hemoglobin synthesis in the rabbit reticulocyte, *Biochem Biophys Res Commun 28*, 647-52.

480. Santos, C. O. dos, Dore, L. C., Valentine, E., Shelat, S. G., Hardison, R. C., Ghosh, M., Wang, W., Eisenstein, R. S., Costa, F. F., and Weiss, M. J. (2008) An iron responsive element-like stem-loop regulates alpha-hemoglobin-stabilizing protein mRNA, *J Biol Chem 283*, 26956-64.

481. Viprakasit, V., Tanphaichitr, V. S., Chinchang, W., Sangkla, P., Weiss, M. J., and Higgs, D. R. (2004) Evaluation of alpha hemoglobin stabilizing protein (AHSP) as a genetic modifier in patients with beta thalassemia, *Blood 103*, 3296-9.

482. Santos, C. O. dos, Zhou, S., Albuquerque, D., Saad, S., Weiss, M. J., and Costa, F. F. (2009) A Natural Variant Sequence in the AHSP Gene May Impact Severity of Beta-Thalassemia. *106*.

483. Santos, C. O. dos, Zhou, S., Secolin, R., Wang, X., Cunha, A. F., Higgs, D. R., Kwiatkowski, J. L., Thein, S. L., Gallagher, P. G., Costa, F. F., and Weiss, M. J. (2008) Population analysis of the alpha hemoglobin stabilizing protein (AHSP) gene identifies sequence variants that alter expression and function, *Am J Hematol 83*, 103-8.

484. Lai, M. I., Jiang, J., Silver, N., Best, S., Menzel, S., Mijovic, A., Colella, S., Ragoussis, J., Garner, C., Weiss, M. J., and Thein, S. L. (2006) Alpha-

haemoglobin stabilising protein is a quantitative trait gene that modifies the phenotype of beta-thalassaemia, *Br J Haematol 133*, 675-82.

485. Kanno, H., Kamatani, N., Hamada, T., Furihata, K., Hattori, Y., Miwa, S., and Fujii, H. (2005) Alpha Hemoglobin Stabilizing Protein (AHSP) Is a Susceptibility Gene to Drug/Infection-Induced Hemolytic Anemia, *American Society of Hematology 106*.
486. Vasseur-Godbillon, C., Marden, M. C., Giordano, P., Wajcman, H., and Baudin-Creuza, V. (2006) Impaired binding of AHSP to alpha chain variants: Hb Groene Hart illustrates a mechanism leading to unstable hemoglobins with alpha thalassemic like syndrome, *Blood Cells Mol Dis 37*, 173-9.
487. Lacerra, G., Scarano, C., Musollino, G., Flagiello, A., Pucci, P., and Carestia, C. (2008) Hb Foggia or alpha 117(GH5)Phe -> Ser: a new alpha 2 globin allele affecting the alpha Hb-AHSP interaction, *Haematologica 93*, 141-2.
488. Brillet, T., Baudin-Creuza, V., Vasseur, C., Domingues-Hamdi, E., Kiger, L., Wajcman, H., Pissard, S., and Marden, M. C. (2010) Alpha hemoglobin stabilizing protein (AHSP): A kinetic scheme of the action of a human mutant, AHSP V56G, *J Biol Chem* 285, 17986-17992.
489. Sambrook, J., and Russell, D. W. (2001) Molecular cloning: A laboratory manual. Cold Spring Harbor Laboratory Press, Cold Spring Harbor, N.Y.
490. Agilent. (2010, December 14) QuikChange II Site-Directed Mutagenesis Kit Instruction Manual (Catalog #200523; Revision C).
491. Agilent. (2010, December 14) BL21(DE3) Competent Cells, BL21(DE3)pLysS Competent Cells, and BL21 Competent Cells Manual (200133-12).
492. GE. (2010, December 13) GST Gene Fusion System Handbook (18-1157-58). GE Healthcare Bio-Sciences Corp.
493. Wiedermann, B. L., and Olson, J. S. (1975) Acceleration of tetramer formation by the binding of inositol hexaphosphate to hemoglobin dimers, *J Biol Chem 250*, 5273-5.

494. Banerjee, R., Alpert, Y., Leterrier, F., and Williams, R. J. (1969) Visible absorption and electron spin resonance spectra of the isolated chains of human hemoglobin. Discussion of chain-mediated heme-heme interaction, *Biochemistry 8*, 2862-7.

495. Antonini, E., and Brunori, M. (1970) Hemoglobin, *Annu Rev Biochem 39*, 977-1042.

496. Antonini, E., and Brunori, M. (1971) Hemoglobin and myoglobin in their reactions with ligands. Elsevier, North-Holland, Amsterdam.

497. Bucci, E., and Fronticelli, C. (1965) A New Method for the Preparation of Alpha and Beta Subunits of Human Hemoglobin, *J Biol Chem 240*, PC551-2.

498. Boyer, P. D. (1954) Spectrophotometric Study of the Reaction of Protein Sulfhydryl Groups with Organic Mercurials, *J Am Chem Soc 76*, 4331-4337.

499. Rossi-Fanelli, A., Antonini, E., and Caputo, A. (1958) Studies on the Structure of Hemoglobin. I. Physiochemical Properties of Human Globin, *Biochim. Biophys. Acta 30*, 608-615.

500. Birukou, I., Schweers, R. L., and Olson, J. S. (2010) Distal histidine stabilizes bound O2 and acts as a gate for ligand entry in both subunits of adult human hemoglobin, *J Biol Chem 285*, 8840-54.

501. Plomer, J. J., Ryland, J. R., Matthews, M.-A. H., Traylor, D. W., Milne, E. E., Durfee, S. L., and Mathews, A. J. N. (1998) Purification of hemoglobin. USA.

502. Baudin-Creuza, V., Vasseur-Godbillon, C., Pato, C., Prâehu, C., Wajcman, H., and Marden, M. C. (2004) Transfer of human alpha- to beta-hemoglobin via its chaperone protein: evidence for a new state, *J Biol Chem 279*, 36530-3.

503. Alpert, B., Jameson, D. M., and Weber, G. (1980) Tryptophan emission from human hemoglobin and its isolated subunits, *Photochem Photobiol 31*, 1-4.

504. Leutzinger, Y., and Beychok, S. (1981) Kinetics and mechanism of heme-induced refolding of human alpha-globin, *Proc Natl Acad Sci U S A 78*, 780-4.

505. Brown, M. P., and Royer, C. (1997) Fluorescence spectroscopy as a tool to investigate protein interactions, *Current Opinion in Biotechnology 8*, 45-49.

506. Beechem, J. M., and Brand, L. (1985) Time-resolved fluorescence of proteins, *Annu Rev Biochem 54*, 43-71.

507. Lakowicz, J. R., and Hirsch, R. E. (2000) Topics in Fluorescence Spectroscopy: Protein Fluorescence; Chapter 10: Heme-Protein Fluorescence. KIuwer Academic Publishers, New York.

508. Gell, D. A., Feng, L., Zhou, S., Jeffrey, P. D., Bendak, K., Gow, A., Weiss, M. J., Shi, Y., and Mackay, J. P. (2009) A cis-proline in alpha-hemoglobin stabilizing protein directs the structural reorganization of alpha-hemoglobin, *J Biol Chem 284*, 29462-9.

509. Schmid, F. X. (1993) Prolyl isomerase: enzymatic catalysis of slow protein-folding reactions, *Annu Rev Biophys Biomol Struct 22*, 123-142.

510. Gryczynski, Z., and Bucci, E. (1993) A new front-face optical cell for measuring weak fluorescent emissions with time resolution in the picosecond time scale, *Biophys Chem 48*, 31-38.

511. Gryczynski, Z., Lubkowski, J., and Bucci, E. (1997) Intrinsic fluorescence of hemoglobins and myoglobins, *Meth Enzymol 278*, 538-569.

512. Rohlfs, R. J., Mathews, A. J., Carver, T. E., Olson, J. S., Springer, B. A., Egeberg, K. D., and Sligar, S. G. (1990) The effects of amino acid substitution at position E7 (residue 64) on the kinetics of ligand binding to sperm whale myoglobin, *J Biol Chem 265*, 3168-76.

513. Olson, J. S. (1981) [38] Stopped-flow, rapid mixing measurements of ligand binding to hemoglobin and red cells, in *Hemoglobins*, pp 631-651. Academic Press.

514. Hargrove, M. S., and Olson, J. S. (1996) The stability of holomyoglobin is determined by heme affinity, *Biochemistry 35*, 11310-8.

515. Smith, M. L., Hjortsberg, K., Romeo, P.-H., Rosa, J., and Paul, K.-G. (1984) Mutant hemoglobin stability depends upon location and nature of single point mutation, *FEBS Letters 169*, 147-150.

516. Alayash, A. I., Patel, R. P., and Cashon, R. E. (2001) Redox reactions of hemoglobin and myoglobin: biological and toxicological implications, *Antioxid. Redox Signal 3*, 313-327.

517. Reeder, B. J. (2010) The redox activity of hemoglobins: from physiologic functions to pathologic mechanisms, *Antioxid. Redox Signal 13*, 1087-1123.

518. Winterbourn, C. C. (1990) Oxidative reactions of hemoglobin, *Meth Enzymol 186*, 265-72.

519. Winterbourn, C. C., and Carrell, R. W. (1974) Studies of hemoglobin denaturation and Heinz body formation in the unstable hemoglobins, *J Clin Invest 54*, 678-89.

520. Faivre, B., Menu, P., Labrude, P., and Vigneron, C. (1998) Hemoglobin autooxidation/oxidation mechanisms and methemoglobin prevention or reduction processes in the bloodstream. Literature review and outline of autooxidation reaction, *Artif Cells Blood Substit Immobil Biotechnol 26*, 17-26.

521. Brantley, R. E., Smerdon, S. J., Wilkinson, A. J., Singleton, E. W., and Olson, J. S. (1993) The mechanism of autooxidation of myoglobin, *J Biol Chem 268*, 6995-7010.

522. Shikama, K. (1998) The Molecular Mechanism of Autoxidation for Myoglobin and Hemoglobin: A Venerable Puzzle, *Chem. Rev 98*, 1357-1374.

523. George, P., and Stratmann, C. J. (1952) The oxidation of myoglobin to metmyoglobin by oxygen. 1, *Biochem J 51*, 103-108.

524. Umbreit, J. (2007) Methemoglobin--it's not just blue: a concise review, *Am. J. Hematol 82*, 134-144.

525. Buehler, P. W., and Alayash, A. I. (2005) Redox biology of blood revisited: the role of red blood cells in maintaining circulatory reductive capacity, *Antioxid. Redox Signal 7*, 1755-1760.

526. Weiss, M. J., and Santos, C. O. dos. (2009) Chaperoning erythropoiesis, *Blood 113*, 2136-44.

527. Kumar, K., Dickson, C. F., Weiss, M. J., Mackay, J. P., and Gell, D. A. (2010) AHSP (α-haemoglobin-stabilizing protein) stabilizes apo-α-haemoglobin in a partially folded state, *Biochem J 432*, 275-282.

528. Vergara, A., Vitagliano, L., Verde, C., Prisco, G. di, and Mazzarella, L. (2008) Spectroscopic and crystallographic characterization of bis-histidyl adducts in tetrameric hemoglobins, *Meth Enzymol 436*, 425-44.

529. Rifkind, J. M., Abugo, O., Levy, A., and Heim, J. (1994) Detection, formation, and relevance of hemichromes and hemochromes, *Meth Enzymol 231*, 449-80.

530. Culbertson, D. S., and Olson, J. S. (2010) Role of Heme in the Unfolding and Assembly of Myoglobin, *Biochemistry 49*, 6052-6063.

531. Brunori, M., Falcioni, G., Fioretti, E., Giardina, B., and Rotilio, G. (1975) Formation of Superoxide in the Autoxidation of the Isolated Alpha and Beta Chains of Human Hemoglobin and Its Involvement in Hemichrome Precipitation, *Eur J Biochem 53*, 99-104.

532. Brunori, M., Fioretti, E., and Rotilio, G. (1978) Effect of drugs on oxidation and precipitation of the isolated chains of human hemoglobin, *Mol Cell Biochem 19*, 43-7.

533. Rachmilewitz, E. A., Peisach, J., Bradley, T. B., and Blumberg, W. E. (1969) Role of haemichromes in the formation of inclusion bodies in haemoglobin H disease, *Nature 222*, 248-50.

534. Tsuruga, M., Matsuoka, A., Hachimori, A., Sugawara, Y., and Shikama, K. (1998) The Molecular Mechanism of Autoxidation for Human Oxyhemoglobin, *Journal of Biological Chemistry 273*, 8607 -8615.

535. Savitzky, A., and Golay, M. J. E. (1964) Smoothing and Differentiation of Data by Simplified Least Squares Procedures, *Analyt Chem 36*, 1627-1639.

536. Mathews, A. J., and Olson, J. S. (1994) Assignment of rate constants for O2 and CO binding to alpha and beta subunits within R- and T-state human hemoglobin, *Meth Enzymol 232*, 363-86.

537. Mathews, A. J., Olson, J. S., Renaud, J. P., Tame, J., and Nagai, K. (1991) The assignment of carbon monoxide association rate constants to the alpha and beta subunits in native and mutant human deoxyhemoglobin tetramers, *J Biol Chem 266*, 21631-9.

538. Olson, J. S., Foley, E. W., Maillett, D. H., and Paster, E. V. (2003) Measurement of rate constants for reactions of O2, CO, and NO with hemoglobin, *Meth Mol Med 82*, 65-91.

539. Kelly, S. M., Jess, T. J., and Price, N. C. (2005) How to study proteins by circular dichroism, *Biochimica et Biophysica Acta (BBA) - Proteins & Proteomics 1751*, 119-139.

540. Yu, X., Mollan, T. L., Butler, A., Gow, A. J., Olson, J. S., and Weiss, M. J. (2009) Analysis of human alpha globin gene mutations that impair binding to the alpha hemoglobin stabilizing protein (AHSP), *Blood* 113(23):5961-5969.

541. Langdown, J. V., Davidson, R. J., and Williamson, D. (1992) A new alpha chain variant, Hb Turriff [alpha 99(G6)Lys----Glu]: the interference of abnormal hemoglobins in Hb A1c determination, *Hemoglobin 16*, 11-17.

542. Marinucci, M., Mavilio, F., Massa, A., Gabbianelli, M., Fontanarosa, P. P., Camagna, A., Ignesti, C., and Tentori, L. (1979) A new abnormal human hemoglobin: Hb prato ([alpha]231 (B12) Arg-->Ser [beta]2), *Biochim Biophys Acta (BBA) - Protein Structure 578*, 534-540.

543. De Marco, E. V., Crescibene, L., Pasqua, A., Brancati, C., Bria, M., and Qualtieri, A. (1992) HB Prato [alpha 31(B12)Arg----Ser] in a Calabrian family, *Hemoglobin 16*, 275-279.

544. Shih, M.-C., Peng, C.-T., Chang, J.-Y., Liu, S.-C., Kuo, P.-L., and Chang, J.-G. (2003) Hb Prato [alpha31(B12)Arg --> Ser (A2)] and alpha-thalassemia in a Taiwanese, *Hemoglobin 27*, 45-47.

545. Lacan, P., Aubry, M., Couprie, N., and Francina, A. (2004) Two new alpha chain variants: Hb Die [alpha93(FG5)Val --> Ala (alpha1)] and Hb Beziers [alpha99(G6)Lys --> Asn (alpha1)], *Hemoglobin 28*, 59-63.

546. Hoyer, J. D., McCormick, D. J., Snow, K., Kwon, J. H., Booth, D., Duarte, M., Grayson, G., Kubik, K. S., Holmes, M. W., and Fairbanks, V. F. (2002) Four new variants of the alpha2-globin gene without clinical or hematologic effects: Hb Park Ridge [alpha9(alpha7)Asn-->Lys (alpha2)], Hb Norton [alpha72(EF1)His-->Asp (alpha2)], Hb Lombard [alpha103(G10)His-->Tyr

(alpha2)], and Hb San Antonio [A113(GH2)Leu-->Arg (A2)], *Hemoglobin 26*, 175-179.

547. Sciarratta, G. V., Ivaldi, G., Molaro, G. L., Sansone, G., Salkie, M. L., Wilson, J. B., Reese, A. L., and Huisman, T. H. (1984) The characterization of hemoglobin Manitoba or alpha (2)102(G9)Ser----Arg beta 2 and hemoglobin Contaldo or alpha (2)103(G10)His----Arg beta 2 by high performance liquid chromatography, *Hemoglobin 8*, 169-181.

548. Giordano, P. C., Zweegman, S., Akkermans, N., Arkesteijn, S. G., Delft, P. van, Versteegh, F. G., Wajcman, H., and Harteveld, C. L. (2007) The First Case of Hb Groene Hart [alpha119(H2)ProSer, CCTTCT (alpha1)] Homozygosity Confirms That a Thalassemia Phenotype Is Associated with this Abnormal Hemoglobin Variant, *Hemoglobin 31*, 179-82.

549. Harteveld, C. L., Delft, P. van, Plug, R., Versteegh, F. G. A., Hagen, B., Rooijen, I. van, Kok, P. J. M. J., Wajcman, H., Kister, J., and Giordano, P. C. (2002) Hb Groene Hart: a new Pro-->Ser amino acid substitution at position 119 of the alpha1-globin chain is associated with a mild alpha-thalassemia phenotype, *Hemoglobin 26*, 255-260.

550. Siala, H., Ouali, F., Messaoud, T., Sfar, R., and Fattoum, S. (2005) First description in Tunisia of a point mutation at codon 119 (CCT-->TCT) in the alpha1-globin gene: Hb Groene Hart in association with the -alpha3.7 deletion, *Hemoglobin 29*, 263-268.

551. Fujisawa, K., Hattori, Y., Ohba, Y., and Ando, S. (1992) Hb Yuda or alpha 130(H13)Ala----Asp; a new alpha chain variant with low oxygen affinity, *Hemoglobin 16*, 435-439.

552. Harano, T., Harano, K., Hong, Y.-F., Than, A. M., Suetsugu, Y., and Ohba, K. (2003) The mutation of Hb Turriff [alpha99(G6)Lys --> Glu (AAG --> GAG)] is carried by the alpha1-globin gene in a Japanese (Hb Turriff-I), *Hemoglobin 27*, 123-127.

553. Mills, M., and Payne, S. M. (1997) Identification of shuA, the gene encoding the heme receptor of Shigella dysenteriae, and analysis of invasion and intracellular multiplication of a shuA mutant, *Infect Immun 65*, 5358-63.

554. Mills, M., and Payne, S. M. (1995) Genetics and regulation of heme iron transport in Shigella dysenteriae and detection of an analogous system in Escherichia coli O157:H7, *J Bacteriol 177*, 3004-9.

555. Varnado, C. L., and Goodwin, D. C. (2004) System for the expression of recombinant hemoproteins in Escherichia coli, *Prot Expr Purif 35*, 76-83.

556. Faggiano, S., Ronda, L., Bruno, S., Jankevics, H., and Mozzarelli, A. Polymerized and polyethylene glycol-conjugated hemoglobins: a globin-based calibration curve for dynamic light scattering analysis, *Anal Biochem 401*, 266-70.

557. Guzman, L. M., Belin, D., Carson, M. J., and Beckwith, J. (1995) Tight regulation, modulation, and high-level expression by vectors containing the arabinose PBAD promoter, *J Bacteriol 177*, 4121-30.

558. (2007, August 23) One Shot Top10 Chemically Competent E. Coli Product Manual. Invitrogen Corporation (Carlsbad, CA, USA).

559. Crowley, M. A., Mollam, T. L., Abdulmalik, O. Y., Butler, A., Goodwin, E. F., Sarkar, A., Stolle, C. A., Gow, A. J., Olson, J. S., and Weiss, M. J. (2011) Hemoglobin Tom's River: A Hemoglobin Variant Causing Neonatal Cyanosis and Anemia, *New England Journal of Medicine, in review.*

560. Medical Dictionary: MedlinePlus, *Merriam-Webster Medical Dictionary [Internet]: Merriam-Webster, Incorporated; Copyright 2011. Cyanosis. Available from http://www.nlm.nih.gov/medlineplus/mplusdictionary.html; accessed January 21, 2011*.

561. Zorc, J. J., and Kanic, Z. (2001) A cyanotic infant: true blue or otherwise?, *Pediatr Ann 30*, 597-601.

562. Avery, A. A. (1999) Infantile methemoglobinemia: reexamining the role of drinking water nitrates., *Environ Health Perspect 107*, 583-586.

563. Reid, T. J. (1982) Newborn Cyanosis, *The American Journal of Nursing 82*, 1230-1234.

564. Nienhuis, A. W., and Stamatoyannopoulos, G. (1981) Organization and expression of globin genes : proceedings of the Second Conference on

Hemoglobin Switching, held at Airlie House, Virginia, June 22-26, 1980. A.R. Liss, New York.

565. Stadtman, E. R., and Levine, R. L. (2003) Free radical-mediated oxidation of free amino acids and amino acid residues in proteins, *Amino Acids 25*, 207-218.

566. Schöneich, C. (2005) Methionine oxidation by reactive oxygen species: reaction mechanisms and relevance to Alzheimer's disease, *Biochimica et Biophysica Acta (BBA) - Proteins & Proteomics 1703*, 111-119.

567. Dean, R. T., Fu, S., Stocker, R., and Davies, M. J. (1997) Biochemistry and pathology of radical-mediated protein oxidation., *Biochem J 324*, 1-18.

568. Kano, G., Morimoto, A., Hibi, S., Tokuda, C., Todo, S., Sugimoto, T., Harano, T., Miyazaki, A., Shimizu, A., and Imashuku, S. (2004) Hb Bristol-Alesha presenting thalassemia-type hyperunstable hemoglobinopathy, *Int. J. Hematol 80*, 410-415.

569. Eberle, S. E., Noguera, N. I., Sciuccati, G., Bonduel, M., Díaz, L., Staciuk, R., Targovnik, H. M., and Feliu-Torres, A. (2007) Hb Alesha [beta67(E11)Val-->Met, GTG-->ATG] in an Argentinean girl, *Hemoglobin 31*, 379-382.

570. Ohba, Y., Matsuoka, M., Miyaji, T., Shibuya, T., and Sakuragawa, M. (1985) Hemoglobin Bristol or beta 67(E11) Val----Asp in Japan, *Hemoglobin 9*, 79-85.

571. Huisman, T. H., with Molchanova, T. P., Postnikov YuV and Pobedimskaya, D. D., Smetanina, N. S., Moschan, A. A., and Kazanetz, E. G., Tokarev YuN. (1993) Hb Alesha or alpha 2 beta (2)67(E11)Val-->Met: a new unstable hemoglobin variant identified through sequencing of amplified DNA, *Hemoglobin 17*, 217-225.

572. Watkins, J. A., Kawanishi, S., and Caughey, W. S. (1985) Autoxidation reactions of hemoglobin A free from other red cell components: A minimal mechanism, *Biochemical and Biophysical Research Communications 132*, 742-748.

573. Tsuruga, M., and Shikama, K. (1997) Biphasic nature in the autoxidation reaction of human oxyhemoglobin, *Biochim Biophy Acta 1337*, 96-104.

574. Noble, R. W. (1971) The Effect of p-Hydroxymercuribenzoate on the Reactions of the Isolated γ Chains of Human Hemoglobin with Ligands, *J Biol Chem 246*, 2972 -2976.